THE BEHAVIOR AND MIGRATORY FATE OF SELECT HEAVY METALS DURING THE DEWATERMENT OF AN EFFLUENT DERIVED SEDIMENT

by

Hayden Tackley

Submitted in partial fulfillment of the requirements
for the degree of Master of Applied Science

at

Dalhousie University
Halifax, Nova Scotia
August 2019

TABLE OF CONTENTS

LIST OF TABLES

LIST OF FIGURES

ABSTRACT

Geotextile filtration has proven to be an effective method of both retaining and dewatering dredged sediments. This option has been considered as a method for the remediation of a contaminated marine sediment in Nova Scotia, Canada. The quality of the filtrate by-product is important to quantify, as it can affect decisions on secondary treatment. The objective of this thesis is to assess the mobility of three metals (Cu, Pb, and Zn), which are present at concentrations elevated above background levels.

Questions regarding metal migration have driven research aimed at identifying the fate and transport of the three metals. Laboratory and field-scale dewatering tests were implemented to evaluate the contaminant reduction potential of the geotextile. With chemical conditioning, reduction in the total metal concentrations of over 99 % was achieved. Analysis of the filtrate and filter cake was used to identify further migration potential of the three metals following treatment.

LIST OF ABBREVIATIONS AND SYMBOLS

±	Plus or minus a given measurement
μg	Microgram
μm	Micrometre
AB	Aeration basin
ABS	Acrylonitrile butadiene styrene (plastic)
AOS	Apparent opening size
AOX	Adsorbable organic halides (dioxins and furans)
ASB	Aeration stabilization basin
ASTM	American Society for Testing and Materials
BH	Boat Harbour
BOD	Biological oxygen demand
CCME	Canadian Council of Ministers of the Environment
CEC	Cation exchange capacity
Cl_2	Molecular chlorine
ClO_2	Chlorine dioxide
Cmol	Centimole
COD	Chemical oxygen demand
D_{85}	85 % of the mass is smaller than the given value
E_H	Oxidation-reduction potential

ESA	Environmental site assessment
GT#	200 mL geotextile test trial number
GT-500	Geotextile #500
H_2S	Hydrogen Sulfide
ha	Hectare (10,000 m^2)
ICP-MS	Inductively coupled plasma mass spectrometry
ICP-OES	inductively coupled plasma optical emission spectrometry
ISQG	Interim sediment quality guideline
JT#	Jar test trial number
L/s	Litres per second
M	Molar
MC	Moisture Content
MFI	Micro flow imaging
mg	Milligram
mL	Millilitre
mS/cm	millisiemens per centimetre
mV	Millivolt
n.d.	No date
NaOH	Sodium hydroxide
nm	Nanometer

NP	Northern Pulp
OD	Optimal dosage of polymer
ORP	Oxidation-reduction potential
PAH	Polycyclic aromatic hydrocarbons
PCOC	Potential contaminants of concern
PEL	Probable effect level
PVC	Polyvinyl chloride (plastic)
RDT	Rapid dewatering test
SC	Solid content
SEM	Scanning electron microscope
SQG	Sediment quality guideline
SS#	Small scale trial number
TSS	Total suspended solids
UVOST	“Ultra Violet Optical Screening Tool”
VOC	Volatile organic compound
WWTF	Wastewater treatment facility
XRF	X-ray fluorescence

ACKNOWLEDGEMENTS

Throughout the course of this research I have received a great deal of support from countless individuals. I would first like to express my appreciation to my supervisor Dr. Craig Lake, without whose insight, guidance, and support, this degree would never have been possible. I would also like to thank my supervisory committee, Dr. Ian Spooner and Dr. Rob Jamieson for their interest, assistance, and dedication.

I would like to acknowledge my fellow graduate students, Xiaofei Song, Kirklyn Davidson, Baillie Holmes, and most of all Masi Alimohammadi whose collaboration, friendship, and comradery throughout this learning process has proven to be invaluable.

I would also like to extend my gratitude to the Civil Department and CWRS. To the lab technicians: Heather Daurie, Dan Chevalier, Jordan Mearz, and Brian Kennedy, thank you for all of your assistance along the way. To Terra Chartrand, Paula Zwicker, and June Ferguson, thank you for your unwavering patience and attention.

I would like to thank Nova Scotia Lands for providing the funding for this research, as without their generous contribution, none of this would have been possible. Finally, I would like to thank my friends and family who have given endless moral support throughout my educational journey.

Thanks!

CHAPTER 1: INTRODUCTION

1.1 PREAMBLE

This chapter provides the problem statement outlining the rationale for this study, identifies the research objectives, and frames the organizational layout of the thesis.

1.2 PROBLEM STATEMENT

Industrial activity can sometimes result in the contamination of the local environment through the emission or discharge of various pollutants. Harmful substances can negatively affect air, water, and soil quality, depending on the source and method of disposal (Martinez & Motto, 2000). Industrial effluent discharge basins have been known to contain high levels of toxins, as low concentrations of contaminants present in the overlying water column can accumulate to considerably higher levels in the sediment over time (Rahman et al., 2014). If pollutants (e.g., metals) are allowed to accumulate to levels above background, remediation of the site may be required.

The removal of elevated metals during sediment remediation is essential to ensure pre-contamination conditions are achieved. High-water content sediments can pose unique challenges during remediation, as the additional process of dewatering is often required to reduce the volume of the material (Mulligan, Yong, & Gibbs, 2001). The implementation of geotextile filtration has proven to be an effective means of dewatering and subsequently containing high water content material on a large scale (Moo-Young et al., 2002; Yee et

al., 2012). As consolidation of the material is achieved, a filtrate by-product is produced and may act as a means of conveyance for both dissolved and suspended contaminants (Muthukumaran & Ilamparuthi, 2006). Chemical and physical properties of both the sediment and filtrate may influence the mobility of contaminants, including metals, and must be considered during any remediation project (Tack et al. 1996).

This study is being conducted with cooperation from Nova Scotia Lands Inc. as part of the Boat Harbour Remediation Planning and Design project; currently ongoing at the Boat Harbour Wastewater Treatment Facility. The facility, located in Pictou County, Nova Scotia, has been in operation for over half a century (commencing in 1967). This facility, which is partitioned into several basins, has operated with the purpose of treating industrial effluent derived from various sources over its lifespan, primarily that originating at a nearby kraft pulp and paper mill (GHD, 2018b), henceforth referred to as 'the mill.' In the past, there have also been other known contributors to the industrial effluent (e.g., chlor-alkali facility). The mill currently transports effluent of unknown constituents through an underwater pipeline to the multi-stage treatment facility at a rate of 87,000 m^3/day (Hoffman et al., 2017). During treatment, the effluent is subject to initial sedimentation, followed by aeration, and finally, a prolonged stabilization period to allow for additional deposition of suspended solids (GHD, 2018a). This treatment process results in a discharge which meets environmental standards outlined by the *Pulp and Paper Effluent Regulations*, enabled by the *Fisheries Act* (Northern Pulp, 2015). This discharge is emitted into the Northumberland Strait (Atlantic Ocean) through a hydraulic control structure.

The largest of the basins at the facility, referred to as 'Boat Harbour' (BH) in this thesis, has been designated as a "stabilization lagoon" (JWEL & Beak, 1993). During this

treatment stage, particulate matter present in the filtrate settles out of suspension over a period of approximately 30 days (Hoffman et al., 2017). Decades of sedimentation have resulted in a deposition of anthropogenically contaminated sediment throughout the basin. This sediment possesses both a high moisture content (> 1000%), as well as various organic and inorganic contaminants (Hoffman et al., 2017).

In June of 2014, a rupture in an undersea pipe resulted in approximately 47 million litres of untreated effluent escaping into nearby Pictou Harbour (Hoffman et al., 2017). Following the incident, the Nova Scotia Provincial Government enacted legislation (i.e., The Boat Harbour Act) ensuring the site would cease operation on no later than the 31st of January, 2020. At the time of this thesis, the pilot phase of a marine sediment remediation project is ongoing at the Boat Harbour.

Due to the physical and chemical characteristics of the sediment, as well as the access granted as a result of the ongoing remediation project, the anthropogenically influenced sediment was selected for this research. Work was completed to help identify the effectiveness of geotextile filtration on the removal and containment of three metals in this sediment; copper (Cu), lead (Pb) and zinc (Zn), which are known to be elevated relative to guidelines. These three metals were chosen as they are known to have varying degrees of solubility under naturally occurring conditions. As a result, the findings discussed here may be used to gain insight into the behaviour of metals which were not considered in this thesis, but share similar solubility profiles. Geotextile filtration has shown to be proficient at reducing total suspended solids in the filtrate produced from the treatment of contaminated sediments (Fowler, Bagby, & Trainer, 2000). Numerous studies have assessed the influence of factors such as water content, solids retention, the pore size of the geotextile,

flow and volume rates, etc., on the efficiency of the dewatering system (Mastin, Lebster, & Salley, 2008; Muthukumaran & Ilamparuthi, 2006). However, research regarding metal migration, as well as that which considers the effect of a growing filter cake on filtrate quality during geotextile filtration dewatering (concerning metal concentration) is lacking.

Understanding the fate and transport mechanisms of these contaminants is essential, as without identifying these parameters, questions regarding the requirements for additional treatment of the filtrate may be left unanswered. It is important to reiterate that the sediment analyzed was selected out of convenience (due to its proximity, high moisture content, and known contamination) and for this research should be considered analogous to any similarly classified sediment (i.e., effluent derived sediment).

1.3 OBJECTIVES

The primary objective of this study was to determine the fate of metals during geotextile filtration of a contaminated sediment. This thesis addresses the following specific research questions:

- What are the fate and migration potential of copper, lead, and zinc during geotextile dewatering of the sediment in question?
- How does an established filter cake deposit on the geotextile influence the migration of copper lead and zinc during these operations?

1.4 THESIS OUTLINE

This thesis is divided into six chapters. Chapter 1 has served to identify the problem statement and necessity for this research, as well as outlining the research questions.

Chapter 2 presents a literature review of previous work pertaining to geotextile filtration as well as metal migration during dewatering. A review of the literature has yielded information relating to the background of the site, both from an industrial and geological perspective. A comprehensive assessment of the contamination known to exist is also included, as much research has previously been done to classify the anthropogenic sediment and identify any pollutants which are thought to be present. A brief explanation of geotextile dewatering, the properties of the materials involved, and the known effectiveness of the method are also included to help aid the reader's understanding of the procedures involved during research.

Chapter 3 presents a detailed methodology of the techniques applied to achieve the research objectives. A research plan was implemented which involved both laboratory analysis as well as site-specific fieldwork. The research plan was divided into five primary steps in order to efficiently and accurately achieve this goal. The steps included: sampling of the sediment, initial characterization, treatment of the sediment, filtration using the geotextile, and analysis to determine the effectiveness of the techniques implemented.

The characterization and preliminary conditioning results gathered through the various methods, as well as analysis and discussion of the findings, are addressed in Chapter 4, with the effectiveness and rationale for potential contaminant migration explored in Chapter 5. Chapter 6 summarizes the findings and identifies areas which may

require additional research. Finally, resources used during this report are identified, and additional information pertaining to the findings is included in the form of five appendices.

CHAPTER 2: BACKGROUND AND LITERATURE REVIEW

2.1 PREAMBLE

This chapter begins with a review of the study location. This review will consist of a brief description of the geologic and geographic characterization of the region where the wastewater treatment facility (WWTF) is located, followed by a summary of the physical alterations to the site made during the period of industrialization. A more in-depth analysis of the effluent treatment process is also included to aid in the understanding of the contaminated sediment. A review of typical bleached kraft pulp and paper effluent and the physical and chemical characterization of the anthropogenic sediment at Boat Harbour are all examined. As mentioned, the emphasis of this report is not on that of the specific contaminated site; instead, it is meant to assess the dewatering technique as it relates to any sediment which possesses similar characteristics (physical and chemical). Details pertaining to the location are relevant, however, as they serve to shed light on the origin of the sediment and its characteristics.

Following this site background is a brief overview of the currently proposed sediment remediation strategy. Details regarding the geotextile dewatering procedure, characterization of the materials and techniques currently being implemented, as well as known effectiveness with respect to both dewatering potential and metals reduction are explored. Additionally, a review of work completed on plausible mechanisms for metal

migration during this process is discussed. Finally, a summary of known knowledge gaps is included to accentuate the need for this research.

2.2 SEDIMENT SAMPLING LOCATION – BOAT HARBOUR

2.2.1 General

The Boat Harbour Wastewater Treatment Facility (WWTF) is located opposite Pictou Harbour near the Town of Pictou in Nova Scotia, Canada. Figure 2.1 displays the location of the facility within the greater maritime region, and Pictou County, Nova Scotia. Figure 2.2 shows the extent of the facility as it exists at the time of this report. Wastewater enters the site (a freshwater embayment) in the southwest of the facility and flows northeast to the discharge point at a water control structure draining into the Northumberland Strait (Atlantic Ocean) (GHD, 2018a).

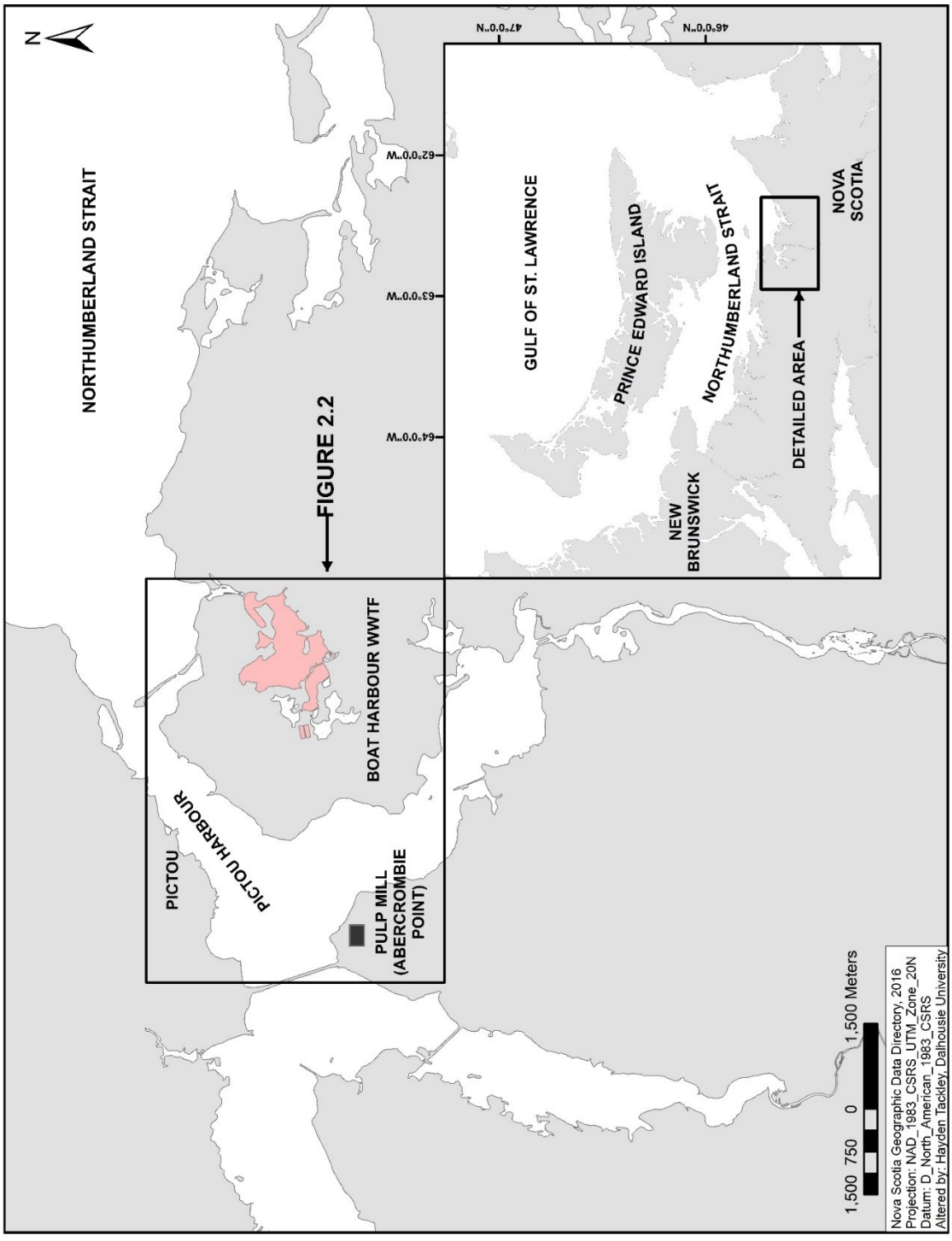

Figure 2.1: Study location in the greater Maritime region.

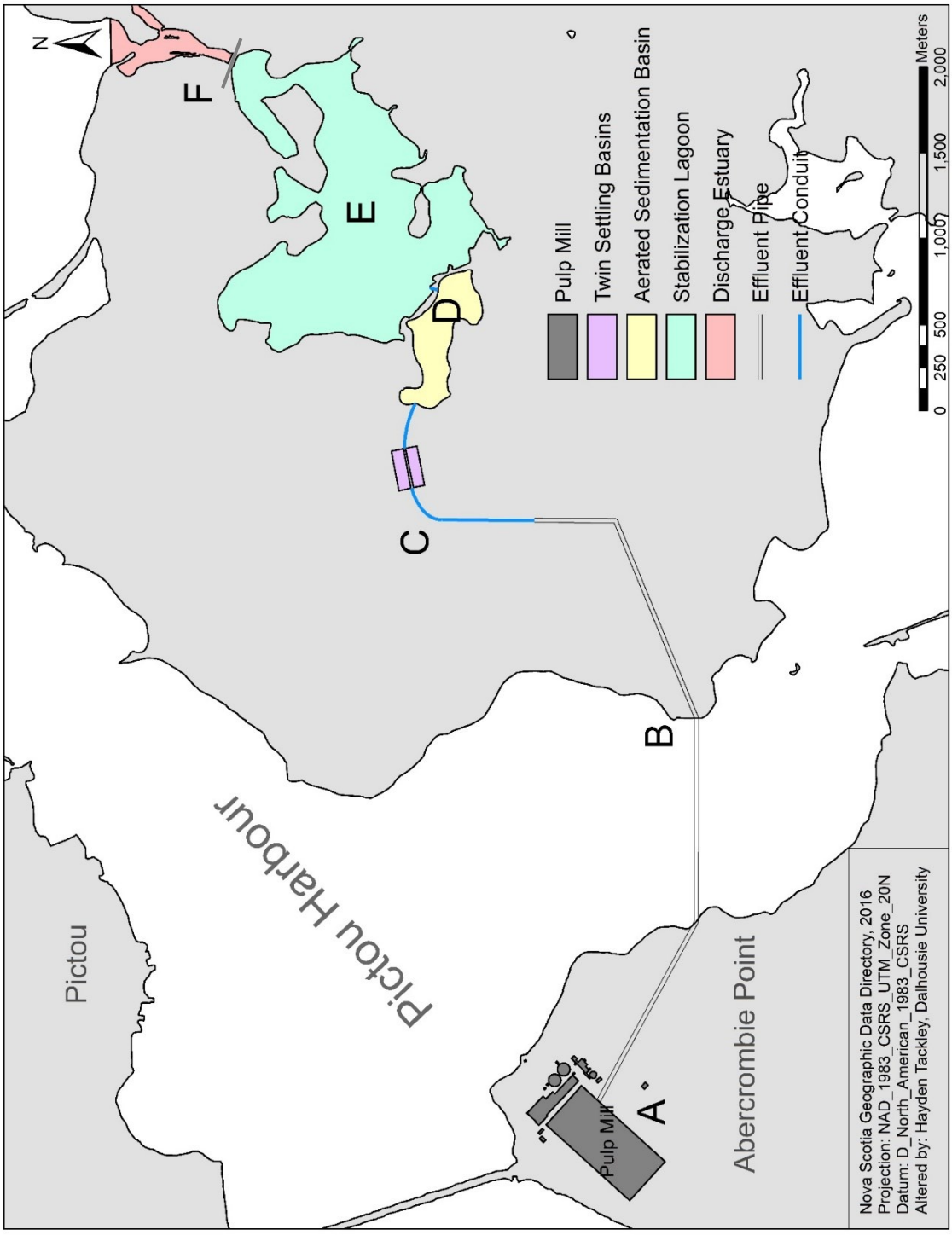

Figure 2 2: Extent of BH WWTF (2019).

2.2.2 Environmental Characteristics

The Boat Harbour WWTF is underlain by Late Carboniferous sedimentary rock belonging to the Pictou Group (JWEL & Beak, 1992). This sedimentary group is composed primarily of fluvial sandstone, arkosic sandstone, floodplain mudstone, siltstone, shale, as well as minor conglomerate and limestone occurrences (Keppie, 2000) (Figure 2.3). The study region is overlain with a regolith consisting of silty till, which was deposited following the last (Late Wisconsinan) glaciation (Keppie, 2000). A sediment known as the Toney River Till is dominant in the area immediately underlying the treatment facility (Keppie, 2000). This deposit consists of a gray-red-brown stony, sandy sediment, which has been moderately compacted. Holocene marine deposits of fine sand, silt, and clay are also present in the area. These sediments are located in the intertidal zone and range from 2-15 m thick (Stea, Conley, & Brown, 1992) (Figure 2.4). Before its utilization as a wastewater treatment facility, BH was a tidally influenced marine estuary (GHD, 2018b). As a result, marine deposits of similar characteristics have been found underlying the anthropogenic deposit throughout the stabilization lagoon (Spooner & Dunnington, 2016). Modification to the estuary was made with the addition of a causeway (dam) at the mouth of the inlet, which became operational in 1967 (Figure 2.2) (Ogden, 1972). This resulted in a rise in water level in the former estuary to approximately 1 m above the high tide level (JWEL & Beak, 1992), thus removing the tidal influence on the area, halting additional deposition of marine sediment.

The settling lagoon currently exists as a freshwater basin (Spooner & Dunnington, 2016). The lagoon is recharged primarily by the inflow of treated effluent, as well as precipitation and localized runoff (GHD, 2018a). An embayment at the northeast terminus

of the facility (Point F, Figure 2.2), is subject to tidal influence. It is at this point, treated effluent from the facility is discharged into the Northumberland Strait.

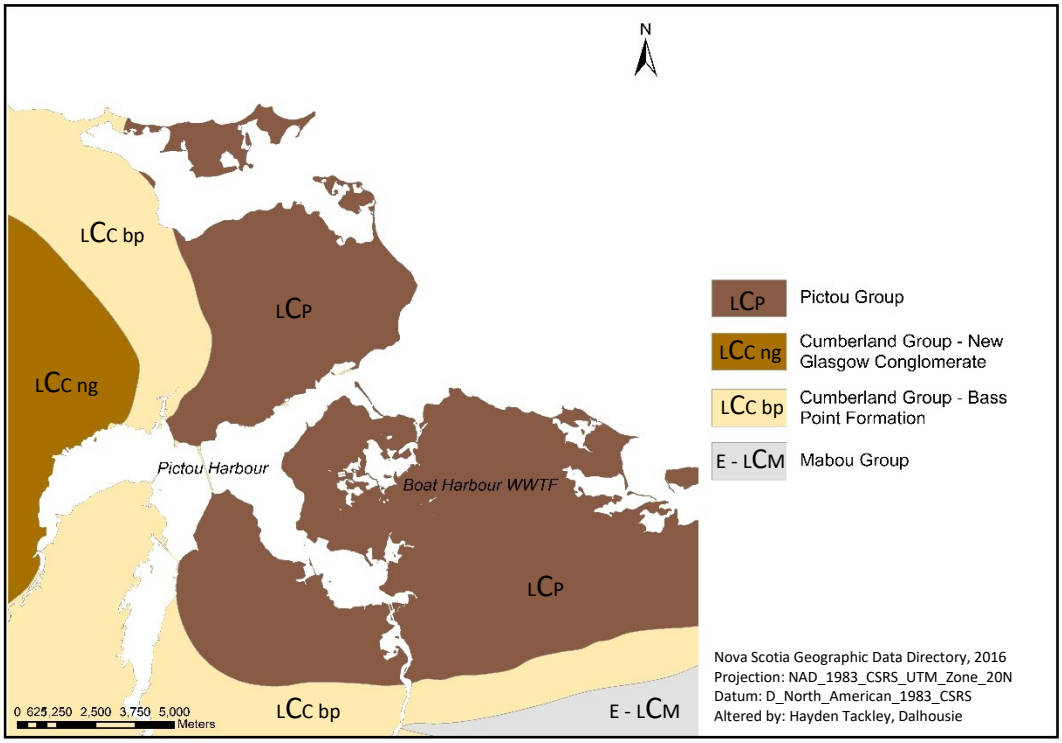

Figure 2.3: Bedrock Geology of Pictou region, adapted from (Keppie, 2000).

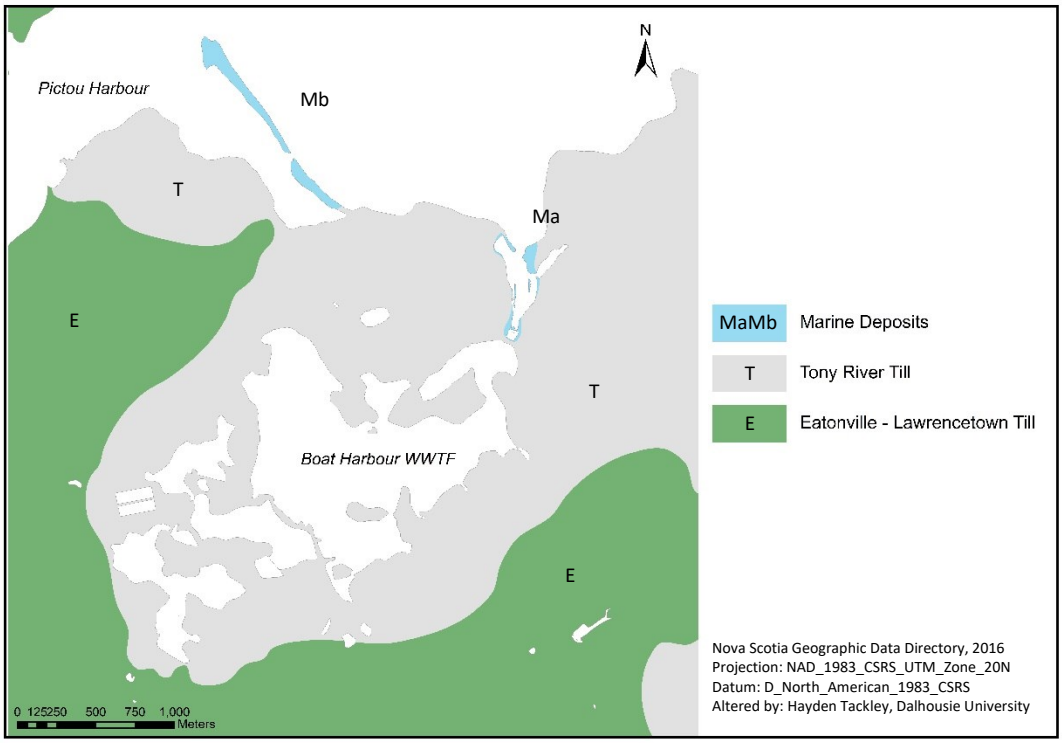

Figure 2.4: Surficial geology of Boat Harbour area adapted from (Stea, et al., 1992).

2.2.3 Anthropogenic Modifications to Boat Harbour

Modification to the Boat Harbor estuary was required to create a suitable wastewater treatment facility. Two water control structures (i.e., dams) were constructed in 1966-67 (Figure 2.5A) (Ogden, 1972; Krauel, 1969). These structures raised the water level in the basin by approximately 2.75 m above mean sea level (JWEL & Beak, 1992), in order to remove tidal influence. The result was the creation of a lagoon which had a considerably higher residence time than previously existed, and therefore would allow for the sedimentation of particulate matter present in the effluent. The basin was initially divided into two sections, the first being a 16 ha "sedimentation basin" where large "settleable solids" (wood chips, etc.) (Ogden, 1972) would be allowed to settle from the wastewater. The second partition, separated from the sedimentation basin by Dam 1 (Figure 2.5A), existed as a "stabilization basin" with a reported surface area of 135 ha (JWEL & Beak, 1992) (however, more recent measurements determined through the course of this study have suggested the original basin had a surface area of approximately 160 ha). This stabilization basin promoted anaerobic/ aerobic growth through natural aeration (oxygenation) (JWEL & Beak, 1992). The added organic influence, combined with additional residence time in the low energy environment, promoted further sedimentation of suspended solids, reducing the amount of particulate matter in the final discharge.

Following five years of operation, a significant retrofit was completed on the facility in response to complaints from the nearby community regarding both increased levels of insects and persistent offensive odors stemming from the site. The retrofit was also designed to improve the treatment process, and reduce the level of contaminants discharged to the Northumberland Strait (Krauel, 1969). This construction, which occurred

in 1972, resulted in the addition of twin sedimentation basins, each approximately 1.6 ha in size (~ 50,000 m^3 volume each), as well as an activated aeration basin (approx. 17.5 ha) which implemented a suite of fixed mounted mechanical aerators. To accommodate these additions, a berm was built which partitioned the stabilization basin, reducing its size to its current extent, approximately 140 ha. A further upgrade to the facility in 1996 introduced a sludge disposal cell, additional aerators, as well as a nutrient feed system (GHD, 2018a; Dillon Consulting Limited, 2019). The physical design of the facility has remained mostly unchanged since 1972 (Figure 2.5B). An additional berm was added in 2016, which partitioned the most southeast section of the main (active) stabilization basin. This section (known as 'Cove A' throughout this report) was selected for pilot research during the remediation project. The remainder of this study will focus on the active stabilization basin (i.e., outside of Cove 'A').

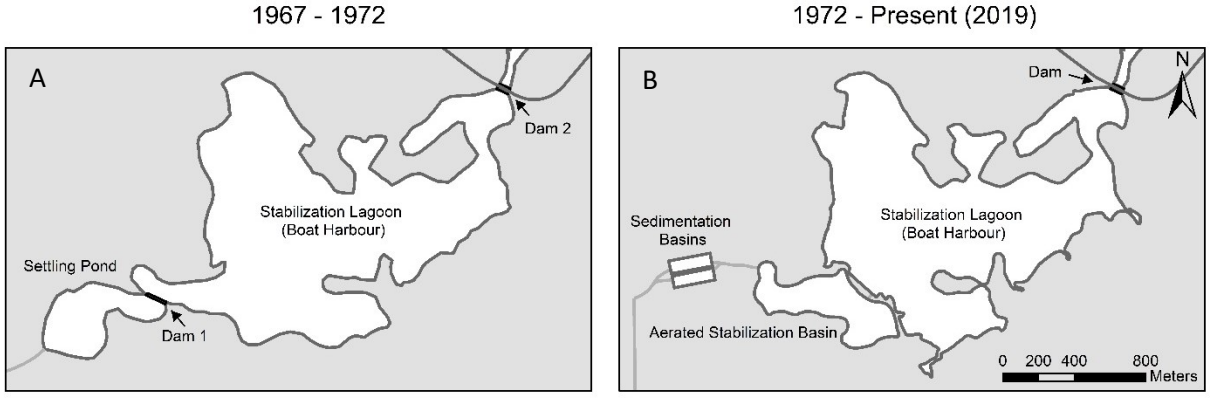

Figure 2.5: BH WWTF temporal comparison. Base maps rendered from historical maps produced by Rust et al. (1970) (A), and JWEL & Beak (1992) (B).

2.2.4 Current Treatment Process

An estimated 577,000 m^3 of contaminated sediment has been deposited in the stabilization lagoon since its inception (GHD, 2018b). This mostly anthropogenic deposit is referred to in this thesis as 'black sediment.'

As outlined by JWEL and Beak Consultants in their 1992 report, the current iteration of the facility operates as follows. The mill at Abercrombie Point disposes of effluent via a 1.1 m diameter pipeline extending under the East River, South of Pictou Harbour. Upon reaching the facility, 87,000 L/day (average) of raw effluent is directed into one of two sedimentation basins (Figure 2.6 - 1) where settleable material is allowed to settle out of the effluent (wood chips, etc.). These basins, which each have a volume of 50,000 m^3 are alternated, allowing for removal of material. Approximately 12 hours is required for a parcel of effluent to flow through this phase of the treatment facility.

Following the sedimentation phase, a mixture of diammonium phosphate and urea is added to promote microbial growth (to aid in further sedimentation) before the effluent enters the 17.5 ha activated aeration stabilization basin (Figure 2.6 - 2). While in this basin, the effluent is subject to mechanical aeration to alleviate the anoxic conditions, and further encourage the breakdown of suspended organic material present in the effluent (Ogden, 1972). This basin has a residence time of approximately five days and has substantial (129,000 m^3) anthropogenic deposits present (GHD, 2018b).

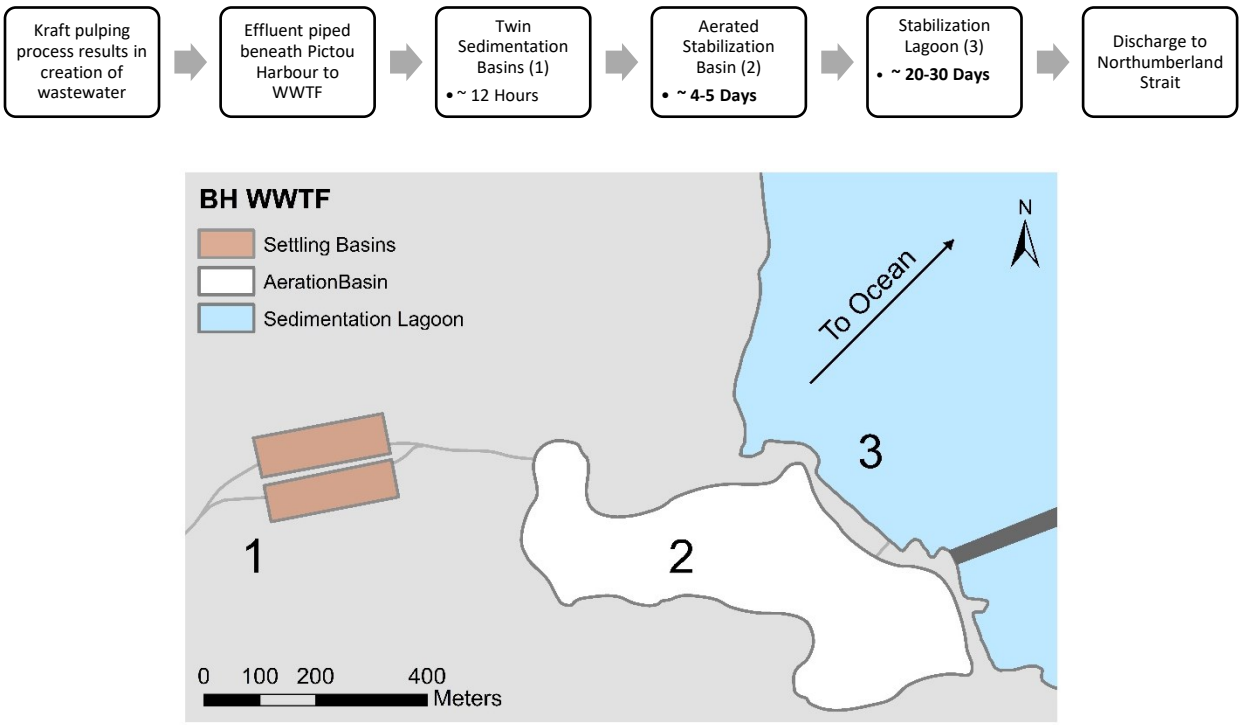

Figure 2.6: Phases of treatment at BH WWTF.

Following aeration, the effluent flows into the 140 ha (3,400,000 m^3) stabilization lagoon (Boat Harbour) (Figure 2.6 - 3). Further sedimentation of fine-grained suspended particulate matter occurs during this late stage over the basin's 20-30 day residence time (Hoffman et al., 2017). Following this phase, the wastewater is discharged to the Northumberland Strait. Compliance monitoring which is conducted prior to the effluent entering the stabilization lagoon (Hoffman et al., 2017) has yielded results which fall within the guidelines set forward by the Canadian Pulp and Paper Effluent Regulations enabled by the Fisheries Act (Northern Pulp, 2015).

2.3 Overview of Chemical Composition of Pulp Mill Effluents

2.3.1 General

The WWTF at Boat Harbour has been in operation since 1967, when it began accepting raw effluent from several industrial services, including a nearby kraft pulp and paper mill. Ancillary to the mill was a chlor-alkali chemical manufacturing plant (Canso Chemicals Ltd.), which operated from 1971 until 1992 (Bennett, 2013; Northern Pulp, 2015). This facility was established to manufacture chemicals utilized in the pulp making process and disposed of its wastewater alongside that of the mills (Cameron, 1972). The treatment of these effluents together has resulted in the accumulation of nearly 577,000 m^3 of unconsolidated anthropogenically influenced sediment in the stabilization basin (GHD, 2018b). The mill currently discharges some 87,000 m^3 of raw effluent per day to the treatment center (JWEL & Beak, 1992), all of which ultimately passes through Boat Harbour.

Analysis conducted on the black sediment has revealed a variety of contaminants exist above various regulatory guidelines within the stabilization lagoon. Testing on the sediment has identified the presence of various metals (Cd, Cr, Cu, Pb, Hg, and Zn), as well as organic compounds (dioxins, furans) (Hoffman et al., 2017; GHD Limited, 2018b). Due to the variability of the effluent, it is difficult to determine with absolute certainty when and how the numerous pollutants have ended up in the basin. As such, a review of the pollutants known to exist in similar industrial effluent and the manufacturing process of bleached kraft pulp is included below, as chemicals used in the process may contribute to contaminants found in the effluent.

2.3.2 Bleached Kraft Pulp Process

The mill, which produces the effluent being deposited in the Boat Harbour WWTF, currently uses a ClO_2 kraft bleaching method in the process of creating white pulp for use in paper products. However, prior to 1997, the mill implemented a bleaching method which utilized elemental chlorine for bleaching (Dillon Consulting Limited, 2019). The elemental chlorine bleaching process previously used in pulp production at this type of mill generates organic compounds such as chloroform, dioxins, furans, and phenols (Hoffman et al., 2017). Kraft pulping involves several stages of heating and chemical treatment to break down wood chips. This process, known as digestion, is done to separate the wood fibres (cellulose), which are turned in to paper, from lignin, a natural binding agent found in the wood (Northern Pulp, n.d.). The amount of lignin in a given wood species can range from 20 – 40 % of the dry mass (Maximova et al., 2001), and as a result, this treatment can result in up to 50% of the original material being dissolved (Smook, 1992). Sodium hydroxide and sodium sulfide are used to facilitate the digestion (*white liquor*) and result in a liquid by-product composed of hemicellulose, sodium carbonate, sodium sulfate, and lignin. A stable compound, rich in cellulose fibres (the main component of pulp (Catalyst Paper, n.d.)) is produced and then separated from the liquid chemical bath for further processing (drying and pressing).

The demand for white paper has resulted in the need for additional chemical treatments during manufacturing. Bleaching occurs in a five-stage process where chlorine dioxide (previously molecular chlorine (Cl_2)), sodium hydroxide, oxygen, and hydrogen peroxide are washed over the fibrous sheets, creating a white pulp (Northern Pulp, n.d., Catalyst Paper, n.d.). Both the pulping and bleaching processes require large amounts of

fresh water for various chemical treatments throughout this practice. Though many of the chemical agents are contained and reused, most of the water is expelled. This water, combined with a fraction of chemical and physical pollutants comprises the raw effluent.

2.3.3 Typical Bleached Kraft Pulp Effluent and Sediment Characteristics

The effluent produced during the bleached kraft pulping process holds a variety of waste matter, and therefore requires treatment before it can be released to the environment. This discharge frequently contains heavy solids (bark, dirt, uncooked wood chips, etc.), dissolved solids (carbohydrates and soluble wood matter such as lignin) as well as chemical pollutants from the pulping and bleaching process (Allan, 1972). These contaminants produce wastewater which can be characterized by suspended solids, toxicity, colour, as well as chemical and biological oxygen demand (BOD & COD) (Pokhrel & Viraraghavan, 2004).

Effluent derived from the kraft pulping process has been studied extensively and shown to contain an abundance of organic material stemming from wood, the primary constituent of pulp. Table 2.1 shows an excerpt from by the US EPA's 1995 report, Profile of the Pulp and Paper Industry, which outlines characteristic pollutants in pulp mill effluent, as well as the stage of manufacture in which each is thought to be produced.

Table 2.1: United States EPA common pulp and paper pollutants (US EPA, 1995).

Source	Effluent Characteristics
Water used in wood handling/debarking and chip washing	Solids BOD Colour
Chip digester and liquor evaporator condensate	Concentrated BOD Can contain reduced sulfur
"White waters" from pulp screening, thickening, and cleaning	Large volume of water with suspended solids Can have significant BOD
Bleach plant washer filtrates	BOD Colour Chlorinated organic compounds

Organic contaminants which have been found in kraft effluent include biocides, resin & fatty acids, surfactants & plasticizers, and other various chlorinated compounds. In addition to these organics, Lacorte et al. (2003) state that at many mills, secondary sludge (material that has flocculated out of suspension following biological treatment of effluent) has been found to contain organochloride compounds such as chlorophenols, chlorocathecols, chloroguaiacols, chlorovanillines, and chlorosyringaldheydes, as well as complex natural polyphenols such as lignin and tannin. The specific biochemical characterization of these organics is beyond the scope of this report.

The presence of 2,3,7,8-tetrachlorodibenzo-p-dioxin (TCDD) (Cabrera, 2017), polychlorinated dibenzo-p-dioxins (PCDD), and polychlorinated dibenzofurans (PCDF) (McMaster, Hewitt, & Parrott, 2006) have also been identified in some kraft pulp mill effluents. The effluent generated from pulp mills utilizing elemental chlorine in the bleaching process has been shown to contain significant quantities of these compounds, known as dioxins and furans (McMaster et al., 2006) or collectively as adsorbable organic halides (AOX) (US EPA, 1995). Studies by Thacker et al. (2007) and Cabrera (2017) suggest that the use of elemental chlorine during the bleaching process is the chief contributor to these toxins. Environmental regulations introduced in the 1980s and 1990s

have significantly reduced the use of this chemical agent, in place of chlorine dioxide (ClO_2) (Suhr et al., 2015), the bleaching agent currently used at the associated mill. However, although elemental chlorine is no longer commonly used in the bleaching process, these toxins are resistant to degradation (Ali & Sreekrishnan, 2001), and as such, sediments deposited from bleached effluent mills prior to this adaptation may still contain AOX.

Naturally occurring wood extractives may also be present in both the effluent and ensuing contaminated sediment. As mentioned previously, chemical treatment and digestion can result in approximately half of the original material being dissolved and separated from the wood fibres during the pulping process. Lignin, carbohydrates, tannins, and resin acids may all be present, and vary in their output depending on the species of wood used (Ali & Sreekrishnan, 2001; Pokhrel & Viraraghavan, 2004).

In addition to both the anthropogenic and naturally occurring organic compounds, pulp mill effluents and effluent derived sediments have also been shown to possess elevated concentrations of various metals (Skipperud et al., 1998a). Allan et al. (1972) note that mercury was a common pollutant released by the manufacture of pulp and paper. This metal served numerous industrial uses including serving as a fungicide to prevent the growth of mould on wood and pulp, as well as a catalyst in the production of bleaching chemicals. The authors note, however, that this practice has since been discontinued and as a result pulp mills no longer discharge mercury originating during the bleaching process (however mercury, which is associated with the wood may still be present in the effluent). Nevertheless, sediments which accumulated before this change in practice may contain elevated levels of mercury. Other metals have also been found in trace amounts in effluent

derived sediments (Skipperuda et al., 1998b; Pokhrel & Viraraghavan, 2004; Lacorte et al., 2003; Wong et al., 2006). Metals such as Co, Fe, Zn, Cu, Pb, among others, are known to exist in sediments derived from pulp mill effluent. These toxins often occur in trace amounts; however, they can pose a significant hazard for diverse biota via bioaccumulation (Furley & de Oliveira Filho, 2000; Mulligan et al., 2001). The bioavailability of these toxins and their effect on local flora and fauna in which they come in contact are beyond the scope of this report.

The raw materials used in the pulping process themselves contain metals (Lewinsky, 2007). The molecules tannin and lignin are examples of polymeric molecules and are major components of plant material. These materials are composed of long chains of phenols, which can adsorb the metals which they encounter (Crist, Martin, & Crist, 2002). These molecules may also contain metals from various sources, which have bioaccumulated over the lifetime of their parent tree (Sawidis et al., 1995). This bioaccumulation is likely the chief contributor to metals in the wastewater. They may dissolve during the pulping and bleaching processes or may remain bound to organics (such as lignin) that ultimately settle in the wastewater treatment facility. Although these metals appear in trace amounts in the effluent, they can accumulate via sedimentation over extended periods.

It is important to note that no two pulp mills produce identical effluent (Ali & Sreekrishnan, 2001), however, by understanding the range of materials which may be present, a general understanding of the nature of the origin of contaminants in the Boat Harbour sediments is obtained.

2.4 BOAT HARBOUR CONTAMINATION

2.4.1 General

Below is a review of previous literature specifically pertaining to Boat Harbour, and contaminants known to be present in the anthropogenic sediment.

2.4.2 Boat Harbour Effluent

A phase 2 environmental site assessment (ESA) was conducted prior to the remediation to assess the contamination present at the site. The ESA has provided a comprehensive overview of the chemical contaminants present at each stage of the treatment facility. The report identifies several areas of potential environmental concern, including the "current raw effluent discharge ditch." Effluent sampled at this location (Figure 2.6 - 1) was done prior to stage one of the treatment process, and as such, can be considered untreated raw effluent. It is, however, only relevant to current effluent and does not necessarily represent historical effluent. Chemical pollutants identified in these samples reported as "potential contaminants of concern," (PCOCs) include; Cyanide, Chlorate/Chlorite, Resin, and Fatty Acids, Sulphate, and Hydrogen Sulphide (GHD Limited, 2018b).

Historical contaminants known to exist in previous BH effluents treated by the facility are also discussed. These include dioxins and furans (AOX), polycyclic aromatic hydrocarbons (PAHs), and hydrogen sulfide (H_2S). The document states that modification to the bleaching process occurred in 1998, and as a result, the use of elemental chlorine and salt were discontinued. The five-stage bleaching process (used currently) was implemented at this time, which utilizes additional amounts of sodium chlorate, sulfuric acid, and hydrogen peroxide, in lieu of the aforementioned chemicals. Other chemical

agents identified in the effluent include chlorine, caustic soda, limestone, alum, salt cake, oxygen, and methanol (GHD, 2018b). These contaminants (along with the elevated amounts of sodium chlorate, sulfuric acid, and hydrogen), however, are not listed as PCOCs by the consultant, as they occur in trace amounts in the effluent. The ESA report did not provide concentrations of any of the pollutants mentioned above in the raw effluent.

2.4.3 Boat Harbour Sediment

2.4.3.1 Distribution

As mentioned previously, an estimated 577,000 m^3 of contaminated black sediment has been deposited in the stabilization lagoon (GHD, 2018b). It is important to understand the distribution of contaminated material throughout the basin. Abundant research has previously been conducted on this material in an attempt to gain accurate volume estimates. Spooner and Dunnington (2016) were able to identify a distinct interface between the two sediment types throughout the basin (the contaminated black sediment and underlying marine silt). The authors report that the interface between these sediment types was easily identifiable, noting a distinct colour change between the estuarine and freshwater deposits. Davidson (2018) and Song (2019) have conducted research pertaining to the migration potential of contaminants in the underlying marine silt. These studies have found the natural sediment has acted, for the most part, as a barrier to transfer, and little mixing of the two sediment types has occurred (Song, 2019). Below the underlying marine silt is a glacial till which is not impacted by the contamination occurring near the surface (Song, 2019).

The thickness of the contaminated sediment is variable throughout the stabilization lagoon. The accumulation of the material has been shown to be somewhat dependant on the morphology of the basin, with higher volumes occurring in low lying depressions (Holmes, 2018). The material ranges in thickness from 0 cm around the shoreline to > 80 cm in the deepest areas (Davidson, 2018; GHD Limited, 2018a). At the time of this report, most recent estimates suggest an average thickness for the black sediment of 24 cm (Alimohammadi et al., 2019b). Thickness measurements presented by Spooner & Dunnington (2016), Holmes (2018), Davidson (2018), and Alimohammadi (2019b) were assembled via the analysis of several methods. Gravity coring was used extensively to collect discrete data from numerous point sources, with percussion coring and UVOST measurements (Davidson, 2020) also used. Seen in Figure 2.7 is an isopach map taken from Alimohammadi et al. (2019a) showing the most recent thickness estimates for the anthropogenically influenced sediment, however large areas of the basin remain under characterized with respect to sediment distribution.

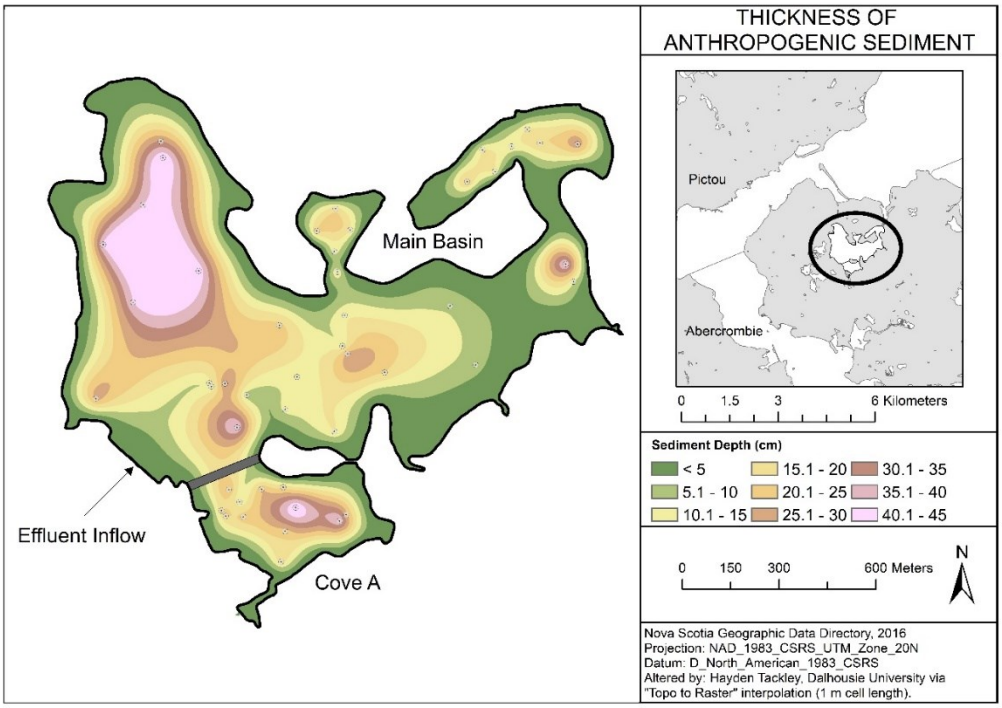

Figure 2.7: Isopach Map showing thickness of contaminated sediment (Colorized) (Alimohammadi et al., 2019).

The effluent derived sediment has been analyzed with respect to temporal distribution, as the cores collected represent a record of the deposition over time. Core extrusions have been done at various increments by Spooner & Dunnington (2016), Holmes (2018), Davidson (2018), and Alimohammadi et al. (2019a), among others, to determine variations in the sediment characteristic throughout the vertical range of deposition. Extrusions were completed on individual core barrels at increments ranging from 1.5cm to 5cm. These discrete samples were analyzed for various characteristics relating to both contamination and physical properties.

2.4.3.2 Reported Physical and Chemical Properties

Sediment which has been deposited within the industrial lifespan is highly organic (Holmes, 2018). The material is known to be very fine-grained, with 85% of particles being finer than 11µm. Grain size analysis has been conducted on numerous samples taken from over 50 locations throughout the basin. No significant variation has been found either spatially or temporally with respect to the physical characteristics (Alimohammadi et al., 2019a).

Preliminary characterization of the contaminated sediment, as well as the overlying water, has been conducted by Alimohammadi et al. (2019b). A summary of the findings which pertain to the stabilization basin (currently in use) as reported by the authors can be seen in Table 2.2.

Table 2.2: Known characteristics of black sediment (Alimohammadi et al., 2019b).

	Unit	Sediment	Water
Solid Content	%	2 – 4	-
Specific Gravity		1.71	-
Organic Matter	%	28.5 – 31.6	-
Zeta Potential	mV	- 28	-24
Cation Exchange Capacity (CEC)	Cmol/kg	62	-
Electrical Conductivity	mS/cm	-	1.5
Ph.		-	7.3
Salinity	ppt	-	0.68
Total Suspended Solids (TSS)	mg L^{-1}	-	25
Total suspended solids (TSS) of sediment diluted to 0.3% solids content	mg L^{-1}	3490	-
D^{85}	µm	11	-

2.4.3.3 Reported Contaminants

Several contaminants of concern (COCs) are known to exist in the black sediment at BH. Known contaminants include metals, polycyclic aromatic hydrocarbons (PAHs), volatile organic compounds (VOCs), cyanide, dioxins and furans (together AOXs), as well as other inorganic and organic contaminants (Hoffman et al., 2015; Holmes, 2018; Stantec Consulting Ltd., 2016).

Hoffman et al. (2017) conducted an in-depth review of secondary data assessing which metals are present in the sediment. The analysis summarized eight reports with relevant chemical data pertaining to metals found in BH sediment. One hundred three individual samples (both core (discrete) and grab (bulk)), taken between 1992 and 2015, were analyzed from 81 locations throughout the stabilization lagoon. The authors were able to identify seven metals (As, Cd, Cr, Cu, Pb, Hg, and Zn) which were found to be frequently elevated above CCME (Canadian Council of Ministers of the Environment) interim sediment quality guidelines (ISQG) for both marine and freshwater. The report noted that six of the metals detected exceeded the probable effect levels (PEL) for freshwater (As,

Cd, Cr, Pb, Hg, Zn), while four exceeded PEL guidelines for marine environments (Cd, Cu, Hg, Zn). The authors note that of the 103 samples analyzed, the majority of samples (69%) represented only the uppermost 15 cm of back sediment, with few samples including data beyond this horizon. Analysis of the samples taken suggests the black sediment has no apparent trend concerning spatial variation with respect to metal contamination throughout the basin (Hoffman et al., 2017; Stantec Consulting Ltd., 2016).

Temporal analyses were also completed by Hoffman et al. (2017), which did identify a trend, wherein a peak in metal loading occurred around 1998 and was followed by a decline in concentration thereafter. The authors attribute this spike in metal concentration to modifications made to the aeration basin around this time, which may have affected the treatment process. Elevated values of the metals identified by Hoffman et al. (2017) (excluding As), can be seen in Figure 2.8. This figure illustrates the level of exceedance over the previously mentioned guidelines which have been found to be present in cores taken from the stabilization lagoon.

As mentioned previously, a phase 2 ESA has been completed on the entire Boat Harbour WWTF site in preparation for the impending remediation. During this comprehensive analysis sediment was sampled from 32 locations throughout the stabilization basin. Samples were obtained by both percussion and gravity coring, which achieved depths of up to 1 meter below the surface. These samples recovered both the contaminated black sediment as well as the underlying marine silt/clay. In contrast to Hoffman et al. (2017), this survey utilized provincial SQGs rather than the federal CCME guidelines for marine and freshwater. Freshwater SQGs were exceeded by As, Cd, Cr, Mn, Hg, Se, and Ag, while the marine SQGs were exceeded at times by Cd, Cu, Hg, Ag, and

Zn. Also found in the sediment were Al, Fe, Tl, and V, which exceeded the "human health criteria." The authors report that Cd and Zn had the highest number of exceedances in the BH settling lagoon, with a spatial trend identified wherein the highest concentrations were found near the effluent inflow pipe, or in areas where accumulation was greatest, and tapered off nearer to the estuary (see Figure 2.7). The study also recovered sediment from a nearby lake (Chance Harbour) which was not believed to have been influenced by the effluent. These samples were used as a comparison to identify the relative elevation of various contaminants found in the basin above background levels. An independent assessment was completed by Holmes (2018) who evaluated metal concentration values for As, Cd, Cr, Cu, Pb, Mo, Ni, Ti, and Zn. The author identified several metals (Cu, Cr, Pb, Zn, Ti), which were shown to be frequently elevated above background levels.

By reviewing the comprehensive assessment produced by Hoffman et al. (2017) and the phase 2 ESA (GHD, 2018a), it is evident that numerous metals are present in the anthropogenic sediment that has accumulated in the stabilization basin. Several potential contributors have been suggested; however, the source of each specific contaminant is beyond the scope of this report. If further information is required pertaining to the origin of the metals, both Holmes (2018) and GHD Limited (2018a) can be consulted.

In addition to metals, trace amounts of various organic contaminants are also known to exist in the black sediment. These include PAHs, VOCs, dioxins, and furans (Hoffman et al., 2017; Holmes, 2018). PAHs and VOCs have also been identified in the anthropogenic sediment; however were not present at levels exceeding applicable guidelines (Stantec Consulting Ltd., 2016). Levels of dioxins and furans exceed applicable guidelines throughout the basin. Amounts of these toxins vary with both depth and location,

showing a generally increasing trend with depth (Stantec Consulting Ltd., 2016). Alimohammadi et al. (2017) provide a comprehensive report on the individual identities of AOXs known to be present in BH sediment. If further information is required regarding these contaminants, the reader can consult this work.

Contaminants known to be present in the BH stabilization lagoon are not unique from what is expected in a similar industrial setting (as outlined previously). Determining how these toxins behave will allow for a better prediction of the fate of the contaminants, following the dewatering and filtering of the material.

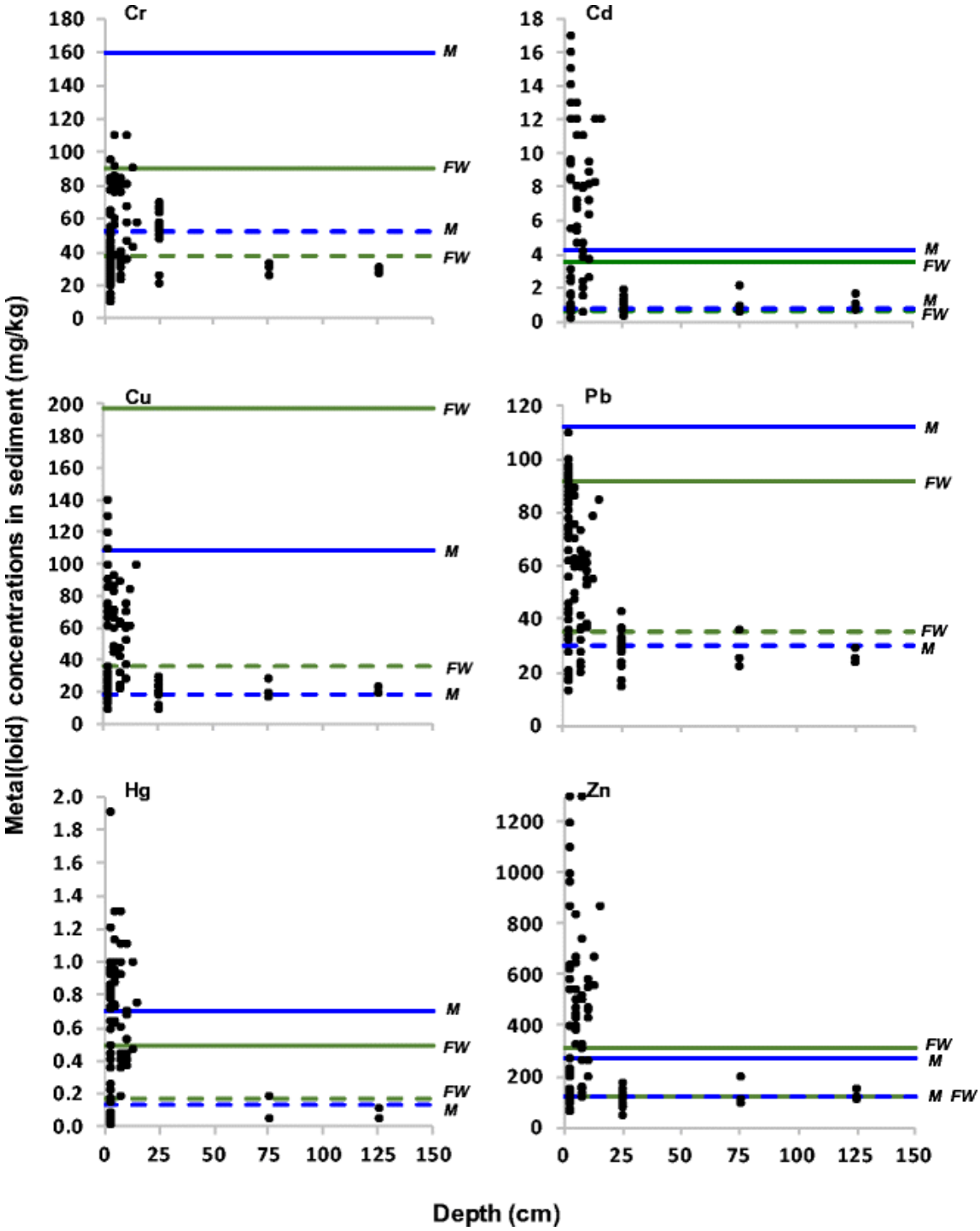

Figure 2.8: Metal contaminants found in BH black sediment. Black dots represent metal concentration (mg/kg) from single samples. Solid lines represent PEL, dashed lines represent ISQG (Hoffman et al., 2017).

2.5 REMEDIATION STRATEGY

2.5.1 General

The literature review and background information provided in this chapter have outlined properties and contaminants found in the black sediment. It has been reported that a volume of approximately 577,000 m^3 of contaminated material resides in the stabilization lagoon at Boat Harbour. The contaminated sediment contains a relatively low solids content, reported to be approximately 10 % (Alimohammadi et al., 2019a). This large volume of water, combined with small grain size (D_{85} < 10μm) has resulted in a high water content material, which will be required to be processed for water content reduction (i.e., dewatered) during the remediation effort. As mentioned in the introduction, for the purposes of this study, sediment collected from this site is meant to act analogously to any similarly contaminated material, when considering an effective dewatering and decontamination strategy. At the time of this report, ongoing pilot work is underway at the Boat Harbour stabilization lagoon to assess the viability of various remediation techniques. Due to the scale of this project, geotextile dewatering is being considered as a practical option for the remediation of the basin. In addition to volume reduction, the ability to reduce contaminants is also an essential aspect of this remediation. Below is a review on geotextile dewatering techniques, a characterization of the geotextile materials involved, and an outline of how it has been implemented previously in similar situations.

2.5.2 Geotextile Dewatering

Geotextile dewatering of contaminated sediments can provide effective storage and consolidation of high water content dredged materials (Fowler et al., 2000). Depending on the physical properties of the sediments, conditioning by synthetic polymers may be required to ensure maximum effectiveness (Mastin et al., 2008). When performed correctly, this method has the potential to retain close to 100% of fine-grained material, and as a result, is also capable of containing many contaminants associated with the sediment (Fowler et al., 2000).

The process utilizes porous containment vessels known as geobags or Geotubes®, to rapidly filter high volume amounts of sediment (TenCate Corporation, 2017). Geotubes® are fabricated from a high strength geotextile, which has the ability to both contain and filter sediment or other unconsolidated material (Watts & Trainer, 2010). For several decades this method has been used for dewatering high moisture content slurries, sediments, and sludges (Fatema & Bhatia, 2018), reducing their volume and making them easier to manage. When compared with other dewatering practices, such as centrifuging, geotextile dewatering has shown to be much less capital-intensive. The implementation of this technique has become both a time and cost-effective alternative for use in the remediation of contaminated sediments (Smith, 2002; Mastin et al., 2008).

When implemented in the dewatering of high water content dredged sediment, the geotextile dewatering method is a relatively intuitive and straightforward process (see Figure 2.9). Sediment is dredged from the contaminated site and pumped, either hydraulically or mechanically, into several openings on the top of the geotextile bag (Fowler et al., 2000). Once inside the bag, the sediment is retained by the woven textile as

it drains, creating what is known as a filter cake (Mastin et al., 2008) adjacent to the geotextile (inside the bag). Water associated with the material (pore water or water introduced during dredging) is then allowed to drain through the bag (and cake) and can be collected for analysis. If effective, upon filtration the substance which remains in the bag will have a higher solid content than the initial sediment. Filtrate quality is a function of the sediment contamination levels and total suspended solids (TSS) (Fowler et al., 2000). If the filtrate is found to contain further contaminants (i.e., metals), additional treatment may be required.

Smith (2002) notes that fine-grained sediment may need to be treated with chemical conditioning agents to aid in coagulation or flocculation. These agents often come in the form of cationic or anionic polymers and are typically added in-line during dredging. The additive(s) chosen, as well as the dosage, are dependent on the properties of the material, as the effect of pH, charge, CEC, and ionic strength must be considered (Rima, 2013). Care must be taken when deciding on the dosage of any chemical additives, as a successful balance will achieve both a fast-draining as well as a clean effluent (Smith, 2002). Figure 2.9 presents a schematic of the geotextile dewatering procedure, as outlined above.

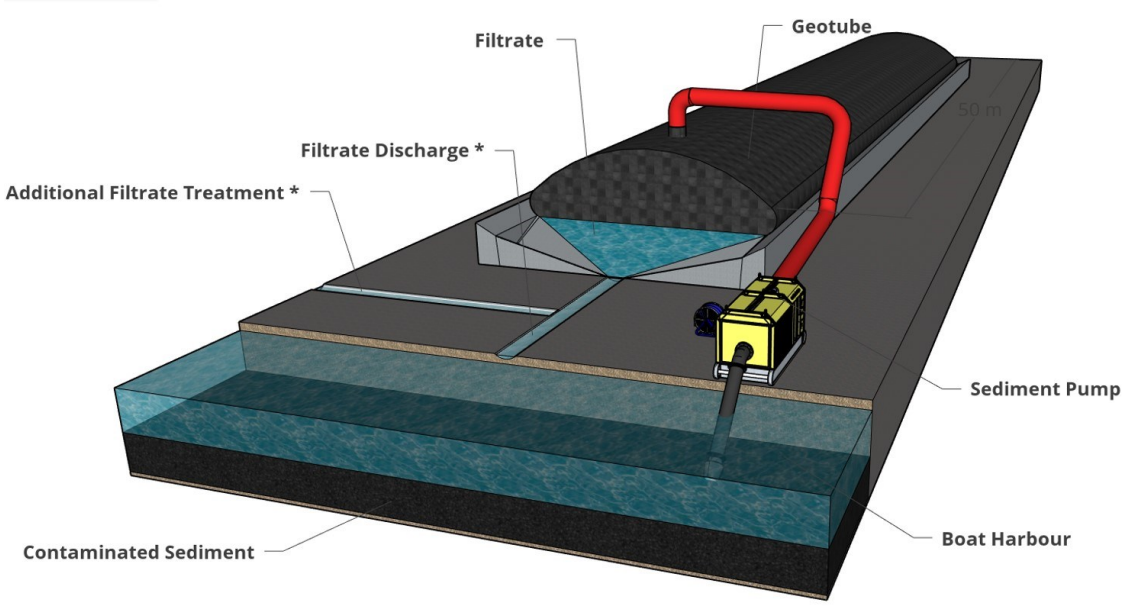

Figure 2. 9: Large scale geotextile dewatering schematic.

2.5.3 Geotextile Characteristics

The geotextile containment vessels (Geotubes®) which have been implemented at the Boat Harbour pilot remediation project are produced by the TenCate Corporation. The tubes are fabricated from a geotextile known as GT - 500. This textile is made of "polypropylene multifilament and monofilament yarns" woven in a manner in which they will maintain their relative position to one another during operation (Watts, & Trainer, 2010). This allows the pore diameter to remain relatively constant throughout use. These bags can be constructed to fit the needs outlined by a specific project, and as a result, come in various sizes.

The GT - 500's apparent opening size (AOS) is reported to be 430 µm and the thickness averages 1.8 mm. The pore size distribution values for O_{50} and O_{95} are 80 µm

and 195 µm, respectively. Table 2.3 outlines some key properties of the material as reported by TenCate Corporation (2015).

Table 2.3: GT - 500 Properties (TenCate Corporation, 2015).

Mechanical Properties	Test Method	Unit	Minimum Average Roll Value	
			MD	CD
Wide Width Tensile Strength (at ultimate)	ASTM D4595	kN/m (lbs/in)	78.8 (450)	109.4 (625)
Wide Width Tensile Elongation	ASTM D4595	%	20 (max.)	20 (max.)
Factory Seam Strength	ASTM D4884	kN/m (lbs/in)	70 (400)	
CBR Puncture Strength	ASTM D6241	N (lbs)	8900 (2000)	
Apparent Opening Size (AOS)	ASTM D4751	mm (U.S. Sieve)	0.43 (40)	
Water Flow Rate	ASTM D4491	$l/min/m^2$ (gpm/ ft^2)	813 (20)	
UV Resistance (% strength retained after 500 hrs)	ASTM D4355	%	80	
Filtration Properties	**Test Method**	**Unit**	**Typical Value**	
Pore Size Distribution (O50)	ASTM D6767	Micron	80	
Pore Size Distribution (O95)	ASTM D6767	Micron	195	
Physical Properties	**Test Method**	**Unit**	**Typical Value**	
Mass/Unit Area	ASTM D5261	g/m2 (oz/yd2)	585 (17.3)	
Thickness	ASTM D5199	mm (mils)	1.8 (70)	

2.5.4 Geotube Effectiveness

Numerous studies have been conducted on the usefulness of geotextiles with respect to dredged sediments. Factors such as initial water content, solids retention, opening size of geotextile pores, flow and volume rates of filtrate must all be considered when assessing the efficiency of the system (Mastin et al., 2008; Muthukumaran & Ilamparuthi, 2006).

The geotextile filtration technique has been proven to be effective at reducing the total suspended solids passing through the geotextile (Moo-Young et al., 1999). By retaining the solid material in a contaminated sludge, contaminants which are bound to

them are also often retained (Mulligan et al., 2009). Much of the research done with respect to geotextile dewatering has been completed on its retention properties.

Alimohammadi et al. (2019b) studied similar sediment taken from the BH stabilization lagoon pilot area (Cove A) and evaluated both dewatering potential and filtrate quality (TSS), following treatment with an optimum dosage of polymer, and filtration through the GT-500 textile. This test consisted of a bench-scale analysis to determine the potential effectiveness of the technique. The test was completed on samples (200 mL each) of sediment/slurry, which had an initial solid content of between 0.3 and 1 %, and a TSS of 2650 mg L^{-1} (0.3%). Following filtration, the authors report a TSS of 31 mg L^{-1} in the filtrate, a reduction of 98.8% from the original input. A total of 195 mL of filtrate was produced (from the original 200 mL input), and a filter cake was found to have accumulated on the surface of the geotextile. This filter cake had a solids content by mass of 7.4 %.

2.6 METAL REDUCTION AND BEHAVIOR

2.6.1 General

The primary objective of this thesis was to determine the fate of three metals; copper, lead, and zinc, during the geotextile dewatering procedure. The specific metals selected for this study were chosen as they had all been shown to be elevated above background concentrations in the BH sediment (Hoffman et al., 2017). These metals, which can often bond strongly with solid particles (organic and inorganic) in sediments (Mulligan et al., 2009), can change both adsorption potential and solubility based on variations in pH, redox potential, ionic strength or other physical and chemical properties (Siepmann, von der Kammer, & Förstner, 2004; Di Luca et al., 2011). However, an increase in solubility, due

to changes in the environmental conditions, can result in greater metal mobility within soils (Reddy, Wang, & Gloss, 1995).

Previous research regarding the geotextile dewatering procedure has proven the methods ability to dewater and contain high moisture content sediment. Analysis of the filtrate and filter cake produced during the dewatering trials (section 3.5) will identify the fate of the metals immediately following treatment. Understanding the migration potential which may exist is necessary when evaluating the long term effectiveness of the method, as processes such as leaching could result in the spread of contaminants throughout the neighbouring environment. This section will review several studies pertaining to the effectiveness of the geotextile dewatering method at retaining metals. Following this review, an overview of the solubility potential for the three metals of concern with respect to the chemical conditions of the environment will be presented.

2.6.2 Metal Migration and Geotextile Filtration

Numerous studies have been conducted on the migration of metals during geotextile filtration. Moo-Young et al. (1999) investigated the migration of contaminants (metals) found in dredged sediment through geosynthetic fabric containers (geotextiles). This study evaluated several metals (including the three which are considered for this thesis) and concluded that through geotextile filtration, a significant amount of the metals present could be removed.

Mulligan et al. (2009) discussed the filtration of a marine sediment sampled from a contaminated waterway. During the study, the authors implemented geotextile filtration and noted the potential for metal reduction via this method. Siepmann et al. (2005), used

geotextiles to determine the reduction potential of metals bound to particulate in urban runoff. This study demonstrated the propensity of metal contaminants found in the water to attach to colloidal particles, and, although were often found to occur in smaller diameters than the filter opening chosen, were retained within the filter cake produced during filtration.

The three studies mentioned support the hypothesis that metal concentrations in dredged sediments can be reduced through geotextile filtration; however, all fail to mention the influence of a changing environment (i.e. factors such as pH or oxidation-reduction potential) on the solubility. The effect of physical retention of sediment (and associated metals) is well documented; however, chemical changes to the system have not been thoroughly investigated.

2.6.3 Solubility Potential

Oxidation-reduction potential (E_H) and pH are both widely recognized as important parameters that can influence the fate and transport of metals (Chuan, Shu, & Liu, 1996). Changes in these two parameters can have a significant impact on the mobility of contaminants in both soil and wastewater (Lange, Rowe, & Jamieson, 2004). Meteorological and biological processes have been shown to alter the pH and redox conditions found inside geotextile containment vessels, and therefore can drastically impact the solubility of these contaminants (Hermann & Neumann-Mahlkau, 1985; Lassabatere, Winiarski, & Galvez-Cloutier, 2004). When implementing the geotextile filtration technique during remediation of a contaminated site, an understanding of the initial chemical conditions present in the environment and how they alter throughout the

operation is necessary to anticipate changes in metal mobility both during and after treatment.

Gambrell et al. (1991) examined the effect of both pH and E_H on the migration of select metals in a contaminated sediment. The study was conducted in anticipation of an impending remediation, wherein the aim was to discover the impact of changes in these two parameters introduced upon disturbance of the sediment, and how these changes may affect the solubility and mobility of certain metals. The material in question was a marine sediment which had a slightly basic pH and low salinity levels (similar to the conditions in the BH stabilization lagoon (Alimohammadi et al., 2019b)). Prior to disturbance, the sediment was found to be highly anoxic, and as a result, was determined to be a reducing environment. Under these conditions, (reducing and neutral) the metals considered (which included Cu, Pb, and Zn) all remained relatively immobile. Upon disturbing the sediment, the pH and E_H were altered, and a high degree of variability in the solubility of the metals was observed. The authors note that if the conditions were to become highly acidic or oxidizing, nearby water systems could be impacted through increased leaching, as the metals become more mobile.

E_H-pH solubility diagrams sampled from Hermann et al. (1984), which were published by Garrels and Christ (1965) and Hem (1972), for copper, lead, and zinc, can be seen in Figure 2.10. It is important to note that the diagrams were developed under laboratory settings and consider very specific conditions. When considering the three solubility diagrams, it is clear that under a reducing and neutral pH environment, the level of dissolved metals would likely be minimal compared to those in the solid fraction. However, if the conditions were to transition to either more oxidizing or acidic, the

solubility of both copper and zinc would likely increase. Solubility fields located in the top left of the graphs indicate that under these conditions, ionic molecules of both copper (Cu^{2+}) and zinc (Zn^{2+}) may both precipitate out of solution (which is in agreement with the findings reported by Gambrell et al. (1991)). Geotextile bags have been found to encourage microbial growth, and as a result, alter the reduction potential of the environment (Lassabatere et al., 2004). As a result, the environment in which the sediment is stored may itself be a factor in the migration potential of the metal contaminants.

Hermann et al. (1984) note that although the figures do not represent the actual conditions which may exist in a given system, they are capable of representing, somewhat accurately, a likelihood of solubility for a given metal. Other species found in the environment may have an effect on the solubility; however, the construction and modelling of E_H-pH diagrams which are representative of the natural system (with all present components considered) are beyond the scope of this thesis. Nevertheless, observing the pH and E_H of the system throughout the dewatering procedure and referencing the levels to the figures may be helpful when trying to anticipate future mobility introduced through changing conditions during and after remediation.

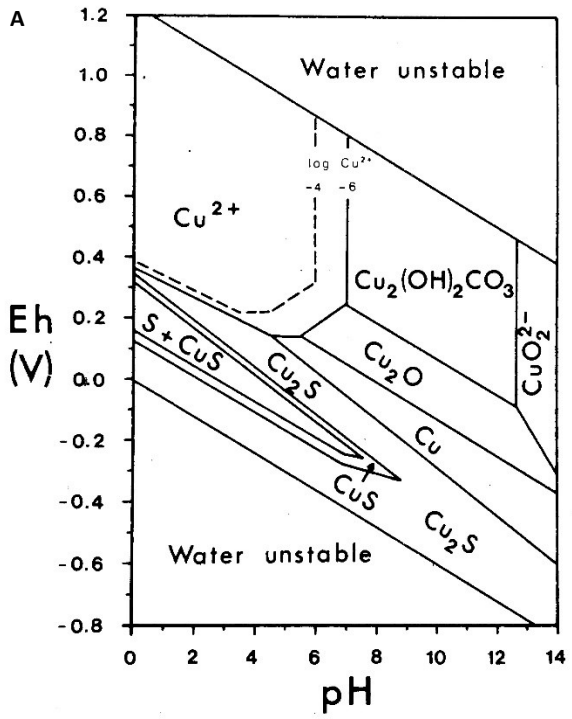

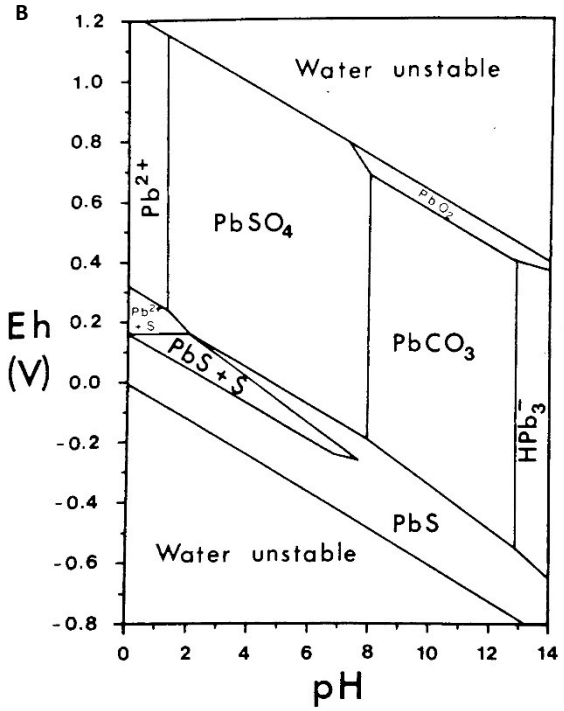

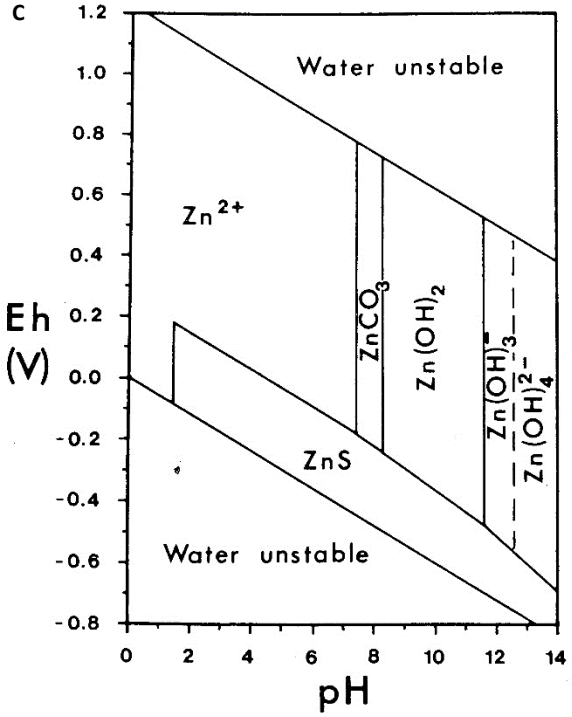

Figure 2.10: Diagrams for Cu(A), Pb(B), and Zn(C) sampled from Hermann et al. (1984).

In addition to reduction potential and pH, the effect of surface charge (zeta potential) on the particles may play a role in the migration of the metal contaminants associated with particulate matter. This factor has been shown to affect the flocculation potential of particulate in solution. If a sediment has a high zeta potential (positive or negative), strong repulsive forces may prevent the material from aggregating, and therefore make it difficult to filter (Larsson et al., 2012). However, low if zeta potential exists, the sediment may have a higher propensity to aggregate, as the repulsive forces can be overcome more readily, allowing for larger material which may be more easily retained by a filter. If the environmental conditions suppress the soluble fraction of metals in the system (and as a result bound them to the sediment), increased particle size through flocculation may be a chief contributor to preventing metal migration. The effect of zeta potential and E_H - pH on the BH stabilization lagoon sediment and filtration by-products will be explored in section 5.6.

2.7 KNOWLEDGE GAPS AND RESEARCH HYPOTHESIS

This chapter has laid the groundwork required for a comprehensive investigation into metal migration during geotextile dewatering of contaminated sediments. Although much research has been conducted pertaining to the potential to dewater sediments, little information could be found describing the mechanisms for contaminant transport through a geotextile. As a result, the effects of contaminant retention via geotextiles require further research (Lassabatere et al., 2004). Information regarding the processes affecting migration, such as solubility, particle speciation, and the association with which metals have with them are all areas which a comprehensive review is lacking. The influence of

the filter cake and its behaviour over time with respect to metal migration is another area which has yet to be explored in detail (Muthukumaran & Ilamparuthi, 2006). The following chapter outlines the research methodology, which was implemented in order to address the research gaps which have been identified. Specifically, this research has pertained to three metals (Cu, Pb, and Zn) and their behaviour during the geotextile dewatering of a contaminated sediment.

CHAPTER 3: RESEARCH METHODS

3.1 PREAMBLE

This chapter outlines the methodologies used to assess the migration potential of select metals during the dewatering of a contaminated sediment. Additionally, several materials which were used throughout the study have been characterized in detail. The sediment chosen for the study was sampled from Boat Harbour, Nova Scotia, Canada. Although this material contained specific levels of contaminants, it is important to note that it is being used analogously to any similarly derived sediment. As such, the methodology discussed here may also apply to similarly contaminated sediments. Experimental methods which were conducted in their entirety by the author are reported in detail. In addition, some analytical methods which required samples to be externally tested are mentioned; however, for a complete procedure, the reader is referred to the reference material cited.

For this thesis, a research plan was implemented which involved both laboratory analysis and site-specific fieldwork. The research plan was divided into five primary steps in order to efficiently and accurately achieve the research goals (see Figure 3.1 below). These steps included: sampling of the sediment, initial characterization of the sediment, treatment of the sediment (i.e., polymer conditioning and modification), filtration using the geotextile (i.e., lab and field trials), and investigating possible mechanisms of metal migration. The test results and related discussion are presented in the following two chapters.

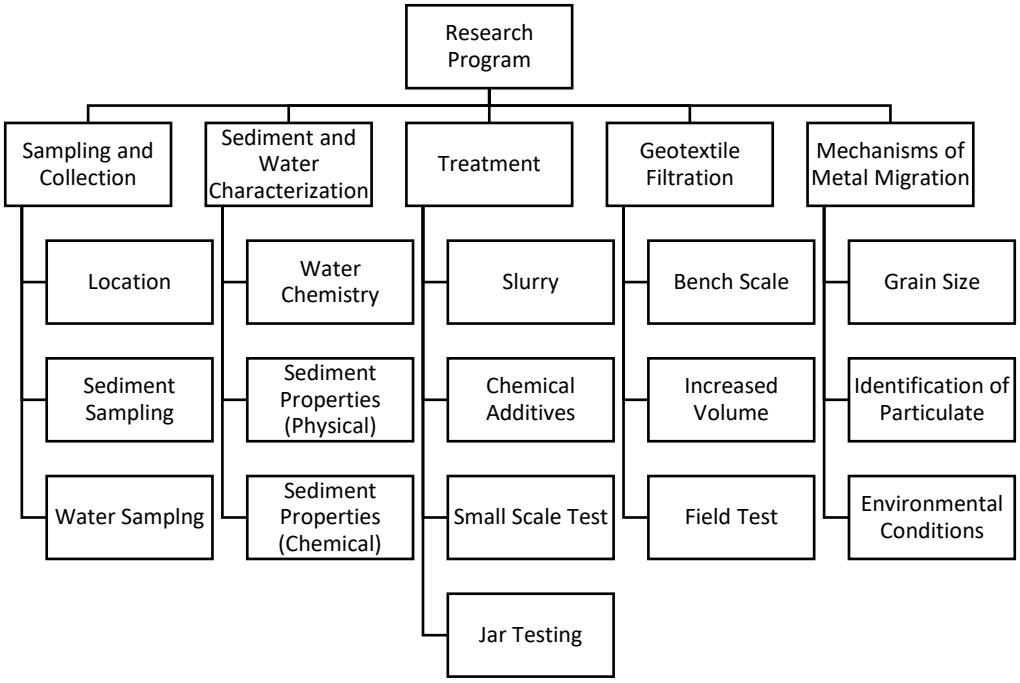

Figure 3.1: Research plan implemented for this study.

3.2 SAMPLING AND COLLECTION

3.2.1 Location

Sediment and water samples were collected from various locations throughout the study area (i.e., BH stabilization basin). Bulk sampling was used to gather the sediment required for the dewatering trials. Figure 3.2 shows the location from which all of the sediment gathered for this thesis was acquired. This site was chosen as it was known to contain a thick deposit of anthropogenic sediment, therefore reducing the chance of contamination by the underlying marine sediment (Davidson, 2018).

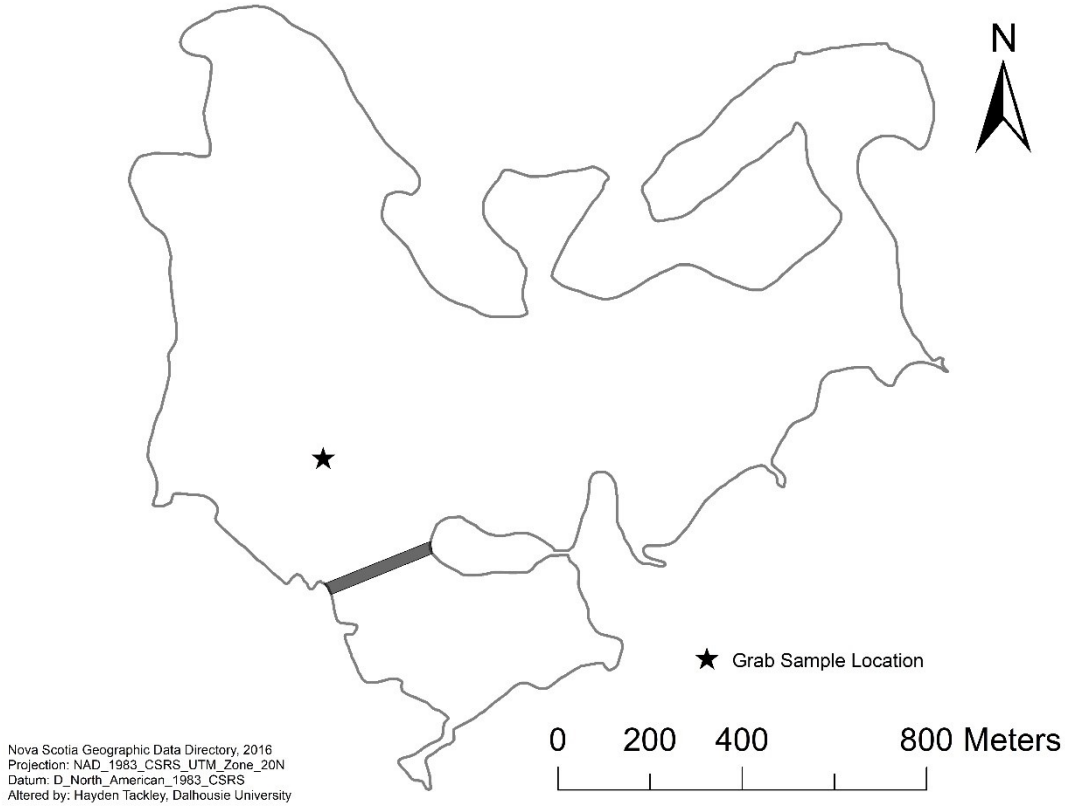

Figure 3.2: BH stabilization lagoon contaminated sediment extraction location.

3.2.2 Sediment and Water Retrieval

All samples which were analyzed during the course of research for this thesis were collected via a wooden/PVC barge measuring 2 m x 4.4 m (Figure 3.3). During sampling, the craft was anchored to reduce drift, and coordinates were recorded.

Figure 3.3: Raft and Zodiac used during sediment and water sampling.

3.2.2.1 Sediment Sampling

Bulk samples of contaminated sediment were collected using a hand-operated Ekman Grab Sampler manufactured by Wildco (model 196-815). The grab measured 150 mm x 150 mm x 150 mm and had a carrying capacity of 3.54 L. Following arrival at the desired sampling

location, the position of the transport vessel was secured via several anchors to limit drift. The grab sampler was lowered over the side and allowed to penetrate the sediment under its own weight. A brass messenger was then lowered along a tether cable, triggering the device. The grab sampler was lifted from the bottom of the basin by rope and removed from the water. The clamshell device was then opened and the contents (contaminated sediment) were drained into a 20 L bucket. This procedure was repeated several times until the desired amount of sediment was collected. The buckets were sealed on-site and transported to Dalhousie University laboratories for chemical and physical analysis.

3.2.2.2 Water Sampling

A large volume of BH stabilization basin water was required for both chemical analysis (metals, pH, etc.), as well as the dilution of the contaminated sediment. This water was collected using a vacuum pump lowered into the basin (to a depth of approximately 0.5 m) from the wooden/PVC barge. In an attempt to reduce added turbidity via the disturbance of suspended solids from both pumping and general movement around the shoreline, the barge was towed approximately 40 m from the boat launch site (South of the sampling location on Figure 3.2). By collecting water at this distance, it was possible to better preserve on-site water conditions (i.e., less lack of suspended solids introduced by disturbance to the basin floor). The pump was lowered over the side of the raft to a level which the intake port was submerged but kept at a height adequate to not disturb the sediment. Opaque 20 L buckets were filled on the raft and sealed for transport to Dalhousie University.

The pump used was an electric 560 Watt submersible sewage pump manufactured by *Powerfist*, and had a cast iron impeller with a suction opening measuring 30 mm. The discharge port was connected to a 15 m long by 50 mm diameter discharge hose via PVC quick release fittings. The pump had a maximum flow rate of 16,000 litres per hour (L/h), which varies by head, reducing to 11,000 L/h at 20 ft. Throughout the experimentation phase of the study, approximately 1,000 L of basin water was drawn from the active stabilization basin using this method.

3.3 SEDIMENT AND WATER CHARACTERIZATION

Initial characterization of both the sediment and water was completed for this thesis. This section outlines the test procedures which were conducted to identify various index properties of the materials with reference to standard methods, where applicable. Individual trials and how these tests were applied to the sediment and water will be discussed in the subsequent sections included in this chapter.

3.3.1 Water Chemistry

Water sampled directly from the active basin was subject to analysis. Any dilution required was done with Milli – Q water (meeting ASTM Type 1 guidelines) (ASTM International, 1999). All water analysis was completed at Dalhousie University's Center for Water Resource Studies laboratory. Many of the tests used for water chemistry analysis of the raw BH stabilization basin water were also implemented on other samples (treated water, filtrate, etc.). As such, the reader should consider Chapter 3.3 as a reference for the methodology if one is not included in a subsequent section.

3.3.1.1 pH

Water pH was measured in accordance with ASTM International (2016a) method D5464. The pH meter (Fisher Scientific Accumet Excel – XL50) was standardized (calibrated) using three pH buffer solutions (4.0, 7.0, and 10.0). Each sample was subjected to a minimum of three trials, with averages recorded to ensure accurate results.

3.3.1.2 Oxidation-Reduction Potential

Reduction potential (E_H) was measured in accordance with APHA, AWWA, WFE (2005), method 2850. A Fisher Scientific Accumet Excel – XL60 millivolt meter in combination with a platinum pin Ag/AgCl combination electrode was used for the procedure, with all measurements being calibrated to 25 °C. A Potassium Iodide ORP standard solution (Orion 967901) was used to standardize the meter prior to each measurement. The technique produced a relative measurement in which the E_H of the system could be determined via Equation 3.1, where $E_{Observed}$ was equal to the sample potential determined by the meter, $E_{Refrence\ Standard}$ was equal to + 220 mV, and $E_{Refrence\ Observed}$ was equal to the potential determined for the reference standard prior to each sample reading.

$$\boldsymbol{E_{H_{System}}} = E_{Observed} + E_{Refrence\ Standard} - E_{Refrence\ Observed}$$

Equation 3.1: Oxidation-Reduction Potential (APHA, AWWA, WFE, 2005)

3.3.1.3 Zeta Potential

Zeta potential was measured to identify the surface charge of particles present in water samples. The analysis was done using a Malvern Panalytical Zetasizer Nano ZS with samples prepared in accordance with APHA, AWWA, WFE (2005). The unit, which was capable of measuring particles ranging from 3.8 nm – 100 nm in diameter, used electrophoretic light scattering to determine zeta potential, accurate to 0.12 um.cm/V.s (Malvern Instruments Ltd., 2019). 1.5 mL of sample was required for each trial, with triplicate analysis being conducted on approximately 20 % of the samples to ensure accurate results.

3.3.1.4 Total Suspended Solids

The amount of total suspended solids (TSS) was measured using a HACH DR 5000 benchtop spectrophotometer. The analysis was completed in accordance with HACH specifications, wherein 10 mL of sample water was placed in a glass sampling jar and inserted into the machine for each trial. The machine was calibrated before each use with a 10 mL sample of Milli - Q water. The unit had an effective measurement range of 5 - 750 mg L^{-1} TSS (HACH Company, 2014). Samples which yielded values in exceedance of the detection limit were diluted to 50, 10, or 1 percent (depending on exceedance) with Milli – Q water and retested. These values were then multiplied by the appropriate dilution factor to yield accurate quantitative results.

3.3.1.5 Metal Analysis

Metal analysis was completed on BH stabilization lagoon water to determine the initial concentration found in the overlying water column. Concentrations found in the Boat Harbour water were determined via ICP-MS analysis, in accordance with ASTM International (2016b) method D5673 – 16. Values for both total and dissolved metals were ascertained through this method.

When considering total metals, sample preparation was completed in accordance with APHA, AWWA, WFE (2005). 10 mL of sample water was treated via the addition of 0.5 mL of concentrated NaOH. Samples were then placed in a block digester (Perkin Elmer SPB 50-24) and subjected to a temperature of 105 °C for 120 minutes. Milli – Q water was then added to return the volume to 10 mL, before being refrigerated until analysis on a Thermo Scientific X Series 2 ICP-MS instrument. The detection limit for the three metals of interest was 0.7, 0.4, and 0.6 ppb for copper, lead, and zinc, respectively.

Dissolved metals were tested in accordance with APHA, AWWA, WFE (2005). Sample water was filtered via syringe through a 45 µm Whatman cellulose nitrate membrane filter (25 mm diameter). Upon filtration of 10 mL of the desired sample, two drops of 0.2 M NaOH were added for stabilization before being refrigerated until analysis.

3.3.2 Sediment Properties (Physical)

The term *sediment* in this chapter refers to the contaminated black anthropogenically influenced material extracted from the active BH stabilization basin via the methods discussed previously. Analysis was completed to determine grain size, particle concentration, moisture content, and solid content (SC) of the raw material. Unmodified

sediment samples were used when possible; however, dilution was required for some tests to allow use in various testing devices. When necessary, dilutions were completed via the addition of Milli – Q water. Similar to the water methodology outlined above, this section contains techniques used for subsequent tests on various other solid fraction materials. Future reference of the same method will be directed to this chapter for a review of the technique.

3.3.2.1 Moisture Content

Sediment moisture content was determined in accordance with ASTM International (2019b) method D2216 - 19. Sediment was mixed using a modified 4 inch diameter stainless steel mixing rod. For each sample, approximately 50 g of sediment was selected post mixing and placed in aluminum weighing dishes for analysis. All samples were dried in an oven (110 °C) for 24 hours.

For all moisture content trials, the dry, empty aluminum dishes were measured prior to the addition of the sediment (M1). Each sample was also measured before entering the oven (M2) and following the 24 hour drying period (M3). Moisture content was then determined via Equation 3.2, with mass values reported being the average of three individual samples analyzed for each test.

$$\boldsymbol{Moisture\ Content}\ (\%) = \frac{\boldsymbol{M2\ -\ M3}}{\boldsymbol{M3 - M1}}\ \boldsymbol{x\ 100}$$

Equation 3.2: Moisture content (ASTM International, 2019b)

3.3.2.2 Solids Content

Sediment solids content was measured in accordance with ASTM International (2019b) D2216 - 19. Measurement data was yielded using the same technique as discussed in section 3.2.4.3, wherein the aluminum weighing dish = M1, the wet sediment + the dish = M2, and the dry sediment + the dish = M3. The equation (3.3) which identifies solids content as a percent is displayed below.

$$\boldsymbol{Solids\ Content}\ (\%) = \frac{\boldsymbol{M3 - M1}}{\boldsymbol{M2 - M1}}\boldsymbol{x100}$$

Equation 3.3: Dry Solids Content (ASTM International, 2019b)

3.3.2.3 Particle Size and Concentration

All sediment and water samples were analyzed for particle size and concentration using a Brightwell Technologies Inc. DPA-4100 flow microscope. The microscope had an effective measurement range of 2 µm – 300 µm and was able to measure material with particle concentrations of up to 175,000 particles per millilitre (Brightwell Technologies Inc., 2009). Raw sediment samples were diluted to 1% of their initial concentration with Milli – Q water. Samples which continued to exceed the limits of the device were diluted again either 0.1% or 0.01% depending on the opacity of the liquid. The procedure consisted of 1 mL of the raw (now diluted) material pipetted out of the solution and placed on the intake cell above the imaging field. The material was then pumped through the field at a

rate of 0.22 mL/min. Proprietary software was used to analyze the images which were taken throughout the trial to determine particle size (as well as several other parameters). During the trials, triplicate analysis was conducted regularly (dependant on the number of samples being analyzed) to ensure accurate results were recorded. The apparatus was normalized prior to each trial by passing approximately 30 mL of Milli – Q water through the imaging field.

Particle concentration in the untreated sediment was also measured using the Brightwell Technologies Inc. DPA-4100 flow microscope. Similar to grain size measurements, raw sediment was diluted to either 1%, 0.1% or 0.01% (depending on initial moisture content) concentration with Milli – Q water prior to analysis. Particle concentration and particle size measurements were performed concurrently, with an average recorded for all samples. The flow imaging device used proprietary software to determine particle concentration (number of particles per mL of sample). The resulting value was then multiplied by the dilution factor to yield a representative value for the raw material.

3.3.2.4 Organic Matter

The total fraction of organic material in the sediment deposited in the BH stabilization lagoon was determined by the ignition of the material in accordance with ASTM International (2014) method D2974 – 14. The percentage of organic matter was determined in a two-step process wherein a 100-300 g sample of the material was oven-dried for 24 hours at a temperature of 110 °C, to evaporate any water present. The sample (M1) was then weighed before being placed in a furnace for a period of 72 hours at a temperature of

440 °C. This heating resulted in the incineration of organic matter, yielding an ash material (M2) which was again weighed and compared to the initial oven-dried sample. The organic matter was then determined by the ratio of the two masses, as seen in Equation 3.4.

$$\boldsymbol{Organic\ Matter}\ (\%) = \mathbf{100} - \frac{\boldsymbol{M2\ x\ 100}}{\boldsymbol{M1}}$$

Equation 3.4: Organic Material (ASTM International, 2014b)

3.3.3 Sediment Properties (Chemical)

Chemical analysis was completed on the untreated sediment to determine zeta potential, E_H, pH, and metal concentration. Untreated sediment samples were used when possible; however, similar to the physical properties, equipment limitations resulted in dilution being required for specific tests.

3.3.3.1 pH, E_H, and Zeta Potential

Sediment pH was measured in accordance with ASTM International (2015) method D2976 – 15. To determine the pH of the sediment, 50 mL of Milli – Q water (reagent) was mixed with 3 g of air-dried sediment. An electrode (Fisher Scientific Accumet Excel – XL50), which was calibrated using three pH buffer solutions (4.0, 7.0, and 10.0) was then inserted into the solution. The pH probe was calibrated before each use via ASTM International (2016a) D5464 specifications.

Zeta potential analysis was performed to identify the surface charge present on the particles in suspension. The analysis was done using Malvern Panalytical Zetasizer Nano ZS (See 3.3.1.3). Trials were completed on sediment samples diluted with water collected from the active stabilization lagoon. The samples were diluted to 0.1% and 0.01% solid content to identify any variability caused by the dilution. Approximately 1.5 mL of sample was used for each trial.

To gain a more representative measurement for the in situ reduction potential, a 10 L sample of sediment was covered and left undisturbed for 1 week in order to reduce atmospheric contamination as much as possible. Following this period measurements were conducted with care taken not to disturb the sample. The same method outlined in section 3.3.1.2 was used to determine E_H of the sediment, with approximately 10 minutes per sample designated for equilibration.

3.3.3.2 Metal Analysis

Two methods were implemented to determined metal concentration in the raw sediment. The various methods were chosen based on the properties of the material being examined. Certain methods were deemed more appropriate for either the liquid or solid by-product produced during the geotextile filtration. As a result, it was pertinent to use methods which could be directly compared, as well as avoid dilution of the material when possible. The first method utilized ICP-MS and was conducted in accordance with ASTM International (2016b) method D5673 – 16. Samples were diluted to 0.1 % concentration with Milli – Q water and digested pursuant to the steps outlined by APHA, AWWA, WFE, 2005. Prior to the digestion of the sediment, 0.5 mL of concentrated NaOH was added to 10 mL of each

dilution and placed in a block digester (Perkin Elmer SPB 50-24) which heated the samples to 105 °C for 120 minutes. The samples were then refrigerated prior to ICP-MS analysis via a Thermo Scientific X Series 2, which was completed by Dalhousie Universities CWRS laboratory.

Quantitative trace element analysis was also conducted at Dalhousie Universities Minerals Engineering Center. The analysis was completed on 200 mL of untreated sediment. Two samples consisting of approximately 1 % and 8 % solids content by mass were analyzed, with the former being diluted with BH stabilization basin water. Upon arrival, the sample was dried and inductively coupled plasma optical emission spectrometry (ICP-OES) was performed to determine the concentration of select metals in the sediment. Both ICP metal concentration measurement techniques reported a precision of ± 5 %. The ICP-OES analysis produced for both dilutions, showing concentrations for 40 metals present in the sediment is shown in Appendix 1.

3.4 SEDIMENT CONDITIONING

The sediment collected from the stabilization basin contained a solid content which was found to be too low to allow for effective geotextile filtration. Multiple tests involving various chemical additives and alterations to solid content through trial and error suggested the efficiency of filtration could be improved under the right polymer conditioning. In order to promote the most efficient separation of solid material from the filtrate, a determination of the *optimal dosage* of additives was required. To ensure results could be easily and accurately replicated modification to the raw sediment was also needed.

3.4.1 Slurry

To establish an optimal dosage of the additives, the sediment was diluted with the addition of water taken from the BH WWTF active stabilization basin in order to create a slurry. For each trial, the raw sediment was diluted to a solid content of between 0.98 and 1.1%. This modified sediment was henceforth referred to as '1 % slurry' and used as the base material for all subsequent tests. The 1% solid content was chosen based on a 'worst case' solids content for dredging operations, with similar solid contents being produced during the remediation effort. The sediment was homogenized prior to the addition of the dilution water and weighed to ensure an accurate and consistent solid content percentage was achieved.

Characterization testing was performed on the 1 % slurry in order to identify any chemical or physical changes which may have deviated from the original material upon dilution. Characterization was accomplished through the same suite of tests, which were performed on the undiluted sediment, and which the methodology for has already been discussed in this thesis (with the exception of the settling time discussed for reduction potential). Tests completed on the 1% slurry are identified in Table 3.1.

Table 3.1: Tests completed on BH 1% slurry.

Physical Analysis	Chemical Analysis
Grain Size	pH
Moisture Content	Zeta Potential
Solid Content	Metal Analysis
Organic Fraction	Reduction Potential (E_H)
TSS	
Particle Concentration	

3.4.2 Chemical Additives

Sediment samples were sent to Bishop Water Technologies (Renfrew, ON) to identify a capable polymer or coagulant, which would promote separation and flocculation of the material. Two additives were identified based on the chemical properties of the raw sediment. Sediment was conditioned with varying amounts of each additive at Dalhousie University, in order to determine an optimal dosage (the dosage which resulted in the highest quality filtrate).

Analysis by Bishop Water Technologies determined that a two-step process would likely be required to efficiently promote flocculation of the solid material. The two additives identified were a water-soluble cationic polymer (Solve 9244) and a flocculating agent (Solve 7118). As recommended by the manufacturer and Bishop Water, the polymers were diluted from their initial concentration using Milli – Q water to 0.5% volume for Solve 9244 and 1% for Solve 7118. Following this dilution, an analysis was conducted to determine the chemical properties (pH and zeta potential) of each additive. This examination was done for both additives in their pure (but diluted) state, as well as after their addition to the 1% slurry (both individually and combined).

3.4.2.1 Bench-Scale Conditioning Test

To establish an optimal polymer dosage, sediment was conditioned via the addition of the two chemicals in varying amounts through trial and error. For the initial trial, precisely 30 mL of 1% slurry was transferred to a 50 mL plastic centrifuge tube. Both Solve 7118 and Solve 9244 were added to the slurry in sequence in various amounts as well as in the reverse order, or mixed prior to treatment. The tubes were then sealed and mixed thoroughly

allowing for the additives to activate and integrate with the particulate matter. Upon mixing, the samples were situated vertically in a holding tray, and the sediment (now amassed as flocs) was allowed to settle out of suspension (Figure 3.4), with the duration of settling monitored for each sample. Following 10 minutes of sedimentation, the clarity of the supernatant was observed visually. The rate of sedimentation and supernatant clarity were used as an indication of the effectiveness of the dosage. Dosages which consistently showed improvement in terms of floc size and supernatant clarity relative to the untreated slurry were selected for further chemical and physical analysis. The initial trial consisted of 25 individual dosages (repeated three times), the concentrations of which can be seen in Appendix 2.

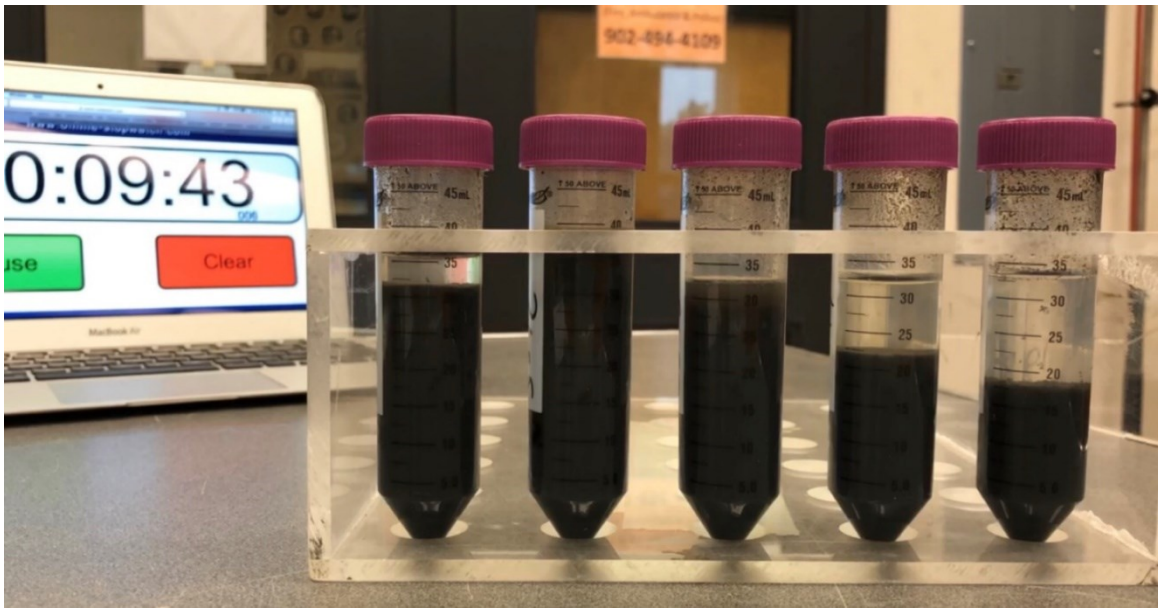

Figure 3.4: 5 of the initial trials to determine influence of additives on the 1% slurry with timer and variation in supernatant quality visible.

3.4.2.2 Jar Testing of Conditioned Sediment

Following the bench-scale tests described above, the samples which showed the greatest improvement in terms of the appearance of the supernatant as well as the rate of sedimentation of the conditioned sediment (compared to the raw slurry) were selected for further analysis. Nine samples were determined to have been positively affected to the degree in which they warranted a more comprehensive analysis of both their chemical and physical properties using jar testing.

For these jar testing trials, 200 mL of the prepared slurry was homogenized in a 500 mL beaker via a Phipps and Bird PB 700 jar testing apparatus, by mixing at 300 rpm for 10 minutes. The volume of coagulant, Solve 7118, which was equivalent in percentage to that used during each corresponding small scale sample was then introduced to the slurry and mixed for a further 3 minutes at 300 rpm. The coinciding volume of the cationic polymer (Solve 9244) was then added to the sample. The combined polymer/slurry solution was mixed at 270 rpm for 1 minute to allow for thorough integration of the polymer with the slurry, in accordance with ASTM International (2019a) method 2035. The jar tester was then slowed to 50 rpm to encourage flocculation. The visual clarity of the supernatant was observed after 5, 10, and 20 minutes. Following each observation, 20 mL of supernatant was decanted from the top of each sample via 5 mL pipette for analysis. Care was taken not to disturb the flocculated sediment during this extraction. The particle size of the flocculated sediment was measured for each trial (discussed in Section 3.6.1). This test was performed three times with each of the chosen dosages (as well as the untreated raw slurry) with identical steps being performed for each trial (30 in total). Figure 3.5 shows five of the trials performed during this stage of the investigation.

Figure 3.5: Jar test on 4 of 9 selected dosages (JT 6 – 9) and raw 1% slurry.

The supernatant which was sampled during the jar test trials was subject to both chemical and physical analysis. Metal concentrations, TSS, particle concentration, and particle (grain) size was performed on each sample pursuant to the steps outlined in Section 3.3.

3.5 GEOTEXTILE FILTRATION AND DEWATERING

Filtration tests using the GT - 500 geotextile were completed at three different "scales" to either aid in determining the optimal additive dosage, or to develop a more comprehensive understanding of the sediment filtrate and how it changes during treatment. Chemical and physical analysis was completed on the filtrate, as well as filter cake produced during the trials.

3.5.1 Bench-Scale Rapid Dewatering Test (RDT): 200 mL Test Volume.

To further identify the concentration of the additive dosage which yielded the best result, the nine concentrations which were found to be most promising (and which were analyzed during the jar test) were subject to filtration using the GT - 500 geotextile (see Table 3.2). A bench-scale rapid dewatering test (RDT) was conducted in accordance with TenCate industry specifications (TenCate Corporation, n.d.a).

Table 3.2: Additive dosages selected for Jar and Geotextile tests. Note samples 3 and 9 were conditioned with identical additives (9 combined prior to mixture with 1 % slurry).

Sample Number	**9244**		**7118**	
	% (Diluted)	ppm (Undiluted Polymer)	% (Diluted)	ppm (Undiluted Flocculent)
1	6.67	333	3.33	333
2	10.00	500	3.33	333
3	5.00	250	5.00	500
4	6.67	333	5.00	500
5	8.33	417	3.00	300
6	8.33	417	5.00	500
7	10.00	500	3.00	300
8	10.00	500	5.00	500
9	5.00	250	5.00	500
Untreated	0	0	0	0

The bench-scale RDT apparatus was comprised of a 150 mm diameter circular piece of the GT-500 geotextile, which was inserted into a 150 mm polypropylene funnel. The lower opening of the funnel was placed in a 250 mL PYREX Erlenmeyer flask to allow for the collection of filtrate (Figure 3.6). During the test, 200 mL of the slurry-polymer mixture (or untreated slurry for the control sample) was poured into the funnel, and allowed to drain through the geotextile. During filtration, the filtrate was collected in the Erlenmeyer flask, while the filter cake was allowed to accumulate on the geotextile.

Following the completion of each trial, the filtrate and filter cake were analyzed for physical and chemical parameters which are discussed below.

3.5.1.1 Filter Cake Moisture Content

During the RDT, the filtrate was allowed to collect for 600 seconds, after which the funnel (containing the geotextile) was removed from the flask. Two samples of filter cake (approximately 40 g wet), which had amassed on the geotextile were carefully removed from each filter to ensure no external pressure was placed on the sediment. The samples from each trial were processed in accordance with ASTM International (2019b) to determine the moisture content of the filter cake.

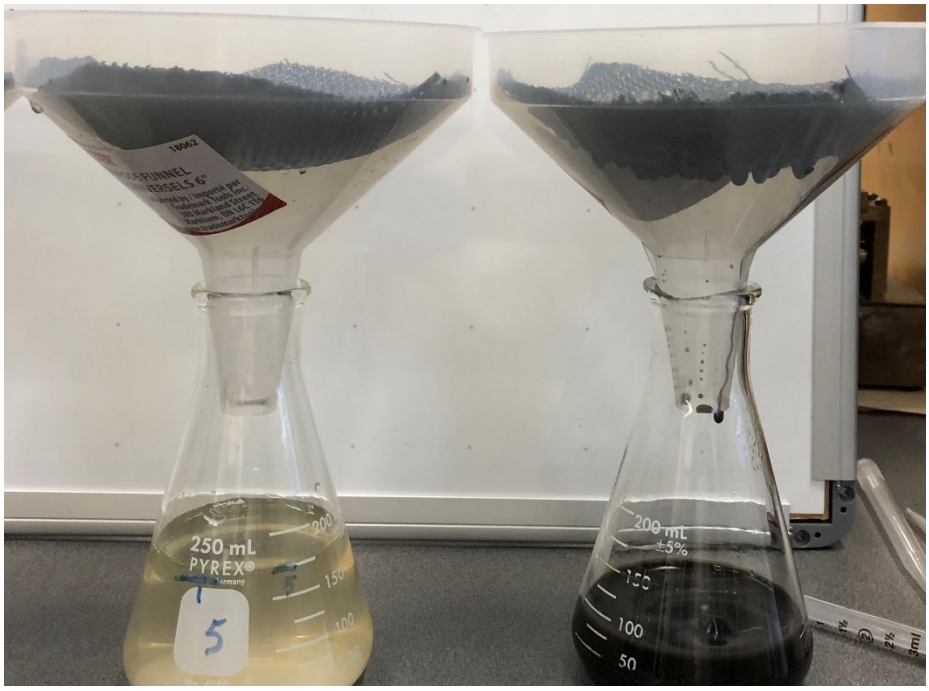

Figure 3.6: Bench scale dewatering trial of raw and treated slurry.

3.5.1.2 Filter Cake Metal Concentration

X-Ray fluorescence (XRF) was used to determine a qualitative metal concentration in the filter cakes. Samples of air-dried sediment were milled into a fine powder in preparation for analysis. The samples were placed in plastic sample holders and were sealed with cellophane. The samples were then transported to Acadia University where they were analyzed via a Panalytical Epsilon 1 XRF measurement device which was calibrated to detect elements frequently found in lake sediments. Each sample was processed three times with the dried sediment disturbed between each trial. The redundant analysis was done to circumvent any potential nugget effect influence, which may have taken place (Gauthier, Burke, & Leclerc, 2012). This method was expressly used to compare the metal concentrations in the filter cakes produced during the determination of the optimal dosage (Chapter 4). The merits of XRF analysis have not been definitively proven at the time of this thesis, and as such, the concentration results were not considered to be quantitatively accurate for use in determining reduction potential during dewatering. Nevertheless, relative qualitative analysis was considered, as the method was both fast and inexpensive.

3.5.1.3 Filtration Rate

The rate of filtration for both conditioned and untreated samples was measured at predetermined time increments during the bench-scale RDT. Filtrate volume measurements were recorded at 60, 120, 300, and 600 seconds for conditioned samples, with an additional measurement taken at 3600 seconds for untreated samples. A time of 600 seconds was selected as the maximum allowable filtration time for conditioned samples, as there was no measurable increase in volume following this period.

Measurements were determined via the stamped volume markings on the PYREX flask (Accurate to within 5% of the shown value).

3.5.1.4 Filtrate Quality

Filtrate collected during the bench-scale RDT trial was analyzed to determine the quality, and in turn, the effectiveness of the polymer in an attempt to find the optimal dosage (OD). For each trial, 50 mL of filtrate was collected immediately following the 600 seconds allotted for accumulation. TSS, pH, particle concentration, particle size, and metal concentration (both dissolved and total) were determined using the analytical methods outlined in section 3.3.

3.5.2 Bench Scale RDT: 4000 mL Test

Based on the measurements yielded during the bench-scale 200 mL RDT experiment, the optimal dosage of both chemical additives was determined. This dosage was applied to all future tests involving the geotextile filtration. A larger-scale test was developed to determine how the geotextile would behave under more realistic conditions, including increased flow volume and pressure, as well as filter cake formation.

The bench-scale RDT test was modified to determine the influence that the filter cake had on both filtrate quality and the rate of filtration. Modification to the funnel used for the initial RDT was required due to the increased volume of sediment which accumulated on the filter. The addition of an acrylic collar (Figure 3.7) allowed for the uninterrupted collection of the larger amount of particulate matter associated with an increased number of samples. Spacers were inserted between the funnel and Erlenmeyer

flask to prevent any change in filtration caused by increased mass and thickness of the overlying filter cake (due to the formation of an airtight seal not present in real-world conditions).

Twenty 200 mL samples of Boat Harbour 1% slurry were prepared using the methods discussed previously. Conditioning was applied to each sample via the addition of the optimal additive dosage. The first 200 mL sample was poured into the funnel and allowed to drain through the geotextile with the filtrate being collected and flow rate identified using the identical method implemented to determine the initial effect of the polymer. Following a collection period of 600 seconds, the PYREX Erlenmeyer flask which was used to collect the filtrate, was removed and the filtrate extracted for analysis.

The funnel then was placed in a clean Erlenmeyer flask, and a subsequent 200 mL sample of optimal dosage conditioned slurry was poured on to the now soiled geotextile filter. The filtrate was allowed to percolate through the previously established filter cake for a further 600 seconds before again being removed for analysis. The time allowed for filtration prior to the replacement of the flask was increased at the 5^{th}, 10^{th}, and 15^{th} trials (to 1200, 1800, 2400 seconds respectively) to allow for the filtrate to pass through the previously established cake. This procedure was repeated for a total of twenty trials, or a total slurry volume of 4 L. The filtrate of each 200 mL sample was analyzed individually following the methods previously outlined. The filter cake was sampled for moisture content immediately following the final trial, and again after 24 hours of settling.

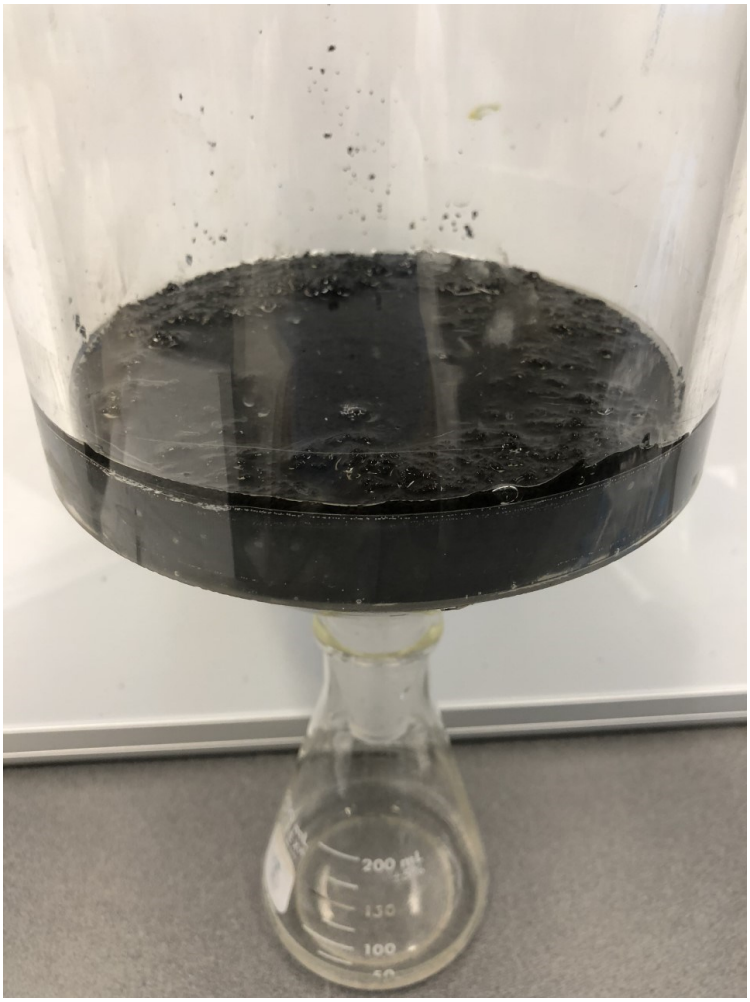

Figure 3.7: Modification to the RDT funnel apparatus. The addition of a 6" collar was required to accommodate the 20 x 200 trial.

3.5.3 Geotextile Bag Filtration Field Trial

A field test using a specially prepared geotextile bag was conducted to test the performance of the geotextile when subject to increased pressure, as well as to examine the three-dimensional effect of the fabric on filtration. Head was increased as a means of raising the pressure on both the geotextile and the accumulated filter cake.

3.5.3.1 Geotextile Bag Properties

Small scale geotextile containment vessels (bags) were acquired from Bishop Water Technologies for field analysis. The bags were woven from the same geotextile material (GT - 500) used previously during the bench-scale analysis. The bags were square with an average side length of 55 cm (±5cm) and stitched together along three of the sides (folded along the remaining side). A 3" ABS female adapter was fitted to one side (the de facto top) of the bag by the manufacturer. This opening was placed in the center of the bag allowing for the input of material. Figure 3.8A shows a bag which has been filled with sediment following the field trial.

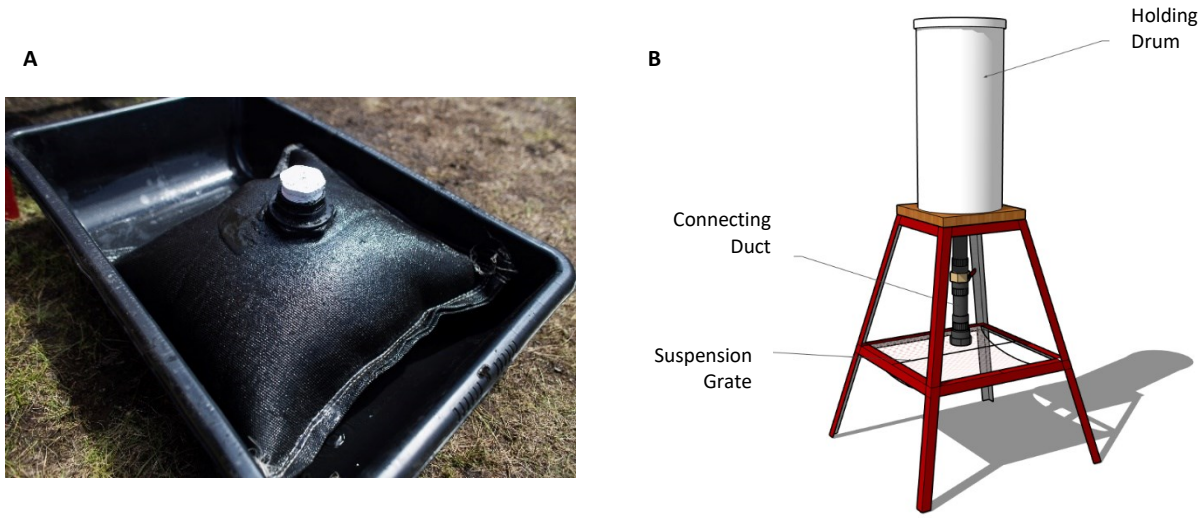

Figure 3.8: A - Field scale geotextile bag immediately following sediment filtration inside catchment basin, B – Annotated interpolation of the field scale geotextile gravity pump (missing catchment basin).

3.5.3.2 Setup and Construction of Apparatus

The device used during the field-scale dewatering trial was designed and constructed at Dalhousie University. The apparatus consisted of four distinct components; a holding drum, a connecting duct, a means of suspending the geotextile bag, and a filtrate catchment basin (Figure 3.8B).

A cylindrical plastic drum measuring 93 cm in height with a 22 cm radius was used to hold the slurry prior to geotextile filtration. The drum was secured atop a steel and wooden frame, resulting in a maximum height at the top of the drum of 170 cm. A 1.5" diameter ABS pipe and flow release valve were fastened to the bottom of the drum. The pipe was stepped up to 2 inches and connected to the bag via a quick release threading system allowing for easy replacement between tests.

The geotextile bag was placed on a PVC net which was fastened to the steel frame at a height of 30 cm above the base. The net was secured in such a manner that it would stretch and contract in relation to the weight of the material that it was bracing. This flexibility allowed for the geotextile bag to remain supported throughout the trial and would limit any influence on filtration (i.e., undue pressure or squeezing of the bag), while still allowing the filtrate to sluice through the geotextile unabated. Below the frame, a 140 L catchment basin was installed in order to better control the output during the trial. The catchment basin was used to allow for a more accessible/ controlled means of sampling the filtrate during the initial surge produced when the control valve was released. An additional 2" release valve was attached to the low point of the basin and connected to a 10 m hose in

order to drain the surplus filtrate. Prior to the test, a field-scale geobag was connected to the drum via the connecting pipe, and the release valve was set to the closed position.

3.5.3.3 Test Procedure

The procedure implemented during the field scale dewatering test was a 5 stage process, designed to be easily repeated. The first stage involved the preparation of a large quantity of 1% slurry (i.e., to be consistent with the bench-scale work described previously). Approximately 13.6 kg of raw sediment was mixed with BH water taken from the active stabilization basin to produce 100 L (for each trial) of the 1% slurry. Both water and sediment were added to the holding drum and homogenized via an electric drill fitted with a stainless steel mixing rod. The slurry was continually mixed at approximately 50 rpm to keep the particulate matter in suspension prior to the addition of the optimum additive dosage.

The second stage of each trial involved the conditioning of the slurry with the optimal dosage of the flocculating agent (*Solve 7118*) with a volume corresponding to the 100 L sample size. The additive was integrated into the slurry by the mixing rod at a rate of approximately 300 rpm for 2-3 minutes to ensure homogenization occurred. The cationic polymer (*Solve 9244*) was then added and stirred at a rate of 300 rpm for between 1-2 minutes, or until flocs were visible, followed by 5 minutes at a reduced speed of approximately 50 rpm to induce further flocculation.

Stage three of the field test began following the formation of visible flocs in the holding drum (Figure 3.9A). Gentile mixing (approximately 50 rpm) of the flocculated material was continuous during this phase, as the material had a propensity to settle out of

suspension (Figure 3.9B). During this stage, the flow control valve on the connecting duct was set to the open position, and the slurry was allowed to drain into the geotextile bag.

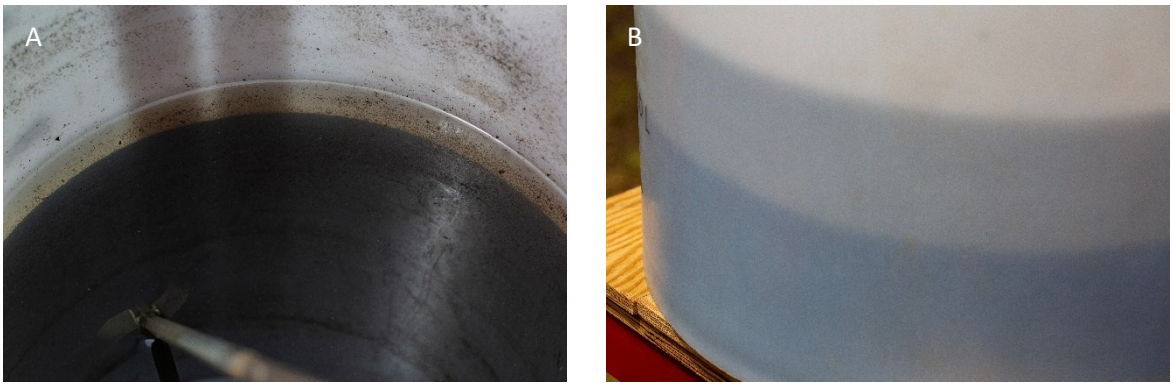

Figure 3.9: A - The formation of flocs following optimal conditioning, B - The settling of flocs in the drum as evident by the change in colour (lighter shade = supernatant, darker shade = settled material).

After the contents of the drum were expelled, the flow control valve was closed. The drum was subsequently refilled using the same method, and the procedure was repeated until the bag was filled with sediment. During the field scale RDT experiment, a total of 200 L of slurry was filtered through the geotextile bag.

The filtrate was recovered at predetermined time intervals during the field experiment (see section 5.3). At each desired interval, sterile plastic centrifuge tubes were placed below a corner of the bag to collect approximately 50 mL of filtrate as it percolated through the geotextile. The filtrate was then analyzed using the same criteria as the bench-scale trials. The field-scale bag was then allowed to dewater for 24 hours before dissection, with moisture content and solids content determined using the same methodology as implemented during the 20 x 200 RDT. Additional MC and SC measurements were taken following 48, 168, and 336 hours of settling.

3.6 FURTHER ANALYSIS OF FILTRATE AND FILTER CAKE

Analyses ancillary to the chemical and physical properties which were discussed in section 3.3 (and applied in section 3.5) were implemented in order to identify mechanisms responsible for metal migration during geotextile filtration. Understanding the behaviour of the flocculated material during filtration was necessary in order to identify any possible means for contaminant transport to occur.

3.6.1 Floc Size

The cohesive strength of the flocs produced from the optimal polymer dosage created an issue in determining grain size. The flocs which were produced via the treatment of the 1% slurry with the optimal dosage of additives were found to be too large for the flow imaging technique implemented previously. Additionally, removal of the flocs from the saturated environment in which they formed resulted in deformation and grain diameters not consistent with 'in situ' (initial) size and shape (Figure 3.10). The grains were found to have a high propensity to break apart or clump together upon disturbance and therefore, an alternative method of determining their size was required.

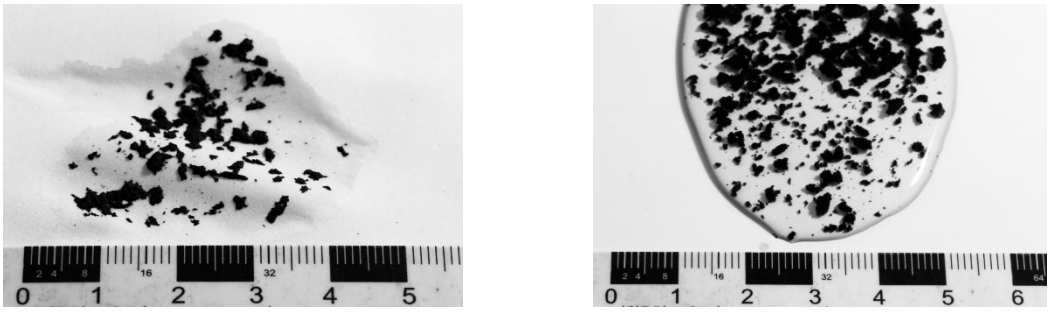

Figure 3.10: Comparison of the deformation of flocs through drying.

To determine the grain size of the flocs, a sedimentation column was constructed out of a 6.35 mm thick transparent acrylic sheet. The column was square in cross-section with each side measuring 50.8 mm (internal), with a height of 60 cm, and having a volume equal to approximately 1.5 L (Figure 3.11A). The column was placed in front of a white background to ensure high contrast between the translucent water and supernatant and the relatively dark-coloured flocs.

Prior to floc size analysis, 1.2 L (80 % of the volume) of water was poured into the column. A 200 mL sample of 1 % slurry was conditioned with the optimal additive dosage via the jar testing procedure outlined in section 3.4.2. The treated material was then poured into the column, and the flocs settled to the bottom. A digital camera was set up to record the flocs as they descended through the water column (Figure 3.11B). The camera was equipped with a polarizing filter to eliminate reflective glare from the acrylic.

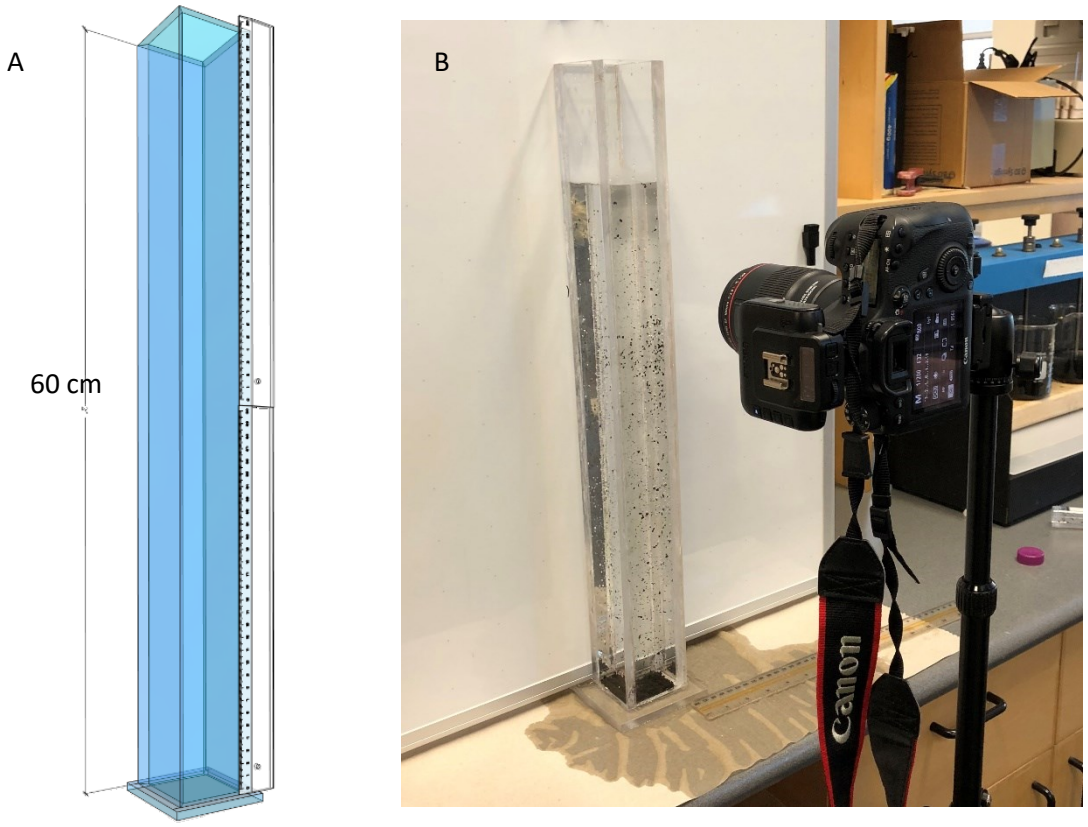

Figure 3.11: A – Rendering of sedimentation column, B – Flocs descending through the water column while being photographed.

The images which captured the settling of the flocs were analyzed using the software 'ImageJ,' the capabilities of which with respect to grain size analysis have been discussed by Igathinathane et al. (2008). Prior to analysis, the images were processed to accentuate the contrast allowing the software to more accurately differentiate between individual flocs. The software analysis was able to produce a qualitative (with respect to the extent of the image field of view) determination of the grain size for all flocs which appeared in a given image. As this analysis was only meant to provide a qualitative idea of the grain size produced by the optimal additive dosage, each floc was assumed to be elliptical in shape. Flocs were measured along the major and minor axis, and the results were recorded in a spreadsheet via the software. The test was repeated for six images for

each of two trials, with consideration taken to choose images which contained various concentrations of flocs. The major and minor axis values were then averaged to yield an estimate of the floc size as it exists prior to filtration.

3.6.2 Identification of Particulate Matter

The filtrate collected during the geotextile trials (both field and bench-scale) contained small amounts of particulate matter. Analysis of this material was conducted to determine any changes which may have occurred throughout the dewatering trials, and which may have an effect on contaminant (metal) migration. Digital imaging via scanning electron microprobe (SEM) was completed on samples taken throughout the conditioning and dewatering process in order to discover any changes which may occur over the course of the treatment.

3.6.2.1 SEM

Scanning electron microscopy testing was conducted on untreated slurry, conditioned sediment (flocs), filter cake, and samples of particulate matter which were isolated from the filtrate. This analysis was done in order to help determine any identifiable surface characteristic of the particulate that passed through the filter cake. Variation in the elemental composition of the sediment during the four stages of filtration, which might suggest a propensity for a given fraction (either organic or inorganic) to flocculate more effectively than the other during treatment, was also considered.

The analysis was completed at the Clean Technologies Research Institute's SEM facility via a Hitachi S-4700 scanning electron microscope. Prior to analysis samples were

prepared in accordance with ASTM International (2002) method E – 1829. Samples were dried at 105 °C for 24 hours before being ground into a powder and homogenized. Following initial preparation the powder was then adhered to a carbon-coated double-sided tape, with the reverse side attached to an aluminum mounting stub. A 20 nm thick gold-palladium sputter coating was then applied via a Leica EM ACE200 vacuum coater in order to increase the conductivity of the sample. Figure 3.12 presents a coated stub prior to SEM analysis. Each specimen was then inserted into the SEM and analyzed in accordance with ASTM International (1998) method E1508 using an accelerating voltage of 20 kV. Peak intensities, which corresponded to gold and palladium were removed, and the weight percentage of the remaining elements was normalized to compensate for the loss in mass. The analytical data and images produced via the SEM can be seen in section 5.3.2, along with a discussion of the findings.

Figure 3.12: Example of sediment mounted to stub for SEM analysis (diameter = 12.5mm).

CHAPTER 4: CHARACTERIZATION AND OPTIMAL DOSAGE

4.1 PREAMBLE

This chapter presents the results and discussion pertaining to both the initial sediment characterization and sediment conditioning with the chemical additives. Initial characterization of both the untreated sediment and water is first introduced to better understand the original material which was to be treated. This characterization includes both index properties as well as contaminant (i.e., metal) concentrations, determined for the untreated water and sediment. The results of the bench-scale sediment conditioning tests which were used to identify the optimal dosage are also presented with a discussion outlining the rationale for the selection.

4.2 SEDIMENT AND WATER CHARACTERIZATION

Effluent derived sediment extracted from the Boat Harbour stabilization lagoon was characterized in accordance with the procedures outlined in Chapter 3. The chemical and physical index properties determined for both water and sediment sampled directly from the lagoon are presented below. Following the initial characterization, both water and sediment metal concentrations are presented and discussed.

4.2.1 Initial Characterization

4.2.1.1 BH Water Analysis

Table 4.1 presents a summary of the chemical and physical properties (pH, E_H, zeta potential, TSS, particle concentration, and particle size) determined for the BH stabilization basin water. The pH of the lagoon was found to be close to neutral (to slightly basic), ranging between 7.5 and 7.9. The oxidation-reduction potential (E_H) of the surface water measured in the laboratory averaged + 375 mV. During this measurement, the probe had to be left undisturbed for approximately 10 minutes in order to achieve equilibrium. The value suggests an oxidizing environment exists throughout the water column; however values ranging from as low as + 45 mV to over + 400 mV were recorded during the 10-minute period, and as a result, some variation to the extent of the potential was apparent. Difficulties in measurement occurred during all redox measurements, and as a result, the averages reported may be better considered an approximation.

Zeta potential of the lagoon water was found to be highly negative, with values measured between - 21 mV and - 25 mV. The strong negative charge detected in the water samples corresponded with the amount of solid material which is stable in suspension (section 4.2.1.3). Total suspended solids in the lagoon water were present at an average concentration of around 38 mg L^{-1}. Chemical properties identified above are explored in detail in section 5.6 of the following chapter.

Mean particle size and concentration were also characterized via Micro-flow Imaging analysis. The particle concentration was found to be approximately 120,000 per millilitre, with an average grain size of 8 µm. Results from the initial water characterization

can be seen in Table 4.1. The values generated during the initial water characterization were in agreeance with those identified by Alimohammadi et al. (2019a), regarding water derived from the active stabilization basin.

Table 4.1: Stabilization lagoon (surface) water chemistry.

Property	Average	Range
pH	7.9	7.4 – 7.9
E_H (mV)	+375	+ 345 – + 385
Zeta Potential (mV)	-22	- 20 – - 23
Particle Concentration (# mL^{-1})	122057	120,000 – 125,000
Mean Particle Size (µm)	8.0	7.9 – 8.2
TSS (mg/L)	38	35 – 40

4.2.1.2 Sediment Physical Properties

Sediment samples were found to have a moisture content and solids content averaging 1182 % and 8 % respectively. Prior to grain size analysis conducted via the microflow imaging device, samples were diluted to 1 % and 0.1 % solid content. The average particle diameter was found to be 5.8 µm (silt-size grains) with approximately 80 % of particles finer than 6.8 µm. Figure 4.1 presents the grain size distribution for the untreated sediment.

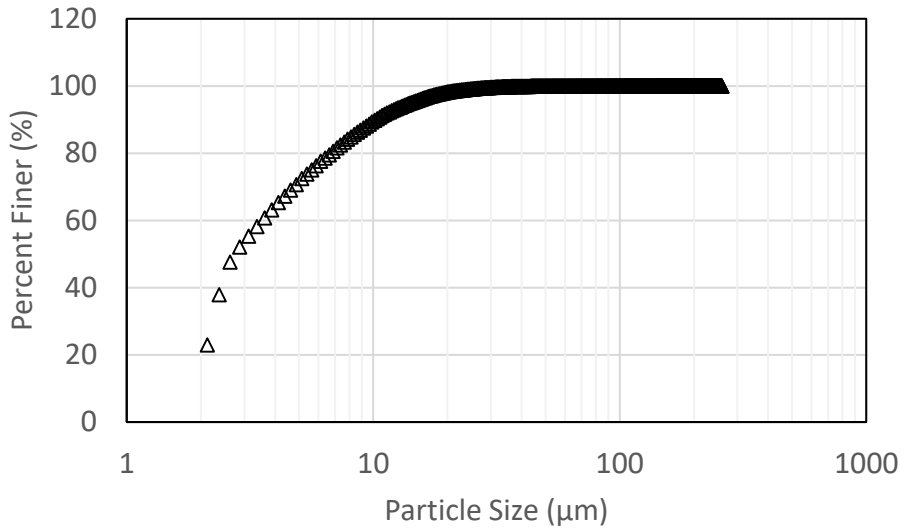

Figure 4.1: Grain size distribution for bulk sample.

The sediment was found to contain an average organic content of approximately 30 % (dry mass). This abundance of organic matter was expected due to the dendritic origin of the effluent and is thought to influence the concentration of metal contaminants through bioaccumulation processes discussed in section 2.3. Table 4.2 presents a summary of the average physical characteristics determined for the stabilization lagoon derived sediment.

Table 4.2: Physical characteristics of untreated sediment.

Characteristic	Ekman Grab Sediment
Mean Particle Size (µm)	5.8
Moisture Content (%)	1182
Solid Content (%)	7.8
Organic Matter (%)	30

4.2.1.3 Sediment Chemical Properties

The pH of the sediment was found to be similar to the stabilization lagoon water, having a slightly basic range, between 7.6 - 7.9. Oxidation-reduction potential (E_H) measurements conducted on the untreated bulk sediment yielded a value of approximately - 268 mV on average (with a range of ± 20 mV following 10 minutes of equilibration). Although it is difficult to confirm in situ conditions (as atmospheric influence may have altered the potential of the sediment upon disturbance during sampling), this result suggests a reducing environment may be present in the basin sediment. Zeta potential of the sediment was found to range from -24 to -26 mV for all dilutions.

4.2.2 Initial Metal Analysis

Metal concentration was determined for both water and sediment sampled from the Boat Harbour Stabilization Lagoon, results of which are presented below.

4.2.2.1 BH Water

All metal concentrations in water were determined via ICP-MS analysis. Water sampled directly from the basin contained total metal concentrations of 46.0 $\mu g\ L^{-1}$ (Cu), 59.0 $\mu g\ L^{-1}$ (Pb), and 758.7 $\mu g\ L^{-1}$ (Zn) on average. The dissolved metal fraction was found to exist at concentrations of 3.5 $\mu g\ L^{-1}$, 34.7 $\mu g\ L^{-1}$, and 246 $\mu g\ L^{-1}$, for copper, lead, and zinc, respectively.

When compared with the total metal load found in the sediment (below), as well as the dissolved fraction in the water, the concentration of metals suggests that the majority of metal contaminants are associated with particulate matter, and therefore can likely be

attributed to the particles present in suspension. Table 4.3 presents the comparison of average total versus dissolved metals found in the basin water.

Table 4.3: Average metals found in the basin water.

	Total Metals (µg L^{-1})	Dissolved Metals (µg L^{-1})	Dissolved Fraction (%)
Cu	46.0	3.5	7.6
Pb	59.0	34.7	58.9
Zn	758.7	246.3	32.5

4.2.2.2 BH Sediment

Metal analyses were completed on the sediment using several techniques. The summary of average total metal concentration in the sediment, as determined by each method can be seen in Table 4.4.

Total metal concentrations found in bulk sediment samples were determined via both ICP-OES and ICP-MS analysis. ICP-OES measurements yielded an average concentration by mass of 124.6 mg kg^{-1} for copper, 82.0 mg kg^{-1} for lead, and 1256.0 mg kg^{-1} for zinc. The ICP-MS analysis yielded average concentrations of 96.9 mg kg^{-1} for copper, 105.8 mg kg^{-1} for lead, and 1162.7 mg kg^{-1} for zinc.

Table 4.4: Summary of metal concentrations in the untreated sediment derived through the two measurement techniques.

	Cu	Pb	Zn
ICP-OES (mg kg^{-1})	124.6	82.0	1255.0
ICP-MS (mg kg^{-1})	96.9	105.8	1162.7

Although some variability was seen between the analytical methods, all techniques measured metal concentration values, which were in exceedance of the sediment quality guidelines outlined by the CCME for the protection of aquatic life (Figure 2.8).

These findings, along with the dissolved concentrations presented for the basin water suggest that the metals which exist in the system are primarily associated with the solid particulate matter (either deposited or in suspension in the basin). The removal of suspended material alongside the deposited sediment during the dewatering procedure would likely result in a significant reduction in the total metals from the system.

4.3 SEDIMENT CONDITIONING

To provide a baseline perspective of the ability of the geotextile to filter the sediment under study, an attempt was made to filter a sample of the effluent derived material using the GT - 500 geotextile. Sediment which had an initial MC of greater than 1100 % (i.e., SC = 8 %) was used for this experiment. Immediately upon pouring the untreated material over the geotextile, the relatively high solids content caused a build-up of sediment on the filter, preventing any further transmission through the geotextile.

As a result of the inability to filter the raw sediment, and based on discussions with consultants involved in the project (Dore, 2018), the sediment was diluted to a SC of 1 % using water extracted from the Boat Harbour active stabilization basin. The 1 % SC material (1 % slurry) was also unable to pass through the geotextile efficiently. Some improvement in the mobility of material was seen, as the dilution resulted in more liquid passing through the filter; however, it also carried a high amount of solid particulate matter with it.

As is common for geotextile tube dewatering projects, the inability of the geotextile to filter fine-grained sediment results in the need for particle size modification via the addition of chemical additives (i.e., polymers). All future trials, including those implemented to identify the optimal dosage of the additives, as well as all dewatering trials using the geotextile filtration techniques outlined in Chapter 3 were conducted on the 1 % slurry material.

4.3.1 Slurry

Analyses were conducted following the addition of the basin water in order to identify any variations which may have been introduced during dilution. The reduction in solids content was shown to have little influence on particle size, zeta potential, pH, or metal concentration (mg kg^{-1}). The organic fraction also remained consistent with that of the undiluted sediment (as it was determined via the dry weight of the material). The solid content was decreased to the desired 1 % for this work. The slurry was found to have a TSS of 13,120 mg L^{-1} on average, and a particle concentration of 1.8 x 10^8 (# mL^{-1}). Of all the characterization measurements conducted, the most significant difference can be seen in the oxidation-reduction potential, which yielded a value of + 375 mV on average. This difference can likely be attributed to the addition of the basin water used for dilution (which had a similar E_H range). This value is therefore not representative of in situ conditions; however, as mentioned in section 3.4, dredging operations during the remediation effort would similarly entrain the basin water with the sediment. As a result, the E_H measurement reported for the 1 % slurry may be considered accurate to the real world conditions upon commencement of the remediation. A summary of the physical and chemical characteristics determined for the 1 % slurry can be seen in Table 4.5. The

properties identified for this material were used as a baseline to compare the effectiveness of all subsequent dewatering and decontamination work conducted for this thesis.

Table 4.5: 1 % SC slurry properties. Used as a baseline comparison for all treated sediment.

Physical Analysis		Chemical Analysis	
Average Particle Size (µm)	*5.8*	pH	*7.65*
Solid Content (%)	*1*	E_H (mV)	*+ 375*
Organic Fraction (%)	*~30*	Zeta Potential (mV)	*- 25*
TSS (mg L^{-1})	*13,120*	Metal Concentration (mg kg^{-1})	
Particle Concentration (# mL^{-1})	*$1.8x10^8$*	Cu	*124*
		Pb	*82*
		Zn	*1256*

4.3.2 Chemical Treatment

Upon dilution to their respective concentrations, the two chemical additives chosen were subject to zeta potential and pH analysis. Solve 7118 was determined to have a positive zeta value ranging between 2.5 mV to 6.4 mV, while the cationic polymer, Solve 9244, yielded a value ranging from positive 84 mV to 100 mV. The pH of the 7118 additive was found to be between 4 and 6, with Solve 9244 having a range from 3 - 4.

The stability of the sediment grains found in the 1 % slurry can likely be attributed to the relatively high negative zeta potential of around - 25 mV (Lu & Gao, 2010). The addition of the cationic polymer (~ + 80 mV) was thought to disrupt this stability and create a surface to which the negatively charged grains would more readily bind, and as a result, encourage rapid flocculation (Betancur et al., 2009). Initial trials using only Solve 9244 resulted in little to no growth in particle diameter, with much of the fine-grained material remaining in suspension. Due to the negative result yielded by the use of only the cationic polymer, dual additive conditioning techniques were considered, as they have been shown to produce significantly larger flocs when dealing with highly stable, fine-grained

sediments (Gregory & Barany, 2011). Although the exact chemical makeup of the two additives is not known, and therefore an exact determination of the processes taking place is not possible, Gregory & Barany (2011) suggest during a dual polymer conditioning, the first additive may produce adsorption sites with a less stable charge, which in turn will encourage increased flocculation.

Zeta potential and pH measurements were taken during and after treatment with the optimal dosage of additive (discussed in detail in the following section). The 1 % slurry treated with only Solve 7118 yielded an average zeta potential of - 15.9 mV and a pH of 7.6. Slurry treated with only the cationic polymer (9244) yielded a zeta measurement of -23.8 on average, and a pH of 7.8. The addition of the combined optimal conditioning treatment (introduced in sequence) altered the charge of the mixture to a value of -18.0 mV, while the pH was reduced to 7.4 (based on the average of three individual tests).

The addition of the first additive (7118) served to reduce the negative charge (bring it closer to zero mV), therefore destabilizing the system and encouraging the particulate matter to coalesce upon the introduction of the cationic polymer (9244). The conditioning resulted in rapid floc growth and a material which was more likely to precipitate out of suspension. As a result of preliminary trials discussed above, both additives were used in sequence during all subsequent research. The identification of the dosage which was most effective is explored in detail below through a series of small scale visual tests and jar testing.

4.3.3 Small Scale and Jar Testing

A small-scale trial and error test was implemented to assist in the initial visual identification of the optimal dosage. Preliminary characterization of the sediment suggested that metal contaminants found in the solution had a propensity to bind to the particulate matter (solid fraction). As a result, an emphasis was placed on floc size and supernatant clarity in the small-scale trials. The eight concentrations (% volume) of the two additives which consistently visually showed the most considerable degree of improvement over the untreated slurry can be seen in Table 4.6. The sample identified as "Jar Test 9" (JT9) was conducted to discern the effect of premixing the additives rather than the two-step process implemented for the other trials. This sample contained an equivalent concentration to that of sample JT3. The concentration of additives used in the small-scale trials can be seen in Appendix 2.

Table 4.6: Additive concentrations selected for chemical and physical analysis.

ID	Solve 9244				Solve 7118			
	mL	%	ppm (.5%)	ppm (raw)	mL	%	ppm (1%)	ppm (raw)
SS4/JT1/GT1	13.33	6.67	66666.67	333.33	6.67	3.33	33333.33	333.33
SS10/JT2/GT2	20.00	10.00	100000.00	500.00	6.67	3.33	33333.33	333.33
SS15/JT3/GT3	10.00	5.00	50000.00	250.00	10.00	5.00	50000.00	500.00
SS18/JT4/GT4	13.33	6.67	66666.67	333.33	10.00	5.00	50000.00	500.00
SS20/JT5/GT5	16.67	8.33	83333.33	416.67	6.00	3.00	30000.00	300.00
SS21/JT6/GT6	16.67	8.33	83333.33	416.67	10.00	5.00	50000.00	500.00
SS23/JT7/GT7	20.00	10.00	100000.00	500.00	6.00	3.00	30000.00	300.00
SS24/JT8/GT8	20.00	10.00	100000.00	500.00	10.00	5.00	50000.00	500.00
SS25/JT9 /GT9	10.00	5.00	50000.00	250.00	10.00	5.00	50000.00	500.00

The concentration of each additive outlined in Table 4.6 was added to 200 mL of 1 % slurry following the procedure outlined in section 3.4.2.2. Supernatant collected at each observation interval (5, 10, and 20 minutes) was tested for TSS, particle concentration, particle size, and metal concentration, the results of which were analyzed to determine the most effective dosage.

Figure 4.2 presents the average particle size found in the supernatant extracted from each of the nine trials. The range of particle size which remained in suspension was similar to that of that found in the untreated sediment; however, some reduction was seen for several of the dosages reducing from 5.8 µm (untreated) to between 2.5 - 3.5 µm for the most promising trails. The majority of the treated material coalesced into flocs, which fell out of suspension before the first measurement. The removal of the bulk of the particulate material through this process resulted in a relatively clear supernatant, in which the size of

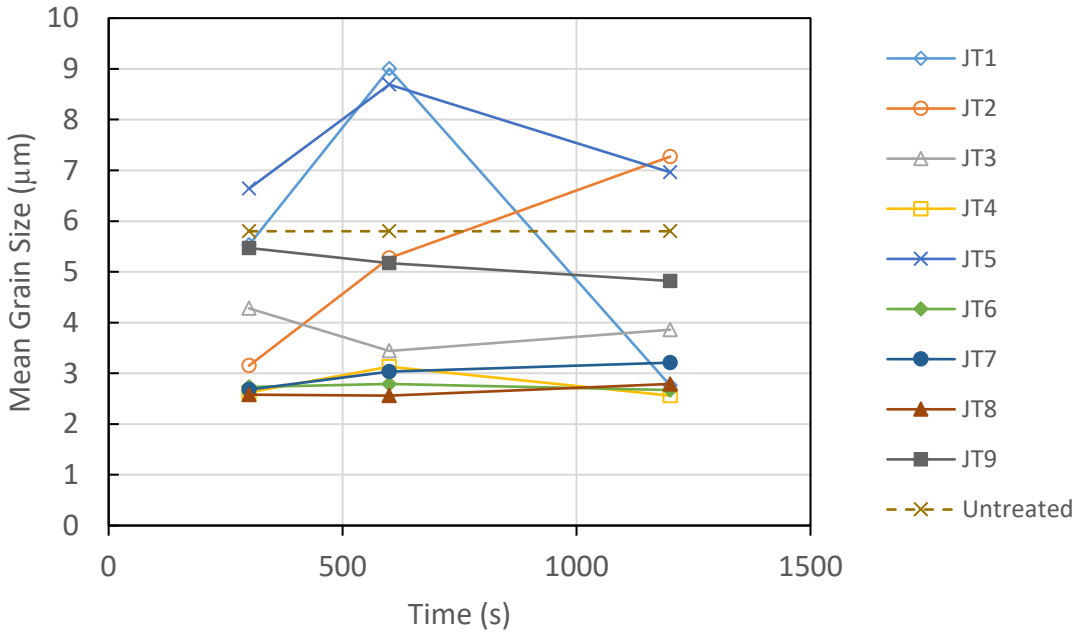

Figure 4.2: Average particle diameter found in jar test supernatant.

the remaining suspended particles stayed generally constant over time. The size of the flocs created during treatment is discussed in section 5.4.

The TSS found in each trial can be seen in Figure 4.3. Little variation was seen between each trial; however, all dosages showed vast improvement in the overall reduction of suspended solids. When compared to the untreated 1 % slurry, a reduction of between 98.9 % and 99.9 % was found for all trials. Solids were reduced from an initial value of 13,120 mg L^{-1}, to between ~ 140 mg L^{-1} to ~10 mg L^{-1} with sample JT3 showing the most significant improvement. Fluctuation with respect to time ranged from limited (80 mg L^{-1}) to nonexistent, as the majority of the particulate matter which flocculated out of suspension during treatment did so immediately, with the remainder being of a small enough diameter to remain in suspension throughout the entire duration of the trial.

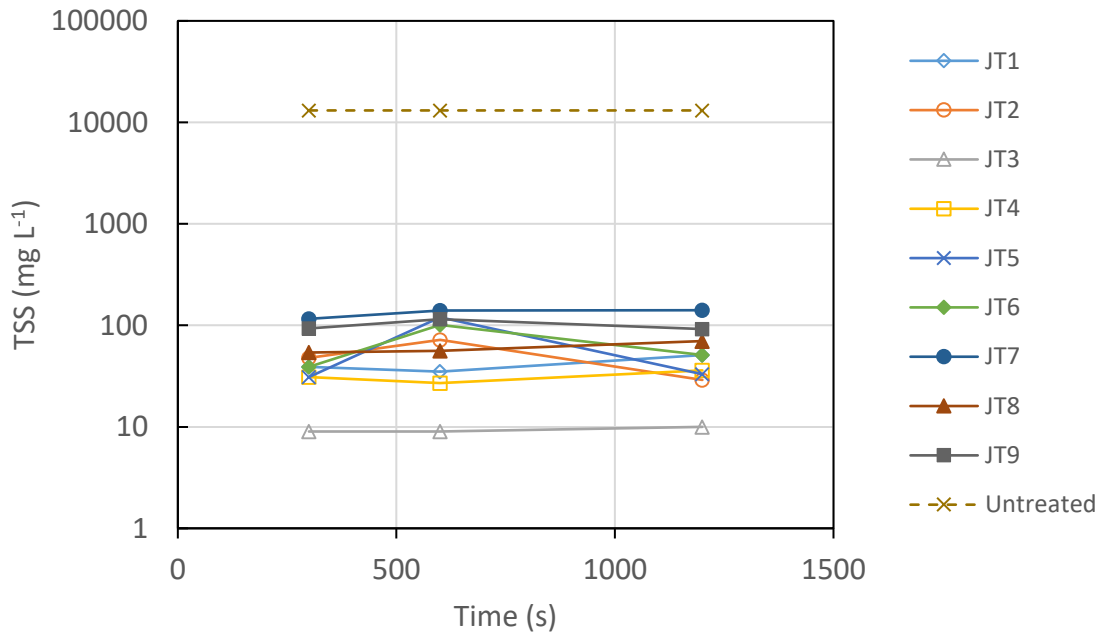

Figure 4.3: Average TSS found in jar test supernatant.

Figure 4.4 presents the concentration of particulate matter found in the supernatant for each trial. Similar to the TSS measurement, the number of particles per millilitre showed a decrease in all trials in excess of 99.1%. Significant variation between each sample was present; however, no clear trend was seen in the concentration, as the number of particles recorded both increased and decreased over the sample period for all nine trials.

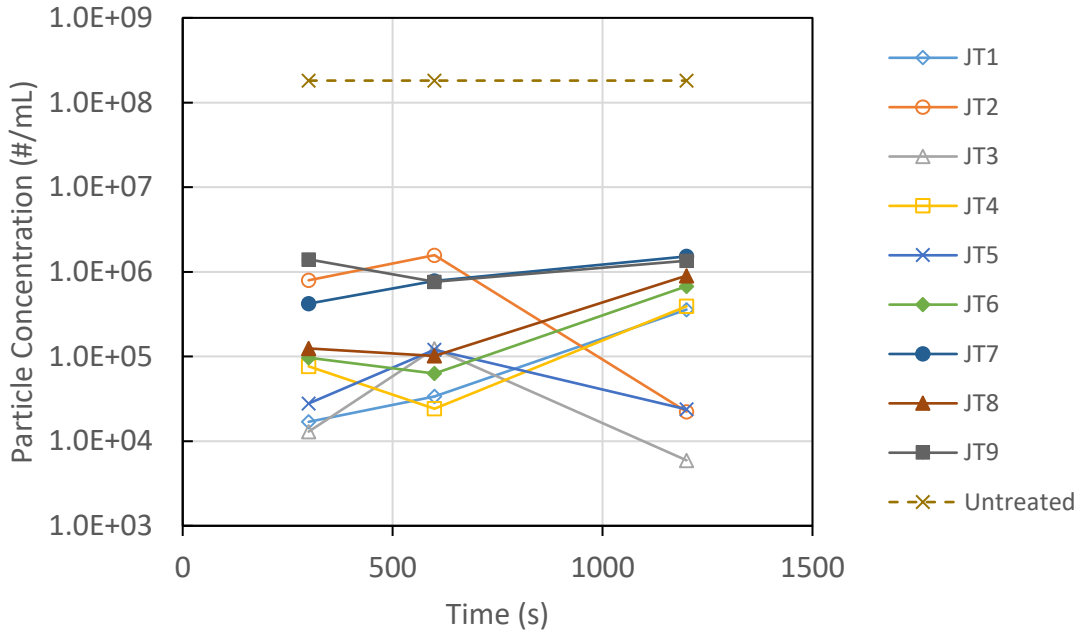

Figure 4.4: Average particle concentration found in jar test supernatant.

Figure 4.5 shows the variation in the total metal concentration found in the supernatant extracted from the jar test samples. Copper concentrations measured in all trials fell to an average of 4.4 µg L^{-1} from an initial amount of 1178 µg L^{-1}. When considering all dosages of the two additives, an average reduction of 99.6 % was seen for this element. Reductions of a similar magnitude were found for both lead and zinc, with corresponding average concentrations falling from 1385 µg L^{-1} (Pb) and 15,750 µg L^{-1} (Zn) to 10.1 µg L^{-}

^{1} (Pb) and 52.6 µg L^{-1} (Zn) following treatment. Measurements taken from samples spanning the duration of the experiment showed little variation over time for all trials.

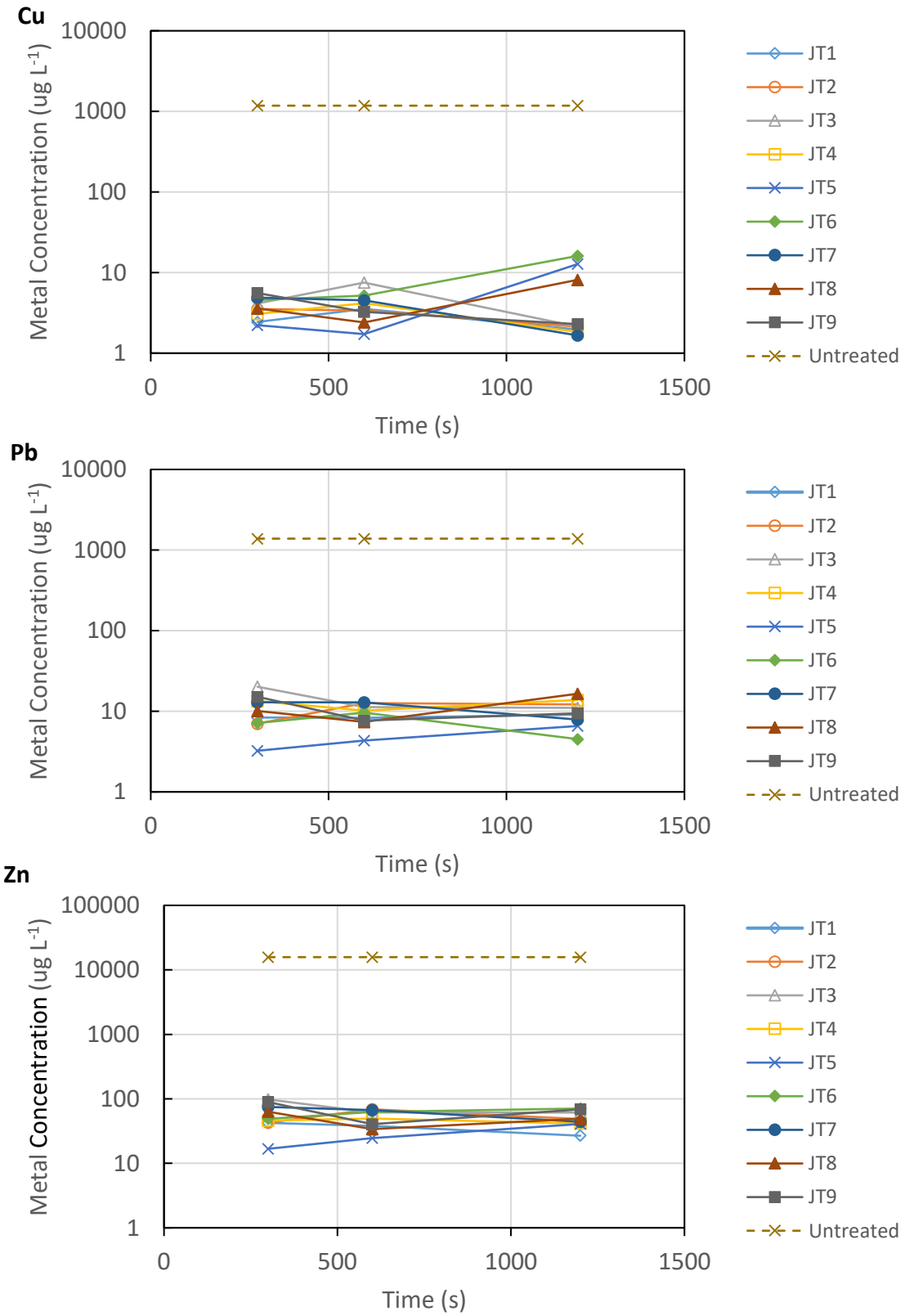

Figure 4.5: Average total metal concentrations found in jar test supernatant.

All polymer dosages selected for the jar test analysis showed vast improvement in supernatant quality when compared to the untreated 1 % slurry. The nine additive dosages which were selected for the trial were effective in reducing the TSS, particle concentration, and total metals, while particles which remained in suspension continued to exist at a persistent diameter. Following analysis of the four parameters considered, no clear measure of additives emerged as the optimal dosage.

To further discern which of the treatments had the most significant improvement on the sediment with respect to geotextile dewatering, the effect of each dosage following filtration via the geotextile was evaluated. The following section reassesses the parameters investigated during the jar test, with an emphasis on the filtrate which passed through the geotextile, rather than the supernatant sampled directly after treatment.

4.4 GEOTEXTILE FILTRATION AND DEWATERING

Filtration using the GT - 500 geotextile was initially completed to assess the impact of each additive dosage on the parameters identified during the jar test procedure. Following identification of the optimal dosage of additives, the test was modified to observe any impact which may occur when filtering a larger volume of material through the geotextile (discussed in Chapter 5). This section outlines the results which were discovered during the analysis of both the filtrate and filter cake produced during the initial trials. Figures are included which represent the data gathered through three repeated tests. Where applicable, statistical data is presented in the form of box and whisker plots (with median and quartiles shown). Also highlighted is the mean value for each parameter, as well as the highest and lowest occurrences represented by the error bars (whiskers).

4.4.1 Bench-Scale RDT: 200 mL Test Volume

The bench-scale rapid dewatering test was implemented to identify the optimal polymer dosage. The nine additive concentrations which were examined during the jar test procedure were each filtered through the geotextile, according to the procedure outlined in section 3.5.1. The filter cake and filtrate produced during each trial were then analyzed with the results presented below.

4.4.1.1 Filter Cake Moisture Content

Figure 4.6 presents the average moisture content of the filter cakes which accumulated during the RDT for each dosage. All trials produced a cake which ranged from 1500 to 1700 percent moisture (with an average of 1578 %). No measurable filter cake accumulated for the untreated slurry, instead the material pooled on the filter once the pores became clogged. When considering the moisture content of the untreated slurry (around 8600 %) the effect of the conditioning on the removal of solid material from suspension becomes evident for all samples. The solids content of the filter cakes was also measured, ranging between 5.6 and 6.2 percent (with an average of 6.0 %), equal to 600 % of the untreated slurry. Similar to the results found during the jar test, no clear optimal dosage was determined, as all trials resulted in drastic improvement when compared to the untreated sample.

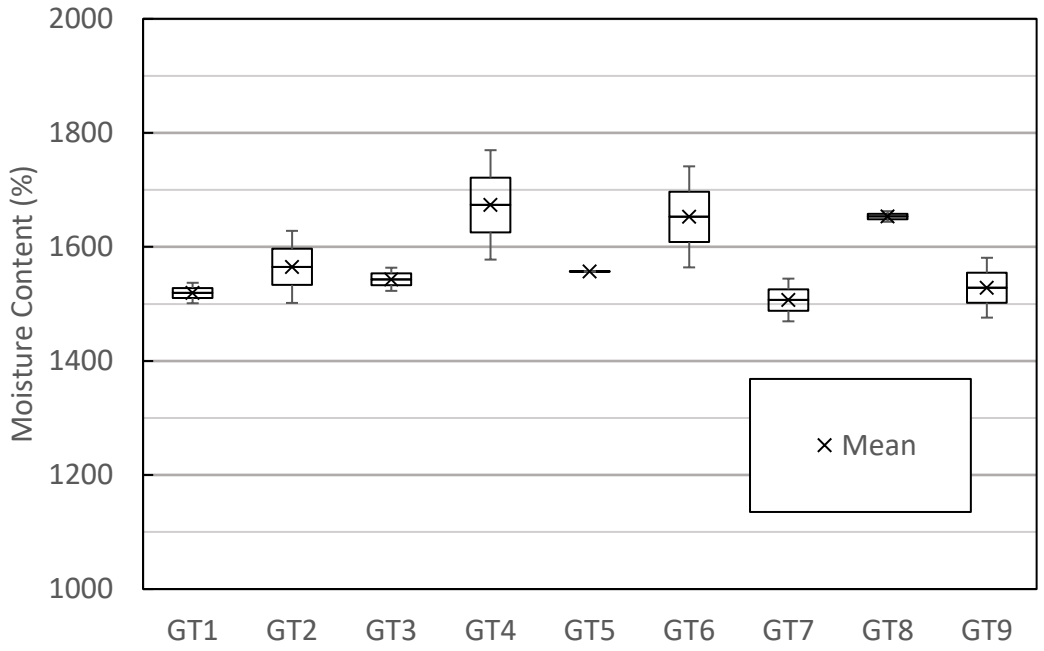

Figure 4.6: Moisture content of filter cakes generated during the optimal dosage identification trials.

4.4.1.2 Filter Cake Metal Concentration

Figure 4.7 shows the average total copper, zinc, and lead concentration found in the filter cakes determined via XRF analysis. Quantitative values were found to be consistently higher than those discovered through ICP techniques. As a result, absolute values comparing the raw sediment to the treated material were not considered relevant for this test; instead, this technique was meant to provide a relative comparison between treatment profiles, in order to identify any variation in reduction potential which may have arisen from a specific dosage.

Mean values for copper ranged between 202.7 and 213.6 mg kg^{-1}, with an average of 209.4 mg kg^{-1} between all trials. Lead concentrations were found to exist in a narrower range, with mean trial values ranging between 78.1 and 87.6 mg kg^{-1}, respectively, with an

average of 82.9 mg kg^{-1}. The amount of zinc present in the filter cakes showed considerably more variability with respect to overall mean concentration, having a range of 1688.5 to 1802.8 mg kg^{-1}, with an average total concentration of 1755.6 mg kg^{-1} when considering all samples. As is evident by the error bars in Figure 4.7, a high level of inconsistency was seen with contamination concentration volume in cakes which were produced using the same additive dosage. Of particular note were erratic levels of zinc found in treatment GT1 and GT2, among concentrations detected from three successive tests, with the broadest margin ranging between 1596.4 and 1776.6 mg kg^{-1}, or a discrepancy of over 10 %.

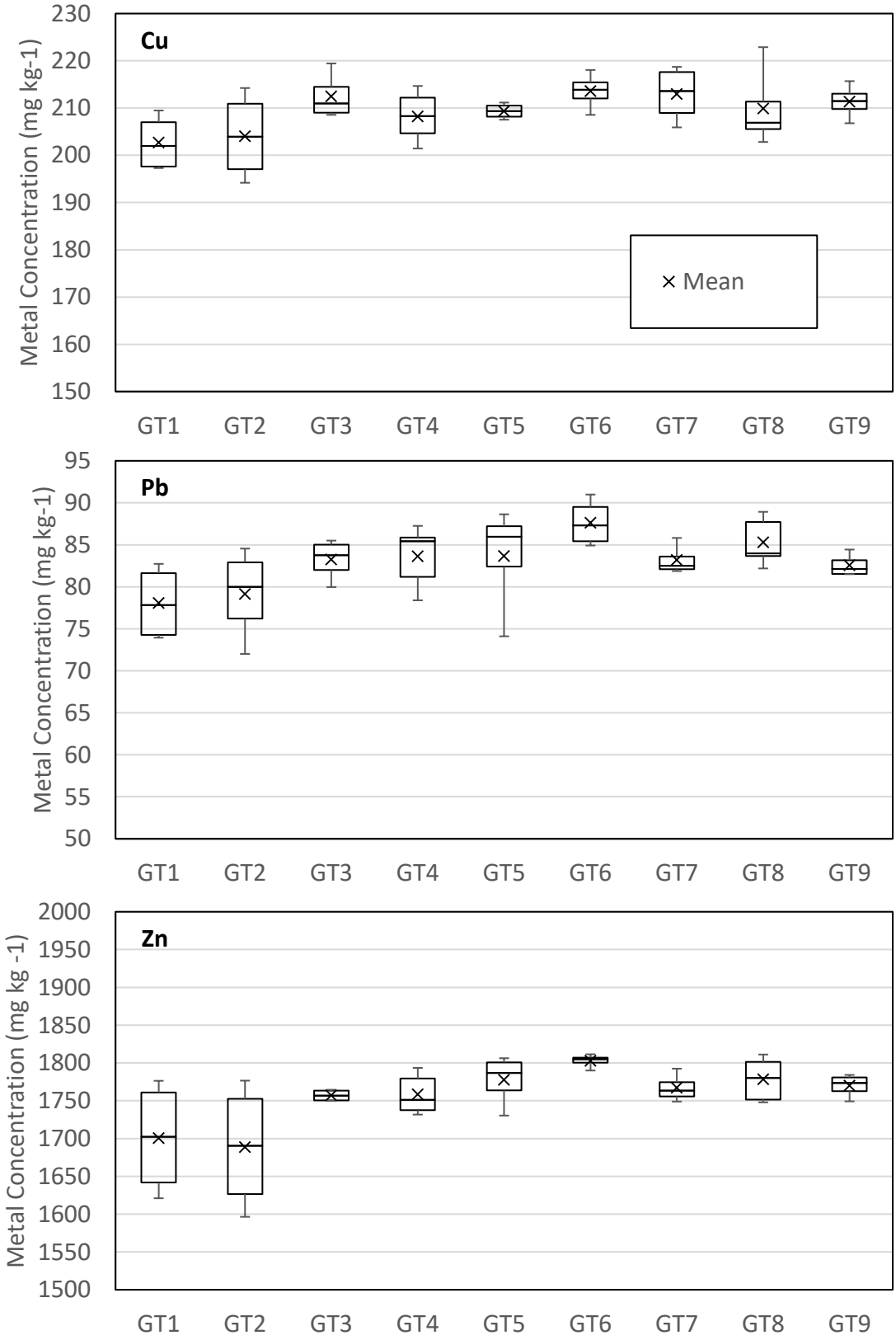

Figure 4.7: Metal concentrations of filter cakes generated during the optimal dosage identification trials (XRF).

4.4.1.3 Filtration Rate and Volume

The rate of filtration was measured for each of the nine additive dosages with average results presented in Figure 4.8. Dewatering volume was shown to be inversely proportional to the elapsed time for all trials, with each reaching equilibrium before 600 seconds. Following this duration, no significant increase in volume was seen in any sample up to 3600 seconds (1 hour).

From the initial input volume of 200 mL, an average of 167.7 mL of filtrate was able to pass through the geotextile during the first 30 seconds of filtration. This average increased to 175.1 mL and 177.1 mL following 5 and 10 minutes of filtration respectively. Some variation was seen with respect to additive dosages, with GT1, GT5, and GT9 filtering at a slower rate than the average. Conversely, dosages GT2 and GT3 passed through the geotextile at a faster rate and produced consistently higher volumes of filtrate when compared to the mean (between dosages).

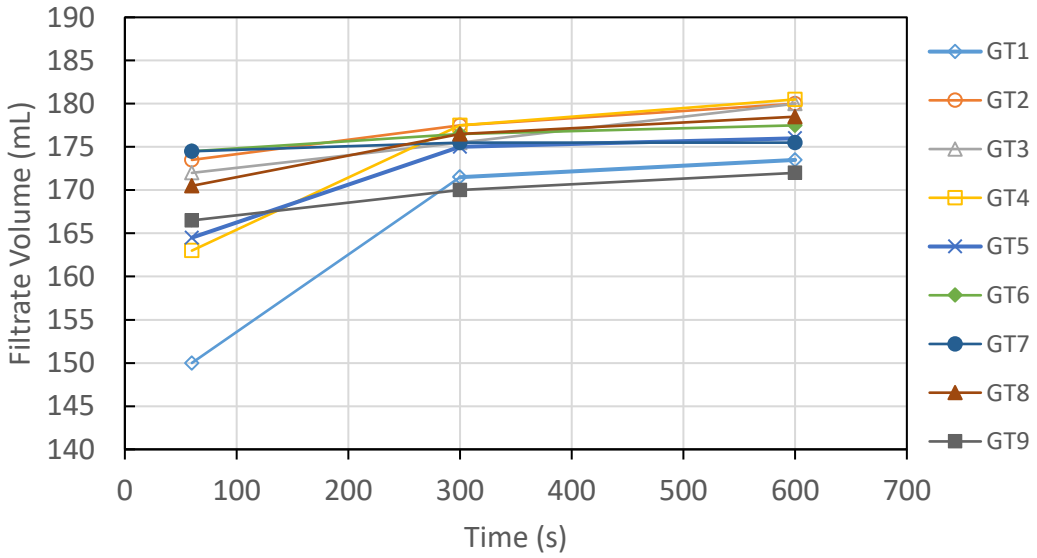

Figure 4.8: Filtration rate measured during the optimal dosage identification trials.

4.4.1.4 Filtrate Quality

Particle size, concentration, and total suspended solids were measured in filtrate samples generated during optimal dosage identification trials. Figure 4.9 presents the average TSS found in each of the samples. A stark contrast exists between trials, with values ranging from a low of 35 mg L^{-1} to a maximum of 193 mg L^{-1}. The results from the TSS test have shown the most significant level of variability when compared to the other parameters measured. Dosages which correspond to GT1 and GT3 consistently yielded the lowest levels of suspended solids (an average of 40 and 35.5 mg L^{-1} respectively), while all other trials produced concentrations which averaged greater than 50 mg $^{-1}$.

Particle size remained relatively constant between 2.5 and 3.5 μm, with an average of 3.2 μm, slightly smaller than that determined for the untreated slurry (5.8). Particle concentrations generally echoed TSS for each of the dosages, with GT1 and GT3 again yielding the lowest values.

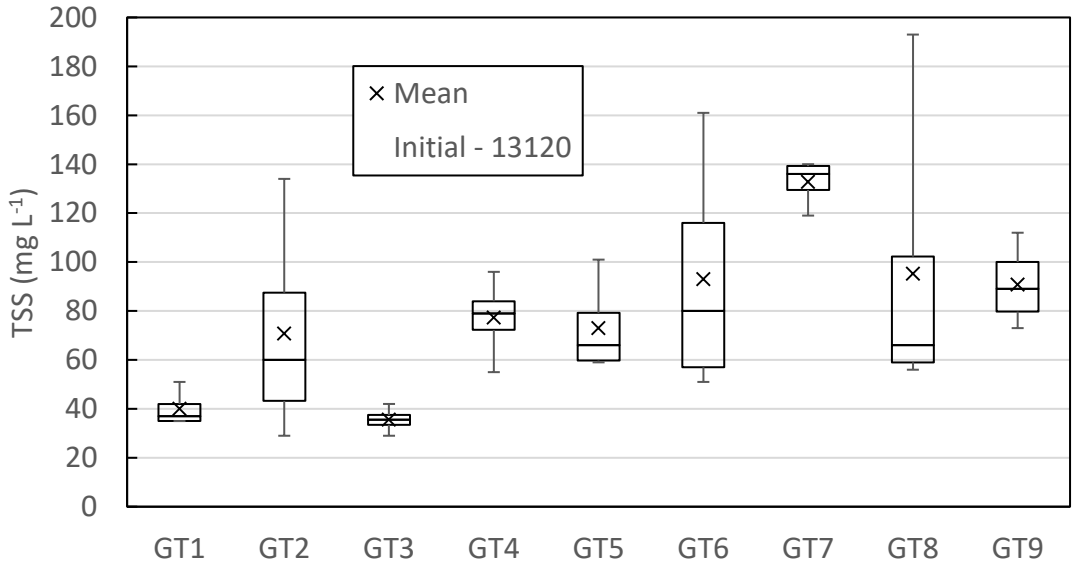

Figure 4.9: Total suspended solids in the filtrate generated during the optimal dosage identification trials.

Total and dissolved metals measured in the filtrate are presented in Figure 4.10. Average total concentrations of copper existed between 6 and 12 μg L^{-1} of filtrate. Total lead was present at a similar concentration, with averages ranging from 3 and 8 μg L^{-1}, while total zinc occurred between 20 and 80 μg L^{-1}. When comparing the dissolved concentrations to total concentrations, values for copper and lead were found to be on average 90 % and 95 % lower for all nine dosages respectively, ranging from a high of 1.6 μg L^{-1} to a low of 0.2 μg L^{-1} for copper and 1.4 μg L^{-1} to 0.0307 μg L^{-1} for lead. Dissolved zinc was generally consistent between dosages, occurring at concentrations of approximately 10 μg L^{-1} on average. This value typically equated to between 25 - 30 % of the total metal concentration; however, dissolved measurements approaching 100 % of the total zinc were recorded. Further analysis which explores some rationale for the dissolved and total metal fractions is discussed in section 5.6.

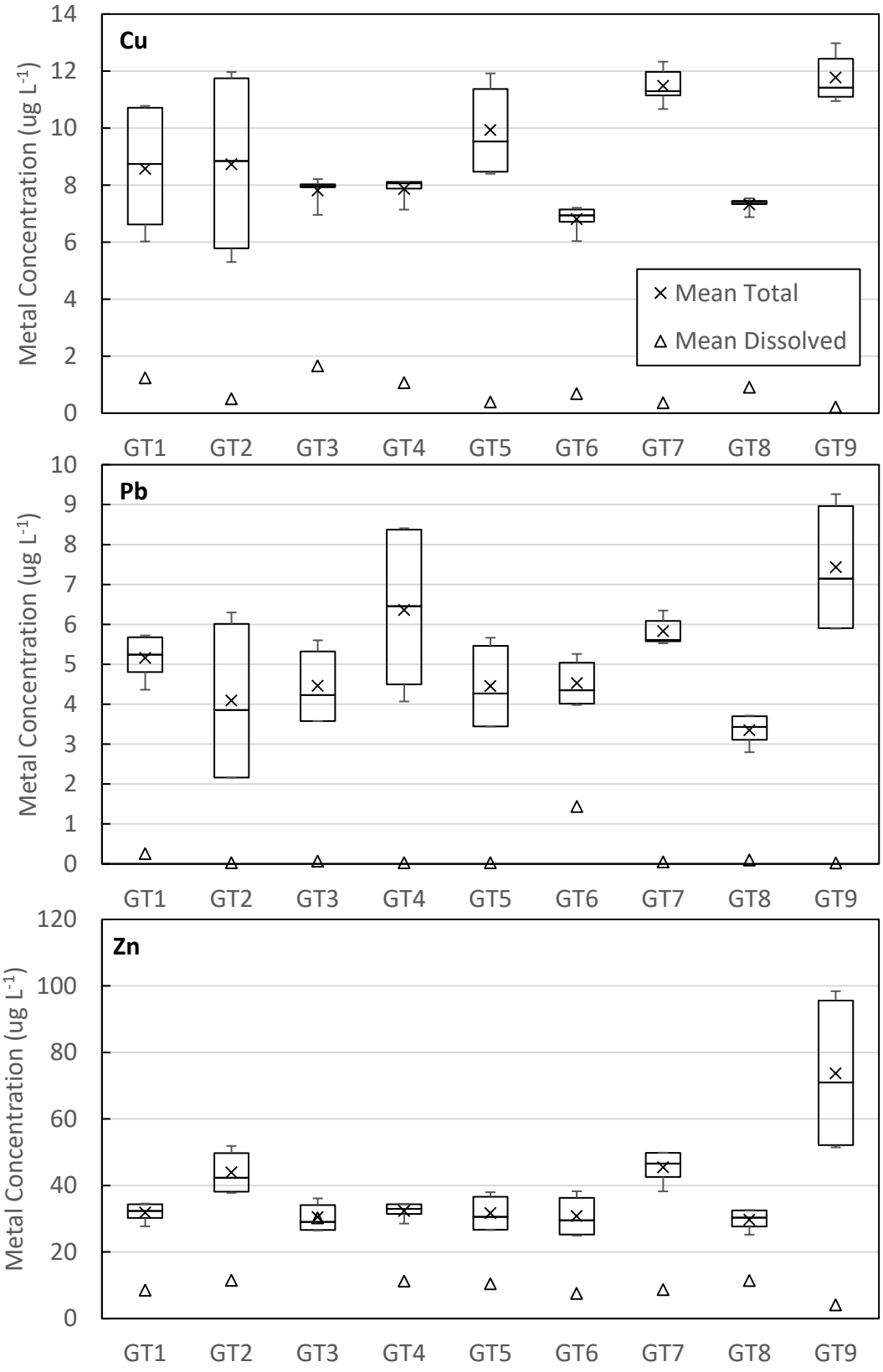

Figure 4.10: Metal concentrations in filtrate generated during the optimal dosage identification trials.

4.5 Optimal Dosage Identification and Results

The optimal additive dosage which would be used for further testing was determined via the results produced during both filtrate and filter cake analysis. No one dosage excelled in all categories; however, sample GT3 showed either average or above average results for all tests considered. This sample produced a filtrate which contained the lowest concentration of suspended solids (on average), as well as produced amongst the highest total filtrate volume and fastest filtration rate. Also considered was the volume of additives required for this dosage, as well as ease of use for the implementation of the dosage during future experimentation. The dosage selected required an amount equal to 5% of the total volume of slurry for both the flocculating agent and the cationic polymer (made down to their respective dilutions). Figures 4.11 and 4.12 present a summation of the initial dewatering results garnered during the bench-scale 200 mL RDT. The figures show a direct comparison of the treatment potential of the now determined optimal dosage with the untreated 1 % slurry.

As a result of the conditioning, TSS showed a reduction of 99.7 % when compared to the initial input. Moisture content could not be compared directly, as no cake developed on the untreated filter, however, a comparison to the initial MC of the 1 % slurry was deemed pertinent, as the filter cake serves as a representation of the solid material which will eventually remain following remediation. The optimal dosage treated slurry produced a filter cake with a moisture content 82 % lower than the untreated material and contained a solid content 600 % greater than the initial slurry (6 % and 1 % respectively).

Particle size distribution results (Figure 4.11) show that 80 % of particulate matter found in the filtrate were finer than 3 μm, with 99.7 % of materials being smaller than 10 μm. When compared to the initial untreated sediment (80 % finer than 7 μm), the size distribution of particulate matter showed some improvement.

Slurry treated with the optimal dosage resulted in an initial dewatering rate (measured following 60 seconds of filtration) 94 % faster when compared to the untreated slurry. The volume produced during the first 60 seconds of filtration was equal to 94.4 % of the total filtration volume obtained using this treatment. Following 10 minutes of filtration, the treated sample reached a maximum of 180 mL, a volume which was 38 % greater than the untreated sample following the same duration. The untreated slurry reached a maximum filtered volume (140 mL) following 1 hour of treatment, which was 17.7 % lower than the treated slurry was able to achieve within the first 60 seconds of filtration.

Also of note was the performance of the GT9 sample, which contained an identical additive volume to that of GT3. This trial generally performed below average in all tests, being among the slowest to dewater, and containing the highest concentration of all metals when compared to the other dosages. It is clear by this result that the two-stage conditioning process was vital to the effectiveness of the dosage.

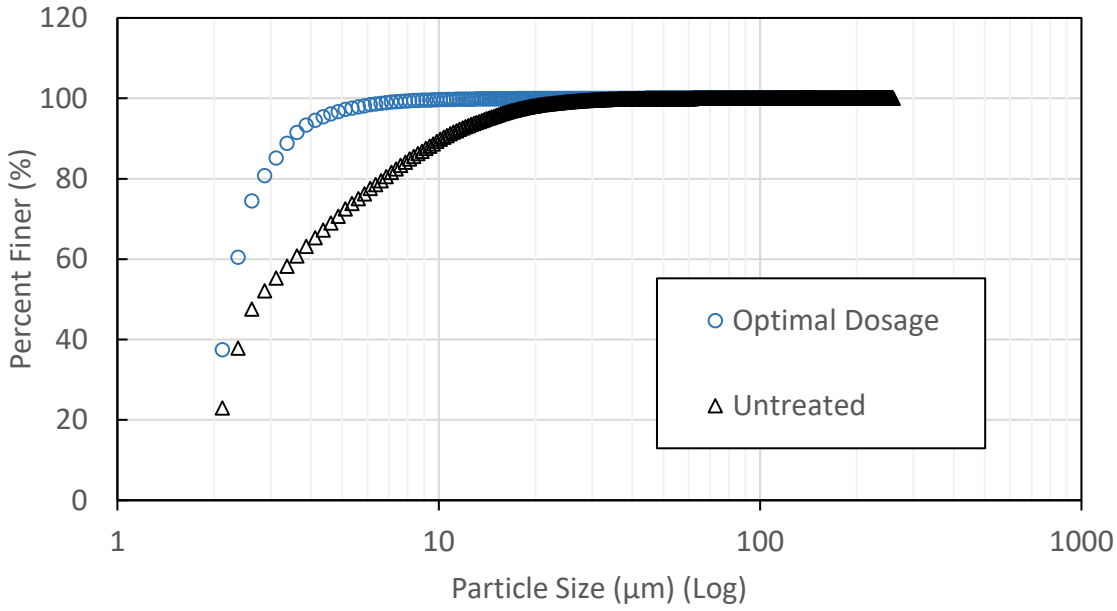

Figure 4.11: Comparison of treated and untreated 1 % slurry.

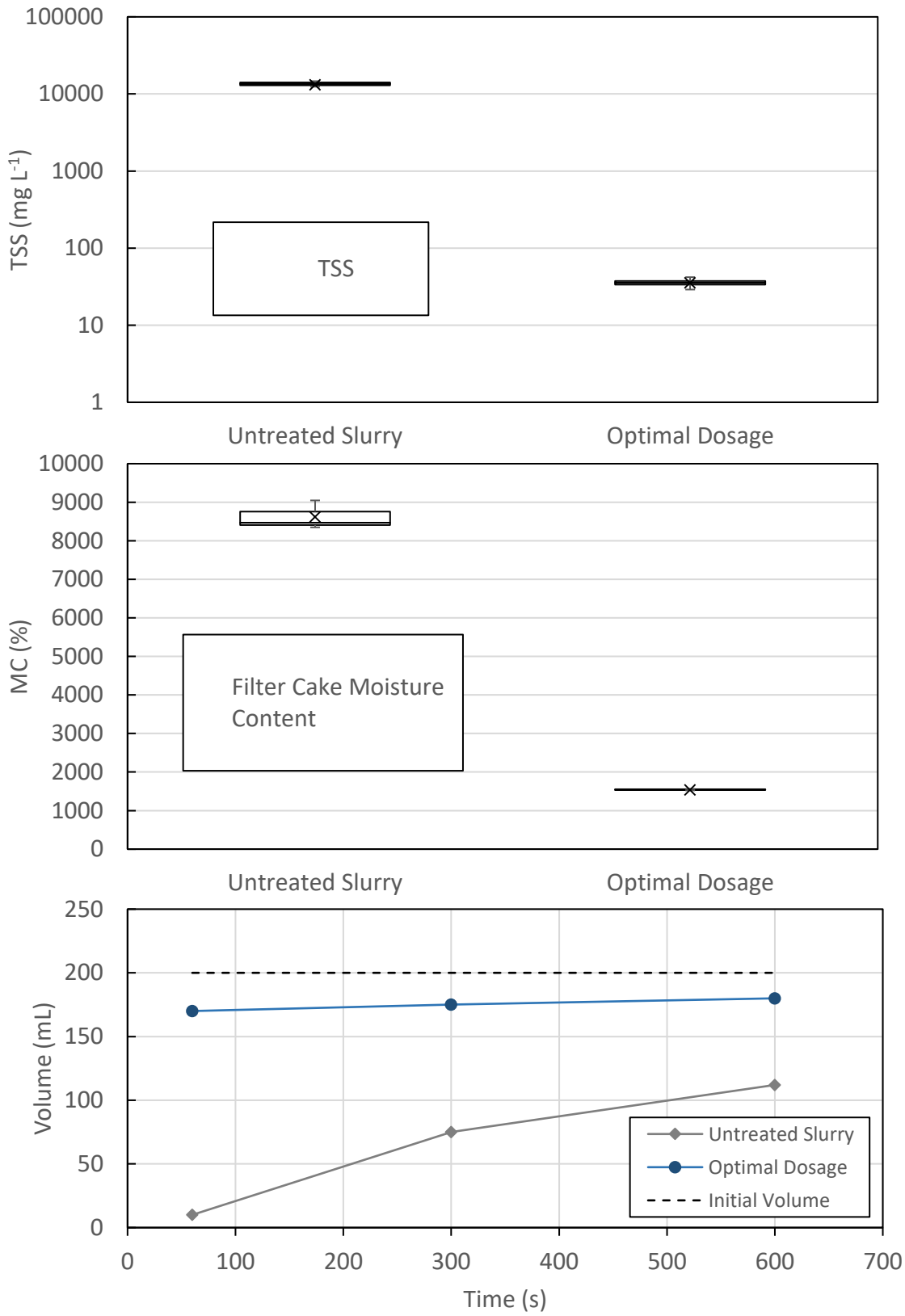

Figure 4.12: Comparison of treated and untreated 1 % slurry.

The metal concentration reduction potential achieved by the optimal dosage conditioning is represented in Table 4.7. Following filtration, over 99% of the solid material (as represented by TSS in the filtrate) has been retained by the geotextile filter. As a result of the low amount of solids present, the filtrate metal concentration is presented in micrograms of metal per litre of filtrate. Average concentrations are shown for both the initial untreated/unfiltered 1 % slurry, as well as the untreated/filtered control trial. Analysis of the filtrate collected from the untreated control sample has confirmed no meaningful reduction in metal concentration could be achieved through geotextile filtration alone, without the implementation of chemical treatment.

Table 4.7: Average metal concentrations in filtrate sampled from optimal dosage conditioned slurry.

	Cu (µg L^{-1})	Pb (µg L^{-1})	Zn (µg L^{-1})
Untreated (Unfiltered)	1177.5	1385.0	15750.0
Untreated (Filtered)	1110	1360	14600.0
Total in Filtrate	7.8	4.45	30.40
Dissolved in Filtrate	1.7	0.07	30.25

When compared to the untreated samples, the optimal dosage produced a filtrate with a reduction in concentration greater than 99 % on average for all metals considered. The filtrate contained total concentrations averaging 7.8 µg L^{-1} of copper, 4.5 µg L^{-1} of lead, and 30 µg L^{-1} of zinc. Figure 4.13 presents the dissolved and suspended metal concentration fractions for both copper and lead. Copper appears in dissolved form on average 21 % of the total concentration, while lead occurs at 2 % of the total concentration.

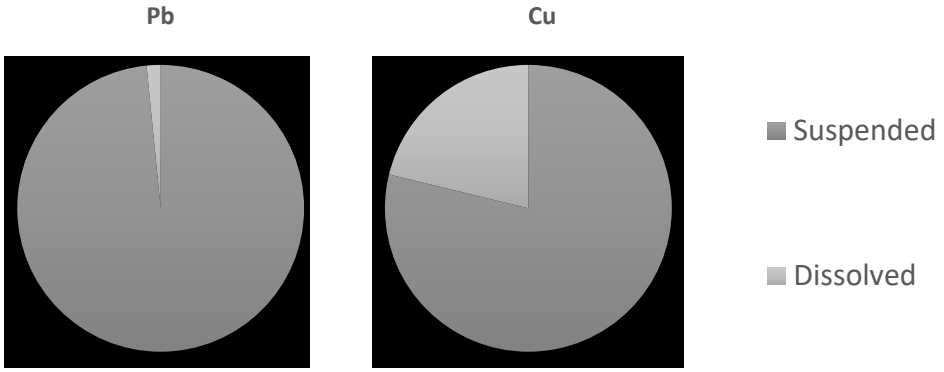

Figure 4.13: Dissolved and suspended metal fraction found in the optimal dosage conditioned filtrate.

The amount of zinc present in the filtrate produced during the optimal dosage treatment was consistently found to be quite variable with values ranging from around 30 % to almost 100 % in the dissolved fraction. Rationale which may explain the dissolved and total fractions of all three metals is presented in section 5.6.

The results generated via the RDT - 200 mL test have shown both the dewatering and contaminant reduction capability of the geotextile. When treated with the optimal additive dosage, stabilization lagoon sediment has shown positive results for all measured parameters. Further tests, which are discussed in the following chapter (5) were applied to investigate the impact of both greater volume and pressure on the filtration process, as well as the effect of increased filter cake thickness on the filtrate quality.

CHAPTER 5: GEOTEXTILE DEWATERING TRIALS

5.1 PREAMBLE

This chapter further explores the effectiveness of the geotextile treatment process, with regard to both metal reduction and dewatering potential. The results from the two increased volume tests will be presented, with significant findings discussed in detail. This chapter also explores the fate of the metals (Cu, Pb, and Zn) during and after the tests, as well as chemical and physical influences, which may have affected their migration.

5.2 BENCH-SCALE RDT: 4000 mL TEST

Bench-scale rapid dewatering trials were conducted with an increased volume of treated slurry in order to observe the impact of the filter cake on filtrate quality (i.e., metal and particulate levels). The filtrate was examined following the filtration of each 200 mL slurry/additive recharge (i.e., "trial"), as outlined in section 3.5.2. Pertinent results are presented below, while average and statistical data pertaining to the 4000 mL RDT can be found in Appendix 3 (where applicable). In this section, figures present the results of the triplicate experiments performed (i.e., three "tests"). As noted on these figures, the mean value of the repeated tests are presented, as well as the maximum and minimum values as identified by the error bars.

5.2.1 Filtrate and Filter Cake Quality

Figure 5.1 presents the mean total suspended solids measured in each trial's filtrate versus the total (cumulative) volume that previously passed through the geotextile. The filtrate was collected for analysis following each 200 mL recharge (i.e. a "trial"). The initial three 200 mL trials which were poured through the geotextile showed considerable variation between the tests. As the experiment proceeded, TSS values in the filtrate generally became more consistent. Shown on the figure is an overall decrease in suspended solids as the filtrate passed through the growing filter cake. The final 200 mL sample (trial 20), which was subject to filtration by both the geotextile and the filter cake established during the preceding 19 trials, produced an average TSS value of 15.6 mg L^{-1}. This amount represents a 67.5 % reduction from the first trial (mean), and an over 99.9 % reduction when compared to the untreated 1 % slurry (13,120 mg L^{-1}).

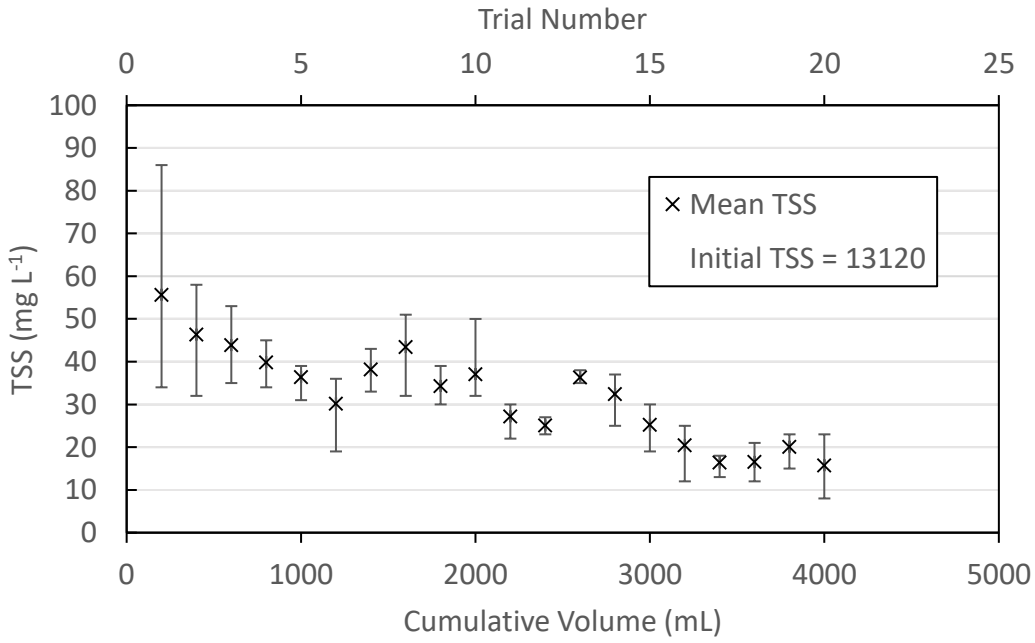

Figure 5.1: Average TSS in filtrate collected during the 4000 mL RDT.

Similar to TSS, a correlation was observed between the total (cumulative) volume passing through the geotextile and the particle concentration present in the filtrate. An apparent reduction in particle concentration is visible in Figure 5.2 as the cumulative volume increased. The chart displays a reduction equal to approximately 75 % when comparing the final 200 mL trial to the initial trials which passed through the unclogged geotextile. (Note that the concentration of particles found in the filtrate associated with the initial trial represented a greater than 99.7 % decrease in particle concentration when compared to the untreated material (reduced from ~ 1.8 x 10^8 particles per mL)).

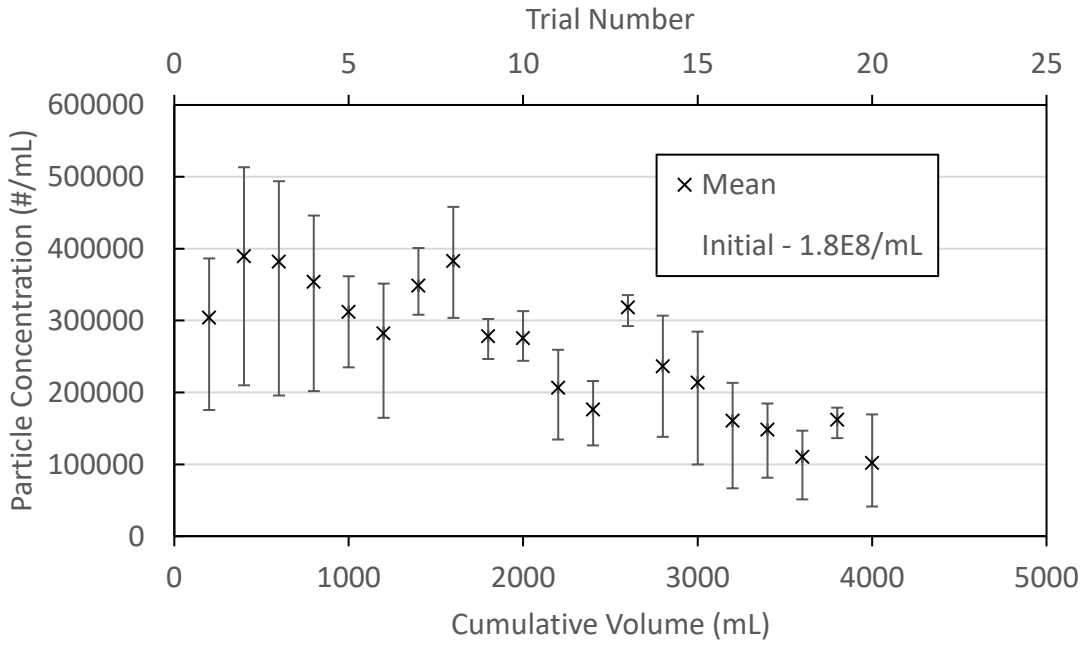

Figure 5.2: Average particle concentration in filtrate collected during the 4000 mL RDT.

The average diameter of the particulate found in the filtrate generally remained consistent throughout the 4000 mL RDT. Figure 5.3 presents the average grain size measured over the course of the trials. When considering the error associated with each trial (determined through the repeated tests), the mean size appeared to remain relatively constant. Although TSS appeared to change over the course of the test, the mean particle size likely didn't change much compared to the initial value (5.8 µm) due to the presence of the filter cake, which when built up reduced the apparent opening size of the pores in the geotextile. These smaller openings preventing the material that had flocculated from passing through; however, material which was yet to aggregate or collect on the cake may have been able to transition the geotextile along with the filtrate.

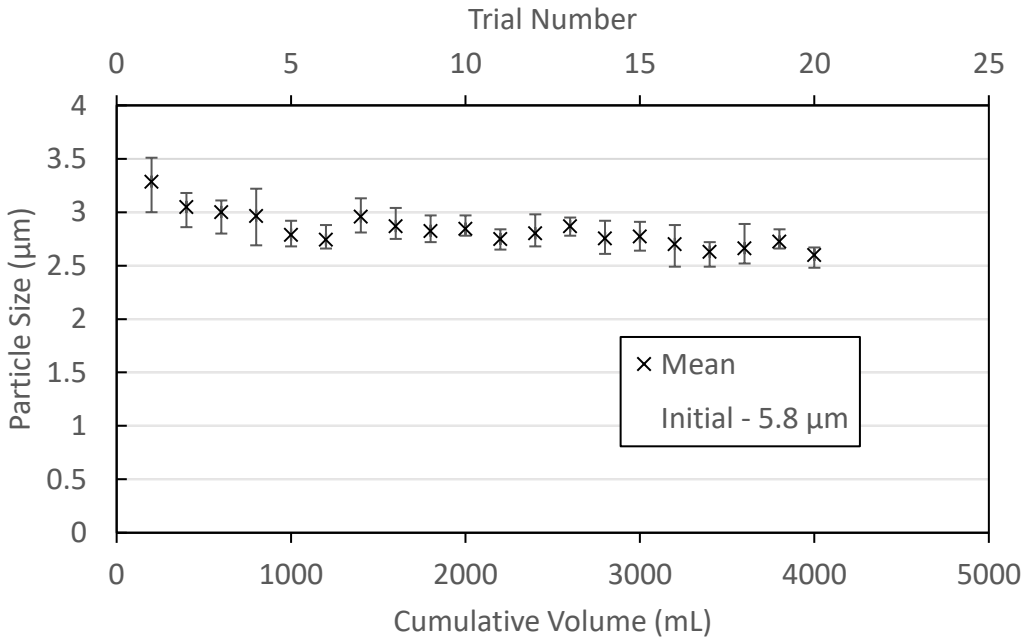

Figure 5.3: Average particle size in filtrate collected during the 4000 mL RDT.

The influence of the filter cake with respect to the filtration rate of material through the geotextile was measured by recording the volume of filtrate collected at pre-determined time intervals (10, 20, 30, and 60 second intervals, and every additional 60 seconds), as well as the total time required for each given sample to reach equilibrium (the time in which the volume of filtrate ceased to increase following each trial). Figure 5.4 presents the cumulative volume for each of the three tests. The figure shows an apparent decrease in filtration rate following trials 1 - 5, as evident by the change in slope seen in all tests. The initial trials (the first cumulative litre) passed through the filter cake and geotextile relatively quickly, and were each able to produce approximately 170 – 180 mL of treated filtrate (and achieve equilibrium) within the first two minutes of filtration.

As the mass of filter cake increased with the addition of subsequent trials, more time was required to produce the same volume of filtrate. When considering the same initial two minutes of filtration, the average accumulation between the three tests for trials 15 - 20 ranged between 75 and 100 mL, and required approximately five minutes to achieve equilibrium. Upon reaching equilibrium, the later five trials were able to yield a maximum filtrate volume ranging between 150 - 170 mL.

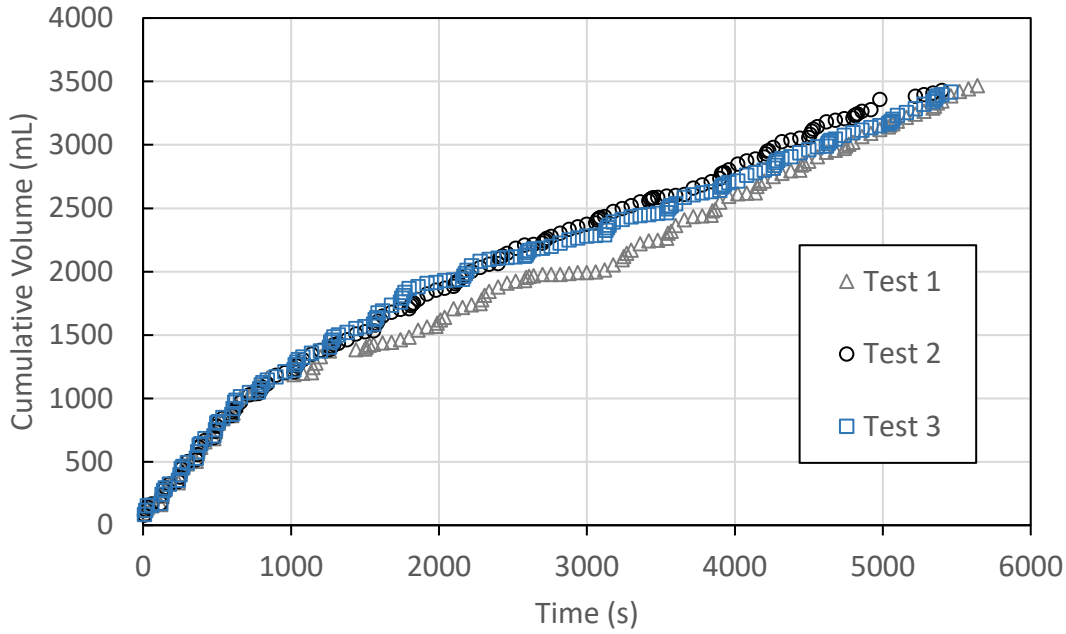

Figure 5.4: Cumulative (Volume and Time) flow rate for 4000 mL RDT.

Total and dissolved metals measured in the filtrate are presented in Figure 5.5. Both fractions were present in similar concentrations to those that were identified in section 4.4.1 (i.e., single 200 mL tests). Filtrate collected from each trial showed a general decrease in the average concentration for all three metals, as a greater volume of the treated slurry was passed through the increasingly clogged geotextile. Copper showed the most consistent reduction throughout the experiment, ranging from an average concentration of 17 µg L^{-1} in the first trial to 4 µg L^{-1} by the twentieth trial. The dissolved fraction of copper was consistent throughout the duration of the 4000 mL RDT, maintaining a concentration of between 4 and 2 µg L^{-1} for all tests.

The total lead remained generally constant in the filtrate with only a marginal trend visible when considering the mean concentration. Filtrate generated during the initial 5

trials was found to contain an average of between 23 to 6 μg L^{-1}, with the range narrowing to between 6 and 4 μg L^{-1} in later trials (final litre). Similar to copper, the average concentration of dissolved lead generally remained consistent, fluctuating between 0.9 and 0.7 μg L^{-1} over the course of the experiment.

The average total fraction of zinc present was again highest in the filtrate sampled from early trials, and similar to copper, began to decrease steadily as an increased mass of filter cake built up on the geotextile. The range of total zinc seen throughout the experiment was generally more extensive than that seen for both copper and lead, with early trial (the first cumulative litre) concentrations reaching 100 μg L^{-1}, before decreasing to between 50 and 30 μg L^{-1} near the end of each test. The dissolved concentration of zinc found in the filtrate averaged 21.6 μg L^{-1} over the course of the RDT. Similar to the other two metals considered, the dissolved fraction of this metal remained consistent throughout the duration of the test, however, was found to represent at a much higher fraction of the total concentration detected.

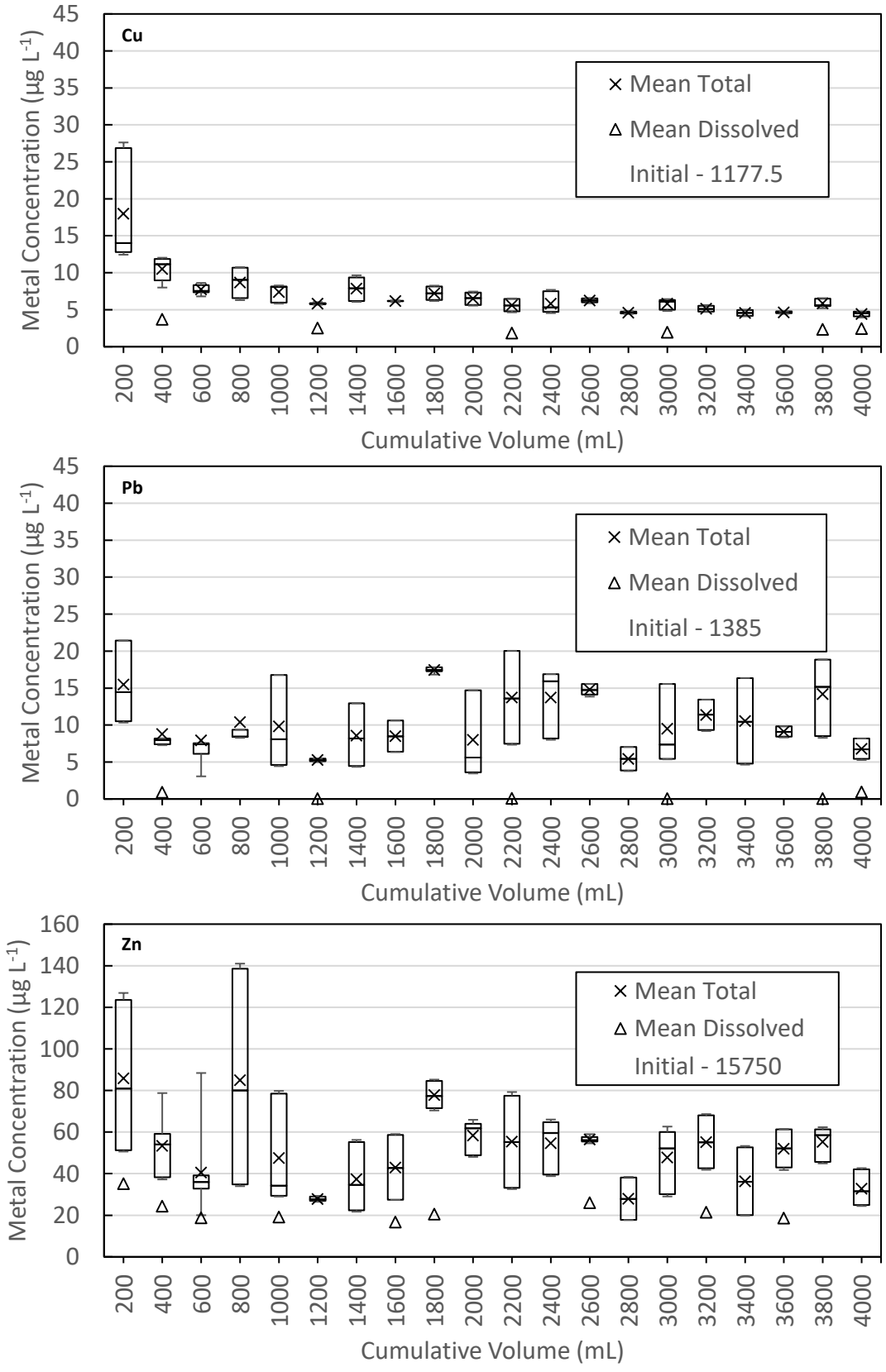

Figure 5.5: Metal concentrations in filtrate collected during the 4000 mL RDT.

The moisture content of the filter cake was measured immediately following each 4000 mL rapid dewatering test, and was found to be between 1230 % and 1330 % (average - 1280 %), while the solids content ranged between 7 % and 7.5 % (average - 7.3 %). MC and SC were also determined following an additional "consolidation" period of 24 hours. Over this time filtrate was allowed to drain out of the material, resulting in a decrease in MC and increase in SC to approximately 750 % and 12 % respectively. When considering the additional dewatering period, the geotextile was able to achieve a filter cake which contained a lower MC (and higher SC) than was found in the original undiluted anthropogenic sediment, sampled directly from the basin (recall basin values of 1182 % for MC and 7.8 % for SC).

5.2.2 4000 mL RDT Discussion

Two spikes can be seen in the measurements for TSS, particle, and total metal concentrations, following trials 6 (1200 mL total), 12 (2400 mL total), and 18 (3600 mL total), lessening in amplitude as trial numbers rose. Increases in the solid and metal concentrations coincide with a lapse in time that occurred while subsequent samples were prepared via the jar test procedure (section 3.4). Due to equipment limitations, only six 200 mL slurry-additive mixtures could be prepared at once. Approximately 20 minutes was required following the sixth trial to prepare the succeeding six samples. During this period, additional dewatering ancillary to that associated with any given trial was found to occur. This dewatering caused a slight compaction of the filter cake during the delay, and upon re-wetting of the cake via the ensuing trial, a more significant disturbance was seen compared to trials conducted in sequence (with no delay). As the spikes were observed in

all tests, it is thought that the disturbance caused a flux in material to pass through the geotextile, and with it contributed to diminished filtrate quality immediately following the delay.

Overall, a reduction in total concentration was seen for all metals, when compared to the initial 1 % slurry (Table 5.1). The majority (~ 98 %) of the reduction generally occurred within the first trial, with levels quickly reducing by the third trial. As each subsequent trial was required to pass through an increased amount of sediment deposited on the geotextile, the filtrate quality with respect to contaminants continued to show consistent improvement. Total values for copper decreased on average to 0.4 % of the initial amount present following the twentieth trial, with similar reductions seen for lead (0.5% of untreated) and zinc (0.2 % of untreated). With effective treatment using the optimal dosage, it is possible to achieve an over 98.9 % reduction in concentration without an established filter cake, with improved performance to 99.6 % upon the buildup of only a small amount of sediment on the geotextile. Table 5.1 presents the average concentration for the initial three and 20th trials as well as total reduction percentages seen for metals over the course of the 4000 mL RDT.

Table 5.1: Average metals and reduction in filtrate collected during the 4000 mL RDT.

	Initial average concentration prior to filtration (µg L^{-1})	Total metals in 1st trial (µg L^{-1})	Total metals in 2nd trial (µg L^{-1})	Total metals in 3rd trial (µg L^{-1})	Total metals in 20th trial (µg L^{-1})	Average minimum reduction	Average maximum Reduction
Cu	1177.5	17.9	11.5	7.9	4.4	98.5 %	99.6 %
Pb	1385.0	15.5	7.7	6.8	6.8	98.8 %	99.5 %
Zn	15750.0	85.9	46.1	36	33.8	99.5 %	99.8 %

In addition to metal reduction, favourable trends were visible for TSS, particle concentration, as well as filter cake moisture content, over the course of the increased volume bench-scale RDT. As an increased filter cake accumulated on the geotextile, a reduction in both filtration rate and total volume of filtrate did, however, become apparent. The reduction in these two parameters was expected to occur, as intuitively, any subsequent trails would be required to pass an increasing amount of material, which would slow and absorb a fraction of the would-be filtrate.

Additional influences, such as increased pressure introduced by the filling of a three-dimensional geotextile bag may alter the performance of the filter cake and the geotextile (i.e., flow rate and contaminant migration). When considering larger-scale conditions, flow rate, volume, particle migration and effluent quality may all deviate from the results presented in this section. Due to the limitation of the bench scale analysis, a larger field test was conducted to better understand full-scale conditions. As described in section 3.5.3, the larger-scale test was designed to test the hypothesis regarding both an increased filter cake and the effect of added pressure, as well as confirm the conceptual results determined through the bench-scale analysis. Results from the large-scale experiment are presented in the following section.

5.3 GEOTEXTILE BAG FILTRATION – FIELD TRIAL

The large-scale field test consisted of two 100 L trials, which were drawn into a single geotextile bag. Included in this section are the physical and chemical test results determined for individual filtrate samples collected at each time interval, as well as a discussion of the contaminant reduction potential, which occurred over the duration of the test. Also

included are the results pertaining to the effect and properties of the filter cake and its impact on the filtrate (i.e., flow rate and contaminant concentration). Average and statistical data pertaining to the field trial can be seen in Appendix 4 (where applicable).

5.3.1 Filtrate Quality

Total suspended solids measured for both trials can be seen in Figure 5.6. The initial trial showed a rapid decrease in the number of suspended solids from the initial measurement of 332 mg L^{-1}, taken 15 seconds after filtration began, to approximately 45 mg L^{-1} after 30 seconds. The TSS values continued to trend downward for the duration of the trial, with a TSS concentration of 18 mg L^{-1} being achieved following 10 minutes of filtration.

The second trial, which was prepared immediately upon the first trial fully draining from the drum, showed an initial spike which peaked at 6.7 mg L^{-1} after 3 minutes of filtration. All values recorded during the second trial were found to be lower than the final value recorded during the initial trial, with a decreasing trend (which was less evident than that identified in the first trial) found following the initial spike. The duration of the second trail was significantly longer than that of the first, culminating after over two hours of filtration. The final TSS recorded value (taken at the two-hour mark) was approximately 2 mg L^{-1}, which was half of the recorded average found in the filtrate following the first 10 minutes of filtration (during the second trial) and equal to 0.6 % of that identified in the earliest sampled filtrate from the initial trial (15 seconds).

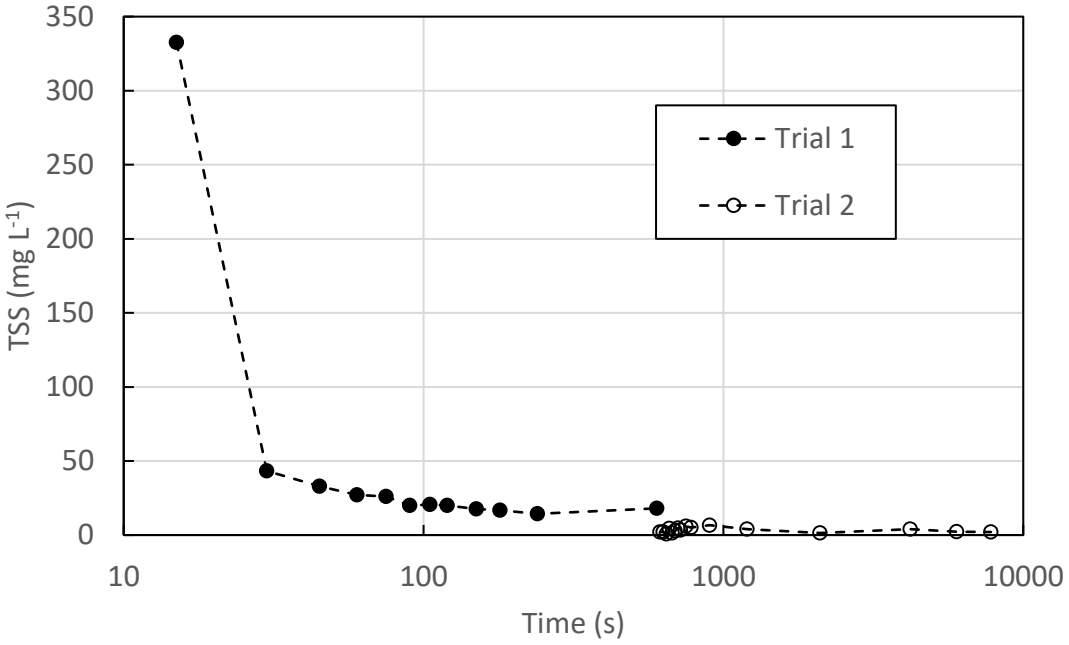

Figure 5.6: TSS in field scale filtrate (200 L) - Log scale.

Figure 5.7 presents the particle concentration data for both trials. Similar to TSS, an overall decrease in concentration can be seen with respect to time. The particle concentration found in the filtrate sampled 15 seconds after the beginning of trial 1 was found to be 2.3 million per mL. This value was quickly reduced, reaching 300,000 per mL in the 45-second sample, and continuing to reduce further as the test proceeded. In the later samples taken from the second trial (1.5 to 2 hours), this concentration was reduced to between 9,000 and 14,000 (# per mL). The decrease seen in particulate concentration is equal to between a 99.4 % and 99.6 % reduction over the course of the test and over a 99.9 % reduction from the initial input of 1.8×10^8 particles per mL.

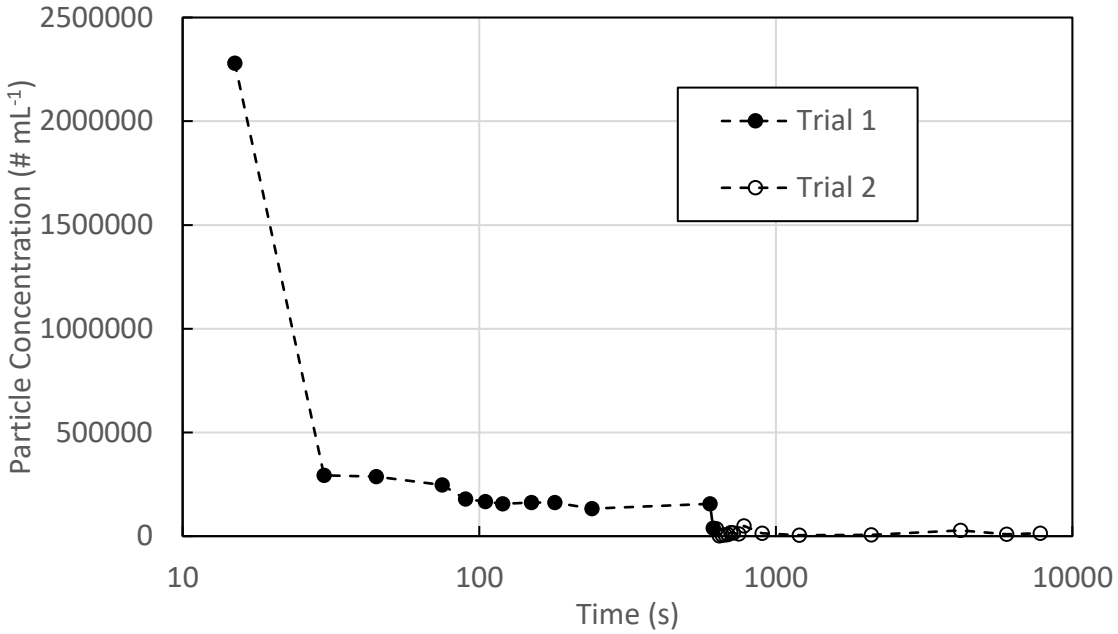

Figure 5.7: Particle concentration in field trial filtrate (200 L).

The size of the particulate matter generally remained constant throughout both the individual trials, as well as the overall duration of the experiment. Little difference to that measured in both the initial (200 mL) and increased volume bench-scale dewatering tests was seen. Particles were found to maintain a constant range between 2.5 µm and 4.5 µm (average of 3.3 µm). This result is similar to that determined during the 4000 mL trial, which was again smaller than the 5.8 µm average found in the untreated material.

5.3.2 Metal Migration

Figure 5.8 presents the total and dissolved metal data for the field scale dewatering experiment. Included on the scale are error bars which denote the highest and lowest concentration determined for each respective data sample (determined by triplicate analysis of each filtrate sample). The initial sample taken after the beginning of the first trial (15 seconds) showed the highest concentration level for all three metals. Following an

additional 15 seconds (i.e., the 30-second sample from trial 1), an immediate reduction in concentration was measured. This reduced concentration in the filtrate was maintained for the remainder of the experiment for all three metals of concern. Similar to TSS and particulate concentration, a minor spike in total metals occurred immediately following the beginning of the second trial. However, some variation was seen, as several measurements taken both before and after this point show values which exceeded this spike for all three metals.

When considering only the first trial, levels of copper were present ranging from a high of 41.2 $\mu g\ L^{-1}$ in the filtrate sampled from trial 1 (15 seconds) to 2.6 $\mu g\ L^{-1}$ after 10 minutes of filtration. Concentrations of lead showed less of a reduction, ranging from 36.7 $\mu g\ L^{-1}$ to 14.8 $\mu g\ L^{-1}$, while zinc ranged from 414.6 $\mu g\ L^{-1}$ to 82 $\mu g\ L^{-1}$, over the same period. Similar to the 4000 mL RDT, the dissolved fraction of copper and lead remained consistent throughout the duration of the trial. Concentrations of dissolved metals ranged from a high of 0.89 $\mu g\ L^{-1}$ down to 0.38 $\mu g\ L^{-1}$ for copper, and 0.27 $\mu g\ L^{-1}$ to 0.11 $\mu g\ L^{-1}$ for lead. A range of 93.2 $\mu g\ L^{-1}$ to 6.1 $\mu g\ L^{-1}$ was determined for dissolved zinc with the highest value occurring in the filtrate sample at the 1-minute mark.

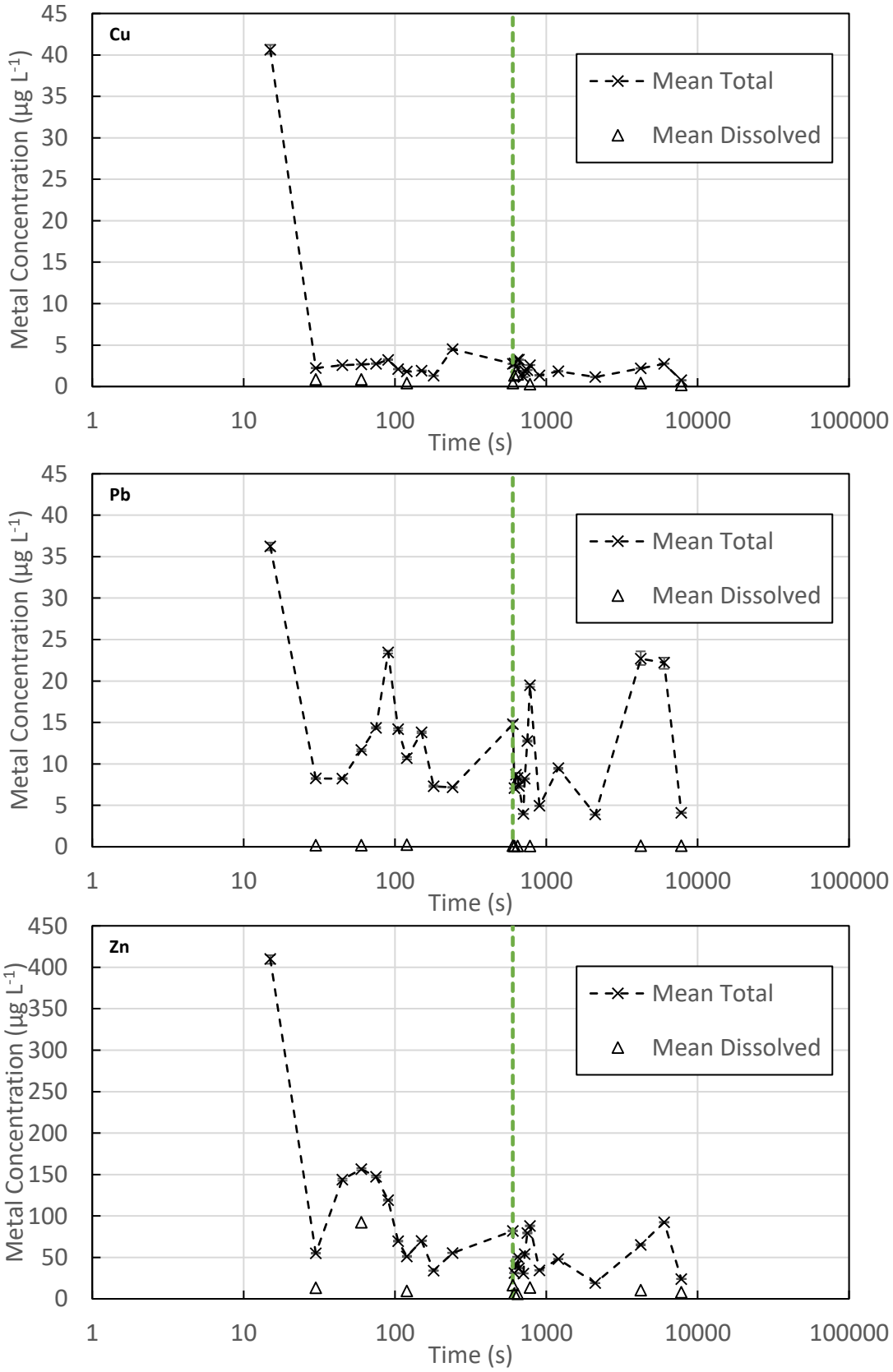

Figure 5.8: Total and dissolved metal concentrations found in field trial filtrate (vertical line denotes beginning of second trial).

Less variation with respect to total zinc and copper was seen in the filtrate collected during the second trial, with values for copper ranging from a high of 3.3 µg L^{-1} (45 seconds) to a low of 0.7 µg L^{-1} (2 hours). Total lead showed a further reduction when compared to the first trial, however, was considerably more variable than the other two metals. Lead maintained a range of concentrations between 22 and 4 µg L^{-1} over the course of the second trial, with maximum values seen in the filtrate sampled between 1 and 1.5 hours. Levels of zinc continued to show an overall decrease during the second trial, with a range of between 92.9 µg L^{-1} and 18.8 µg L^{-1}, however, similar to lead some variation was seen (see figure 5.8). Dissolved metals generally maintained similar concentrations to the first trial, averaging 0.74 µg L^{-1} and 0.10 µg L^{-1} for copper and lead respectively, while dissolved zinc averaged 9 µg L^{-1}.

Metals in the filtrate were generally found to be reduced as an increased filter cake was established over the course of the experiment. A small spike in total metals was found in the initial filtrate sampled from each trial. This spike was comparable to that seen in the results for both particle concentration and TSS, and was thought to originate from a similar mechanism as that seen in the 4000 mL bench-scale test (increased disturbance following a period of settling)

The greatest evidence of metal reduction potential via the geotextile can be seen by comparing the amount of metals measured in the filter cake, to that found in the untreated 1 % slurry. Total metal concentrations by mass were determined for the filter cake via ICP - OES. A comparison of the filter cake results with those determined from the untreated sample (Table 4.5) is presented in Figure 5.9 (error bars represent a 5 % margin of error reported for this method). The concentration of total copper in the filter cake was found to

be 130 mg kg^{-1}. Lead was present at a concentration of 85 mg kg^{-1}, while zinc was present at 1229 mg kg^{-1} (concentrations of copper and lead determined for the filter cake were slightly higher than the initial values, however, fall within the range of error of 100 % of the untreated sediment). When considering all three elements, greater than 99 % (by mass) of the total which was identified in the initial system is accounted for in the filter cake. The remaining metals (< 1 %) have likely passed through the geotextile with the filtrate over the duration of the 200 L field test (either dissolved or associated with particulate); however, as discussed previously, appear in only trace amounts. The metal concentrations determined for 40 elements in the filter cake can be seen in Appendix 1.

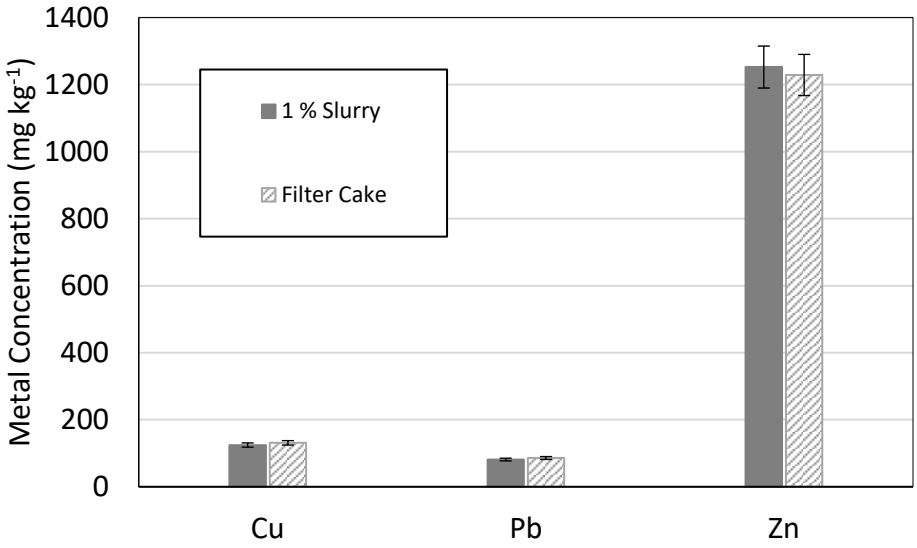

Figure 5.9: Metals comparison by mass of untreated sediment and field scale filter cake.

The geotextile bag has proven to be effective at retaining metal contaminants throughout the duration of the experiment. However, if a rise in metal solubility were to occur due to changes to the environment, an increase in mobility through processes such as leaching may be possible. Influences which may affect the mobility of these metals

through the geotextile during filtration, such as pH, oxidation-reduction potential, and charge, are discussed in section 5.4.

5.3.3 Dewatering Results

Although an established filter cake served to improve the filtrate quality, as an increased volume of conditioned slurry passed through the bag, the filtration rate was slowed considerably throughout the course of both each trial and the overall experiment. The flow rate did increase during the initial stage of the second 100 L trial (first 30 seconds), with the flow rate at the beginning of the trial surpassing the final measurement recorded at the end of the first trial. This higher flow rate was thought to be a result of the increase in pressure upon opening the flow control valve. As the trial commenced, the flow rate decreased, as a result of reduced head and a growing filter cake.

The total time required to complete the filtration of the first 100 L (trial 1) was approximately 26 minutes. In contrast, the second trial, which contained the same volume of conditioned slurry (and hence same initial total head), required a filtration period approximately five times longer (2.5 hours). This overall reduction of the filtration rate can intuitively be attributed to the increase in sediment volume within the geotextile bag, and the growing thickness of the filter cake. Figure 5.10 presents the total flow rate measured as the slurry exited the containment drum for both trials. The graph shows a consistent decrease in the slope as the experiment progressed. The change in slope highlights the reduction in filtration rate, which decreased as an increased volume of filter cake amassed

within the geotextile bag, from an initial 2.3 L s^{-1} at the beginning of the first trial, down to 0.005 L s^{-1} at the end of the second trial.

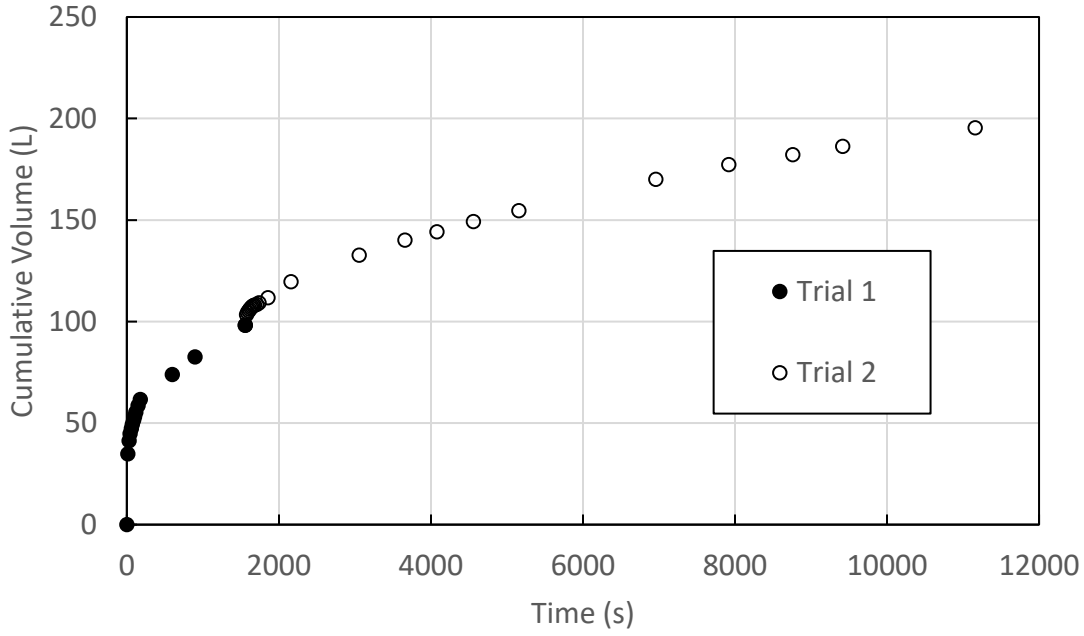

Figure 5.10: Flow rate of the field scale trial (200 L).

Upon completion of the second trial, the geotextile bag was transported to Dalhousie University where it dewatered for an additional 24 hours based on manufacturer recommendation, as the contents were too saturated to allow for dissection (TenCate Corporation, n.d.b.). Following this period, the filter cake was tested for moisture and solids content. Two locations within the bag were sampled in order to gain a better understanding of the geotextiles ability to dewater the material. Triplicate samples were taken from the center of the bag near the surface, as well as from a location near the edge of the bag. The moisture content varied with location, with an average value of 856 % (± 20) for the middle of the bag, compared to an average of 724 % (± 40) measured near the

edge. Results for solid content were similar to that of MC, with the middle of the bag, averaging 1.7 % lower than the edge (middle = 10.5 %, edge = 12.2 %).

Samples were also taken from the same two locations following 48-hours, 1-week, and 2-weeks from the completion of the test. The additional 24-hour consolidation time (i.e., 48 hours total) resulted in a decrease in the MC found in the middle of the bag (805 % ± 5), while the edge maintained a similar value as the 24-hour measurement. The solids content showed a similar trend, resulting in a reduction in variation between the two sampling locations (middle = 11.1 %, edge = 12.2 %).

The MC and SC results generated via the use of the three-dimensional enclosed bag were generally in agreement with those measured for the open-air bench-scale RDT filter cake following 24-hours of drying (recall and average MC of 748 %, and SC of 12 %). Following the two-week dewatering period, the filter cake achieved an absolute solid content value of 16 %. This dewatering period has resulted in an over 100 % increase in the SC as compared to the initial SC of the untreated basin sediment (7.8 %). Although not identical to real-world conditions (as this test did not explore the effect of pressure exerted on the exterior of the bag) the result produced over this relatively short dewatering period indicate the effectiveness of the geotextile to both filter and dewater the sediment in question. Figure 5.11A presents the “bloated” geotextile bag post-filtration, while Figure 5.11B shows the bag immediately following dissection. Values for MC and SC for both sample sites over each interval can be seen in Tables 5.2 and 5.3.

Figure 5.11: Geotextile bag following 200 L filtration trial (A), and immediatly following disection (B).

Table 5.2: Field scale filter cake moisture content.

Moisture Content (%)	24 Hours	48 Hours	168 Hours	336 Hours
Middle	856.3	805.4	667.6	574.5
Edge	723.8	726.3	656.2	516.0

Table 5.3: Field trial filter cake solid content.

Solid Content (%)	24 Hours	48 Hours	168 Hours	336 Hours
Middle	10.5	12.2	13.0	15.5
Edge	11.0	12.1	13.2	16.2

5.4 DEWATERING DISCUSSION

During the field scale dewatering trial, all parameters measured that contributed to filtrate quality (TSS, particle, and metal concentrations) achieved reductions greater than those found during the bench-scale 4000 mL test. The TSS, which had reduced from an initial 13,120 mg L^{-1} in the untreated slurry to a low of approximately 15 mg L^{-1} during the 4000 mL RDT, was further reduced to a concentration reaching 2 mg L^{-1} at the end of the field-scale trial. Similarly, particle concentration, which decreased from 180 million per mL to approximately 100,000 per mL during the bench-scale test, continued to decrease with an increased filter cake to between 14,000 and 9,000 per mL during the field test.

When considering additional metal reduction during the field scale, it is important to recall that over a 99 % reduction was seen for all total metals during the 4000 mL RDT. The highest concentrations of total metals detected (all three) during the field-scale trial occurred in the first sampled filtrate collected upon commencement of the test. Concentrations of copper and zinc measured in the filtrate did trend lower than those observed during the bench-scale analysis (with final mean concentration measurements for zinc reaching 32 µg L^{-1} for the bench scale and 24 µg L^{-1} for the field scale, and copper reducing from 4 µg L^{-1} to 0.75 µg L^{-1} at the end of the two tests respectively). Total lead did occur in lower concentrations during the field trial than were identified in the 4000 mL filtrate; however, due to the somewhat irregular concentrations produced (i.e., a less evident trend), it can not be said that a definitive reduction has occurred over this test.

The concentrations of dissolved copper in all field scale filtrate samples showed a reduction when compared to the amounts found in the 4000 mL RDT filtrate, as well as

that determined for the basin water (~5 μg L^{-1}). However, values for this metal fraction maintained a consistent range over the course of both experiments (respectively). A lower concentration of dissolved copper was identified in the earliest filtrate analyzed (30 seconds) than was seen in any bench-scale sample. Due to the relatively low amount of established filter cake at the time of sampling (as evident by the values for total metals, TSS, and particle concentration), as well as the consistent concentration through the duration of the test, the discrepancy found between the two experiments can likely be attributed to the chemical conditions present in the slurry, rather than the presence of the filter cake.

When comparing the dissolved zinc concentration measured in the field scale test filtrate to that identified in the bench scale RDT, little variation can be seen. The field-scale filtrate yielded dissolved lead concentrations which generally maintained a consistent level throughout the test with only minor fluctuations. The results yielded through this experiment indicate that the development of a filter cake has little influence on the dissolved fraction of the metals present in the filtrate, however, it can significantly affect the total concentration.

Although there appears to be an overall reduction in TSS, particle concentration, total copper, and total zinc as an increased volume of slurry is filtered, values which did not follow the apparent trend were identified for all parameters listed. This may be attributed to variations within the geotextile that were not anticipated. The three-dimensional effect of the geotextile filtration procedure may have resulted in a section of filter cake where filtrate was more readily able to transition (due to micro-scale changes in density, variations in pore opening, etc.), which may have momentarily increased the flow

rate of filtrate, and with it increased the amount of particulate which was able to pass through. Additionally, the location at which the filtrate permeated through the geotextile was unknown, as samples were collected as the material drained off the corner of the bag. Sediment movement within the bag during filtration may, therefore, impart minor effects on filtrate quality (and may serve as some explanation for the non-linear reduction in lead concentrations seen during the test).

Regardless of the micro-scale variation in metal and particle concentration within the filtrate, the results discussed in this section have further confirmed the improved contaminant reduction potential of the geotextile, which exists upon the establishment of a filter cake. All TSS, particle, and metal concentrations measured showed the highest values at the beginning of the test. Following the initial 15 seconds, it is evident that enough sediment had amassed on the geotextile to begin to influence concentrations. The correlation between filtrate quality and the presence of the filter cake can likely be attributed to the propensity for the particulate matter to aggregate, as it did during the initial formation of the flocs in the treated slurry. As the mass of the filter cake is increased, the pore size is reduced relative to the AOS of the geotextile, causing more material to be filtered and encouraging the entrapment and binding of particles to the already established cake.

In addition to the retention of solids, over 99 % of metal contaminants found in the untreated slurry were contained in the geotextile bag. The result of the concentration of metals in both the filtrate and filter cake confirms the earlier hypothesis that metals present in the basin are likely bound to the solid particulate. As a result of the association between these constituents, the reduction found in the concentration of metals can likely be

attributed to the physical retention of the sediment, upon treatment and filtration via the techniques discussed previously.

The concentration of TSS found in the filtrate suggests that the flocs (and additional accumulated material which remained un-flocculated) were almost entirely retained by the geotextile. This result is likely due to both the attractive qualities of the sediment, as well as the fact that the average apparent opening size of the geotextile fabric (430 μm) was smaller than that of the diameter of the flocs. Both the size of the flocs, as well as a rationale for the metal contaminants propensity to associate with the sediment is explored in the following section.

5.5 Further Analysis of Flocs and Particulate Matter

5.5.1 Floc Size

Floc size was determined using the method outlined in section 3.6. Analysis by the ImageJ software determined the shape of the flocculated material tended to be elliptic rather than uniformly spherical. As a result, values were calculated for both major and minor axes, the average of which was determined to be 960 μm and 610 μm respectively. The floc size measured using this technique represents an increase in the average size of between 16,000 % and 25,000 % (or growth by a factor of approximately 200), when compared to the untreated slurry. When considering the filtration properties (Table 2.4) of the geotextile, it should come as no surprise that the geotextile fabric was able to retain the treated slurry

effectively. Figure 5.12 presents the slurry following conditioning with flocs clearly visible.

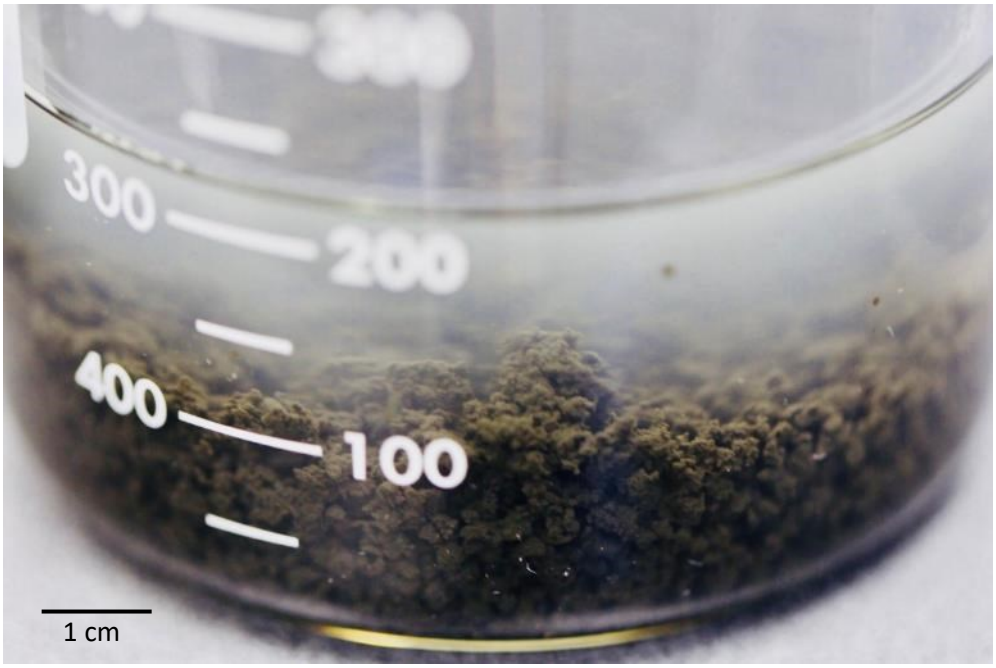

Figure 5.12: Flocs post conditioning.

Due to the fragile nature of the flocs, a great deal of fragmentation and reunification occurred during the preparation of samples arranged for floc size determination (this was also apparent in samples produced for the bench and field-scale analyses). As a result, floc size varied considerably between samples from the same trial and were inconsistent when considering duplicate trials. In addition to the disturbance generated during treatment, interaction with the geotextile and existing filter cake immediately transformed the free-floating particles into a more cohesive, uniform substance, lacking any individually discernible grains.

Particle size analysis of the flocculated material was conducted merely to gain insight into the effect of the additive treatment before filtration, rather than characterize a specific grain size. As a result of the variability identified during this test, the size of the grains is qualitative. This average size was found to be larger than both the original, untreated particles, as well as the AOS of the geotextile. The pore size of the filter cake was not determined, however, based on the reduction in filtration rate seen during the field and bench-scale analysis; a reduction likely occurred resulting in a smaller pore diameter than the AOS of the fabric.

As the pore size becomes smaller with an increasing filter cake, the size of particles which may be effectively retained by the filtration system would likely decrease. As a result, the flocs need only be larger than the AOS until a suitable filter cake is developed (however treatment is still required to prevent clogging of the pores). Based on the ImageJ floc size analysis, and the retention seen during experimentation with treatment via the optimal dosage, it is evident that a large enough average floc diameter has been achieved. The particulate matter which was not incorporated into the filter cake, instead, passing through with the filtrate, is discussed in the following section.

5.5.2 Identification of Particulate Matter in Filtrate

In order to provide insight on the metal migration observed during the bench and field scale trials, a scanning electron microprobe was used to determine to a better degree the identity of the particulate matter which had passed through the filter. Although concentrations were similar to those present during the bench-scale tests, filtrate collected during the field-scale trial contained a higher overall volume of solid material and was therefore chosen for this

analysis. Particles were analyzed to discern any identifiable morphometric quality that may render them more susceptible to migration through both the filter cake and geotextile, as well as identify any affinity the metals may have for a given particle, which might enhance the transfer of the metals through the geotextile. It is important to note that, as a result of the preparation (which involved grinding the material) the results generated via this technique are considered relative, and therefore the measurement should be considered a qualitative comparison of the elemental composition. Scanning electron microprobe (SEM) images and findings are presented below, with the full data set available in Appendix 5.

5.5.2.1 Qualitative Identification of Particulate Matter

Figure 5.13A presents a high magnification SEM image of the particulate matter collected from the filtrate produced during the initial 15 seconds of the field-scale test (no other individual test yielded the required amount of solid material needed for this analysis). Two locations on this image were analyzed for elemental composition, which corresponded to two visually distinct surfaces. The left surface (site 1), which can be characterized by its more rounded features, appeared as an anomaly at this scale. Surrounding the rounded anomaly was a more sheet-like surface, which appeared to be visually representative of the majority of the sample. Location 1 yielded peak intensities which corresponded with a high degree of carbon (> 92 % by mass), and a moderate amount of oxygen (7.3 %). In addition to oxygen and carbon, trace amounts of silicon, calcium, and aluminum were detected on this surface. Adjacent to the carbon-rich site, the second measurement location (representing the sheet surface) yielded a composition rich in both carbon and oxygen (54 % and 35.8 % by mass, respectively). The SEM also detected peak intensities which

corresponded to a silicon concentration equal to 8.7 % by mass, along with trace amounts of several other elements (Mg, Al, Cl, K, Ca, Mn, & Fe). The high degree of carbon found at both the anomaly and site 2, which appeared to represent the majority of the sample, suggests organic material may be prevalent in the particulate found in the filtrate.

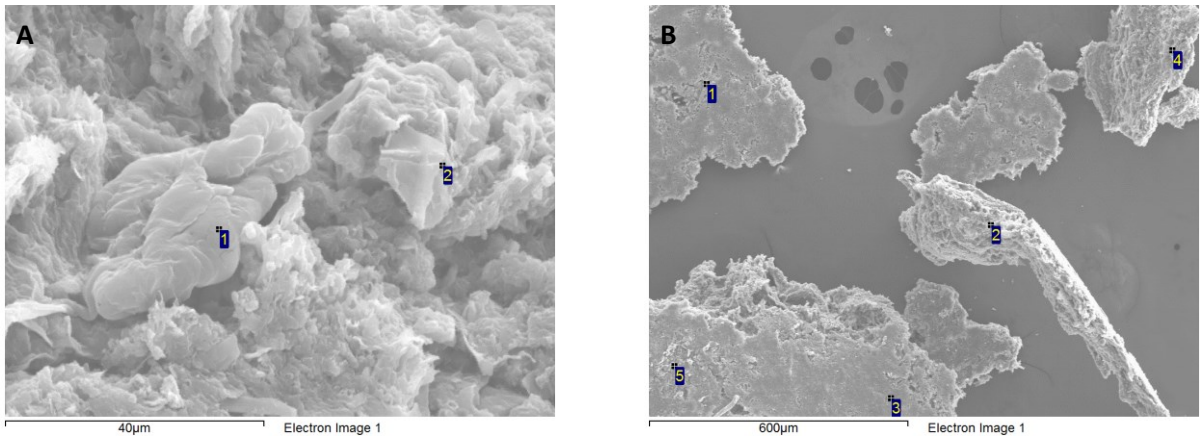

Figure 5.13: SEM image of particulate matter sampled from the initial field scale filtrate.

Figure 5.13B presents the same sample (solids in the filtrate) under reduced magnification. Five locations were chosen, which corresponded to several individual grains present on the sample. All measurement sites indicate a weight percentage for carbon of between 50 and 70 %. This element may be over-represented in the data; however, as the sample was adhered to the stub via a carbon-coated double-sided tape (the presence of this artificially introduced carbon may have skewed the measurement).

Of particular interest was the mass of both silicon and oxygen present on the sample surfaces. Sites 1 and 2 contained relatively high amounts of silicon (7 % and 11 %, respectively) when compared to the other three sites analyzed (1 -3 %). Oxygen levels approximately twice that of the silicon were present in sites 1 and 2 (15.5 % and 18 % respectively), with the other three sites reporting oxygen values approximately ten times

that of silicon. The relative weight percentages of silicon, carbon, and oxygen relating to the particles in the filtrate (Figure 5.15B) can be seen in Table 5.4.

Table 5.4: Major elemental constituent composition of particles in the filtrate.

Site	C	O	Si
1	58.8	15.5	7.1
2	49.1	18.2	11.2
3	65.2	27.1	2.3
4	68.8	25.9	1.3
5	61.5	29.5	3.4

Little variation can be seen when considering visual observation of the SEM images at this scale. When considering the elemental analysis, however, some insight into the type of material present may be gained. Sites which contain a high degree of silicon may be representative of inorganic material (such as quartz or other silicates). In addition, sites which contain relatively low silicon and high oxygen (which were also those which showed the highest overall fraction of carbon) may be indicative of the existence of the organic fraction in the filtrate.

As discussed in chapter two, a significant proportion of the organic matter present in the effluent is thought to originate during the pulping process, and contain high amounts of both lignin and carbohydrates (the primary constituents of trees). Pettersen (1984), notes that the overall elemental makeup of deciduous trees (common in Nova Scotia) is roughly 50 % carbon to 44 % oxygen. The relatively high degree of these two elements identified in the results generated for sites 3, 4, and 5 may, therefore, be indicative of organic material stemming from the pulping process. As well as the organic constituents, it is thought that many of the metal contaminants which have been identified in the BH stabilization basin

have bioaccumulated in these trees (see section 2.3.3). Therefore, if particulate matter identified in the filtrate has stemmed from an organic origin (such as what we may see here), it may also serve as the method of conveyance for metals, which are adsorbed on their surface, or otherwise associated with the molecular structure through biological processes.

Due to the relative data and instrument limitations concerning the detection of carbon, it is difficult to determine accurately the percentage of organic and inorganic matter which was able to transition through the geotextile. When considering both scales, however, the relatively high and consistent presence of carbon, oxygen, and silicon, suggests that both organic and inorganic matter is present. As mentioned, the results of the SEM analysis should be considered qualitative; however, when considering the constituents present, there appears to exist no prejudice for the exclusive removal of either the organic or inorganic fraction during conditioning and filtration.

5.5.2.2 Comparing Stages of Filtration

Relative analysis considering variations over the course of the filtration process was also determined via SEM. Figure 5.14 presents four images, each representing one of the four stages of the dewatering test: the untreated sediment (A), the conditioned flocs (B), the filter cake (C), and an additional location from the sample representing the particles found in the filtrate (D). The apparent particle size seen in the images is not representative of the actual grain size at this stage, (as each coalesced into a large mass upon drying); instead it can be attributed to the propensity of the material to break apart during preparation via grinding of the sample (note the filtrate particulate was not ground).

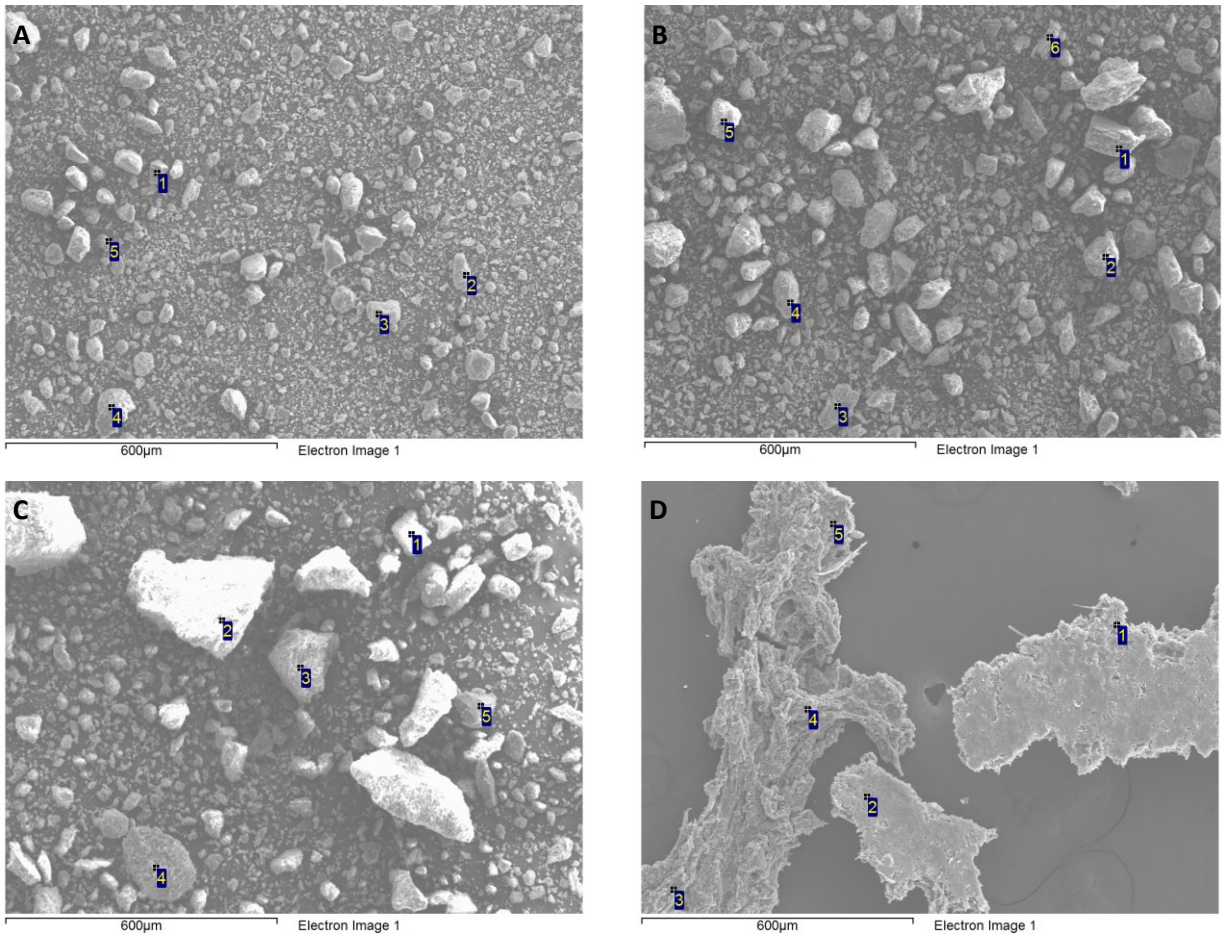

Figure 5.14: SEM images representing the four stages of filtration. (A – Untreated, B – Flocs, C – Filter Cake, D – Particles in Filtrate.

Between four and five sites at each stage (which appeared visually diverse) were selected for analysis. When comparing the stages of filtration, individual sample sites were not considered. The data from the sample sites for each dewatering stage was averaged to produce an elemental weight percent, which represented the stage as a whole. As discussed previously, the carbon tape used to adhere the samples to the stub may have influenced the results. Due to this possible source of error, the weight percentage of carbon was omitted from further analysis, with the remaining elements normalized to 100 % to account for the loss in mass. The weight fraction determined for the remaining elements were then compared between the four phases of filtration. Oxygen, which was consistently the second

most abundant element was also removed to allow for a more discrete analysis of the remaining trace constituents.

Table 5.5 presents the weight percent determined for each of the trace elements (and silicon), averaged over the four (or five) sites from each stage. When comparing the averages for each element, very little change is seen between stages. Figure 5.15 presents the data from Table 5.5 as a bar graph, which when considering the minimum and maximum values (shown as error bars) clearly shows no trend toward either reduction or amplification for any element over the course of the filtration procedure. This result indicates that the particulate material which has been able to pass through geotextile possesses no identifiable characteristic (organic, inorganic, etc.) which has made it more susceptible to mobility. Rather, the particles have likely passed through based on size during the initial stages of filtration, prior to the reduction in pore size as a result of the increased thickness of the filter cake.

Table 5.5: Average element percentages by weight seen in each stage of filtration.

	Untreated	Conditioned (flocs)	Filter Cake	Particles in Filtrate
Na	9.4	4.5	1.5	2.4
Mg	9.0	6.9	5.9	7.1
Al	8.7	10.5	9.8	13.2
Si	25.7	35.2	42.9	26.3
S	14.0	13.2	16.3	14.6
Cl	16.1	12.1	8.8	9.8
K	2.4	3.9	2.9	2.3
Ca	8.6	9.0	14.3	15.7
Mn	1.5	1.1	1.3	2.6
Fe	4.6	6.1	7.4	6.6
Cu	1.5	1.5	1.3	2.7

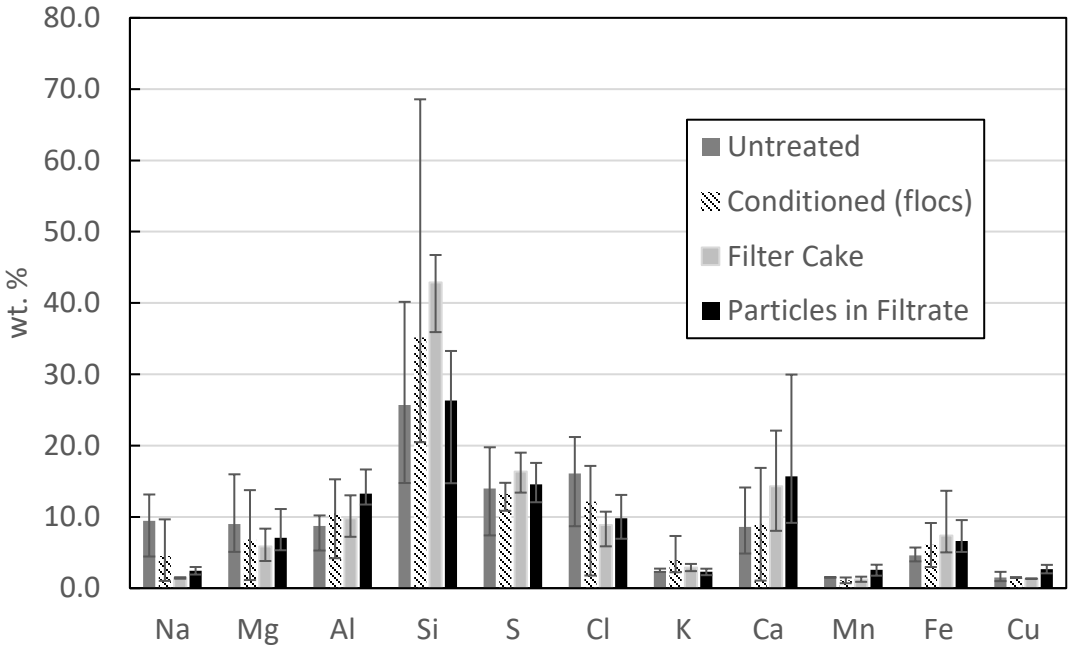

Figure 5.15: Comparison of average element weight percentages found in each stage of filtration.

5.6 METAL FATE AND MIGRATION

5.6.1 Initial Fate

The results presented in this section will discuss the fate of the three metal contaminants during the geotextile dewatering procedure. As apparent by the preliminary characteristics presented in Table 4.8, and confirmed via the bench and field-scale dewatering trials, the filtrate which was produced following the optimal dosage treatment contains trace amounts of the three metals of concern. When comparing the total mass of metals found in the untreated sample to those found in both the filter cake and filtrate produced by conditioning with the optimal additive dosage, over 99 % of the metals examined in the untreated sample have been retained by the geotextile. This result indicates that the majority of metals examined in this thesis (i.e. Zn, Cu, Pb) are likely adsorbed or associated in some other way with the solid particulate matter. The geotextile has been proven to be effective at retaining the sediment and therefore, serves as the primary contributor to the removal of these contaminants from the filtrate; however, a question still remains to the migration potential of the metals.

5.6.2 Migration Mechanisms

The secondary aim of this research was to assess the mechanisms responsible for the migration of metal contaminants both during and after geotextile filtration of the material. Results determined over the course of this thesis suggest that both physical and chemical processes may be responsible for the fate of heavy metals found in the filtrate. When combined with chemical additives used to aid in the flocculation of the sediment, the geotextile filtration technique has proven to be highly effective with respect to the

dewatering and filtration of the material. As a result of the apparent affiliation seen between the two contaminants (TSS and metal concentration), an increased reduction in solid particles may, therefore, increase metal reduction as well.

5.6.2.1 Zeta Potential Influence

Zeta potential measurements conducted on the filtrate following both the bench and field-scale dewatering tests resulted in a sharp increase when compared to the untreated sediment. The initial zeta potential determined for both the water and sediment was reasonably consistent, ranging from around -21 mV to -25 mV for both mediums. The negative charge associated with the material is likely the primary factor which has resulted in the high degree of repulsion seen between particles prior to treatment (Larsson, Hill, & Duffy, 2012), and therefore has contributed to their inability to coalesce without the aid of the chemical conditioning. Upon filtration, the zeta potential determined for the filtrate from the 4000 mL RDT was increased to an average absolute value of + 6.3 mV. Filtrate sampled during the field-scale test yielded similar zeta measurements, ranging between + 4.7 and + 7.7. Figure 5.16 presents the average zeta potential determined for each of the filtrate samples collected during the bench-scale tests, which shows a consistent measurement approximately 30 mV higher than that seen in the initial material (BH sediment and water). The addition of the cationic polymer (recall a zeta potential of + 100 mV) has served to change the charge of the system and resulted in the much lower value (closer to zero).

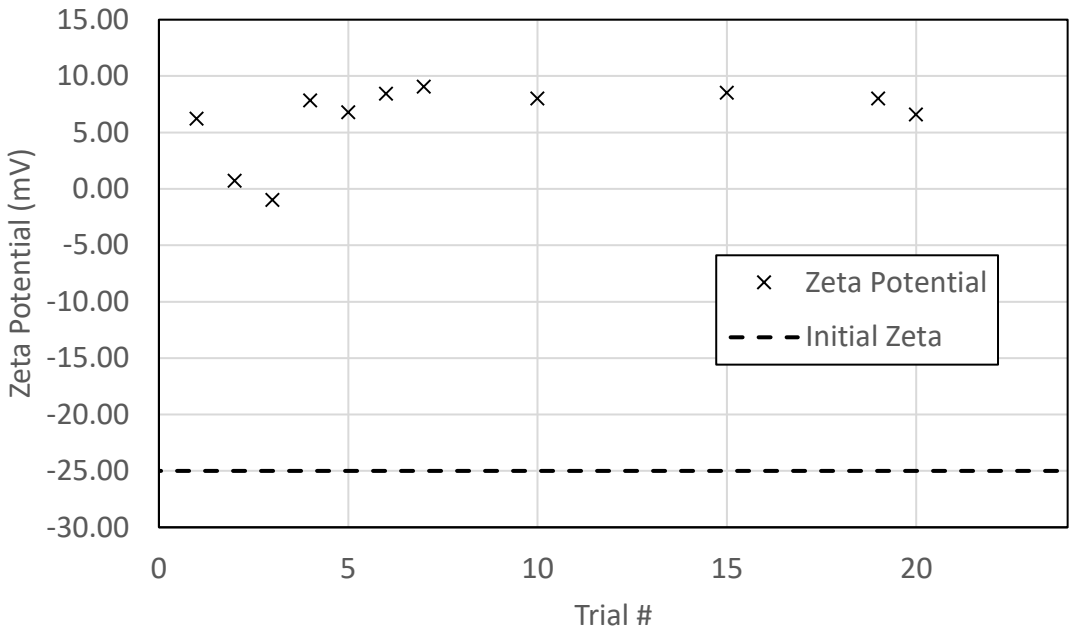

Figure 5.16: Zeta potential determined for 4000 mL RDT.

The effect of the low zeta potential seen in the filtrate is a reduction in the repulsive force between the individual particles, therefore improving the flocculation potential (Larsson et al., 2012). The majority of metal contaminants which were present in suspension (associated with the particulate matter) were likely bound to the flocs during treatment or amassed on the filter cake as additional contact between particles increased. With an increase in particle size becoming greater than the AOS, a physical limitation in the amount of metal contaminants able to pass through the geotextile arose. Metals which were not associated with particulate matter (dissolved), or bound to particles failing to coalesce into flocs larger than the AOS (or be retained by the established filter cake) may have been able to permeate through the geotextile, and as a result, accumulated in the filtrate.

This hypothesis is substantiated by particle concentration, TSS, and mean particle size results, as well as the total and dissolved metal concentrations identified in the filtrate during the tests discussed above. Filtrate generally and consistently contained both lower particle concentrations, and lower total metal concentrations as each test proceeded and the filter cake grew, while dissolved metals remained mostly consistent throughout the experiments.

5.6.2.2 Oxidation-Reduction Potential and pH Influence

When considering the concentrations of both the total and dissolved fractions of copper, lead, and zinc in the filtrate, it is clear that the majority is present in solid form. Chemical analysis of the sediment, water, filter cake, and filtrate was conducted during both field and bench-scale experiments. Throughout the chemical conditioning and dewatering trials, all pH values remained generally consistent, ranging between 7.4 and 7.9, indicating a neutral environment close to that of freshwater. The pH of the chemical additives was found to be acidic (ranging from 3-6); however, upon the treatment, the relatively small amount of additives introduced had little effect on the overall pH of the slurry.

Similar to the pH, the E_H (oxidation-reduction potential) generally remained constant throughout the treatment and dewatering procedures for all mediums. An initial average value of + 380 mV (oxidizing) was determined for the untreated 1 % slurry. This value was determined following the dilution from the initial raw sediment in the laboratory and was therefore subject to atmospheric influence through disturbance. This disturbance may have introduced oxygen to the system and had an effect on the measurement (Tack et al., 1996). However, these results mimic those conditions that might occur during the

sediment extraction (dredging), during the geotextile filtration, and treatment of the sediment, and therefore this result may be considered representative of the environmental conditions during remediation (Gambrell et al., 1991).

The addition of the chemical additives had little effect on the E_H of the system, increasing the voltage to + 394 mV prior to filtration, before reducing to + 358 mV on average as measured in the filtrate produced during the 4000 mL RDT, and ranging between + 327 mV and + 365 mV during the field scale trial. Following filtration, both the pH and reduction potential of the filtrate remained generally consistent, with no apparent trend in either metric identified over the duration of any test. It should be noted that the accuracy of the oxidation-reduction potential measurements may be less reliable than that of other parameters evaluated during the experiments. Identical samples produced 'stabilized' values, which fluctuated more than 30 mV at times, with no trend identified with respect to settling time. This finding is consistent with Gambrell et al. (1991), who investigated the effect of changes in E_H and pH of a similar sediment (section 2.6). Gambrell et al. (1991) determined that minor changes in the material may prevent a consistent measurement, yet an approximation can still be made based on the values generated. The variation in E_H for a given sample may help explain the fractions of both total and soluble metals in the filtrate.

The three E_H-pH solubility diagrams (section 2.6) which were sampled from Hermann et al. (1984) are reproduced in Figure 5.17. Superimposed on each of the three diagrams is a red marker (crosshair) which represents the average location of the pH and E_H condition of the filtrate produced during the 4000 mL RDT. An error of approximately 0.75 for pH and 0.075 V was included to compensate for variations seen throughout the

analysis. The location the marker on each diagram (pH ≈ 7.5, EH ≈ + 350 mV), suggests a qualitative rationale as to the occurrence of the dissolved and suspended metal fractions identified in the filtrate.

Figure 5.17: Solubility Diagrams for Cu(A), Pb(B), and Zn(C) sampled from Hermann et al. (1984).

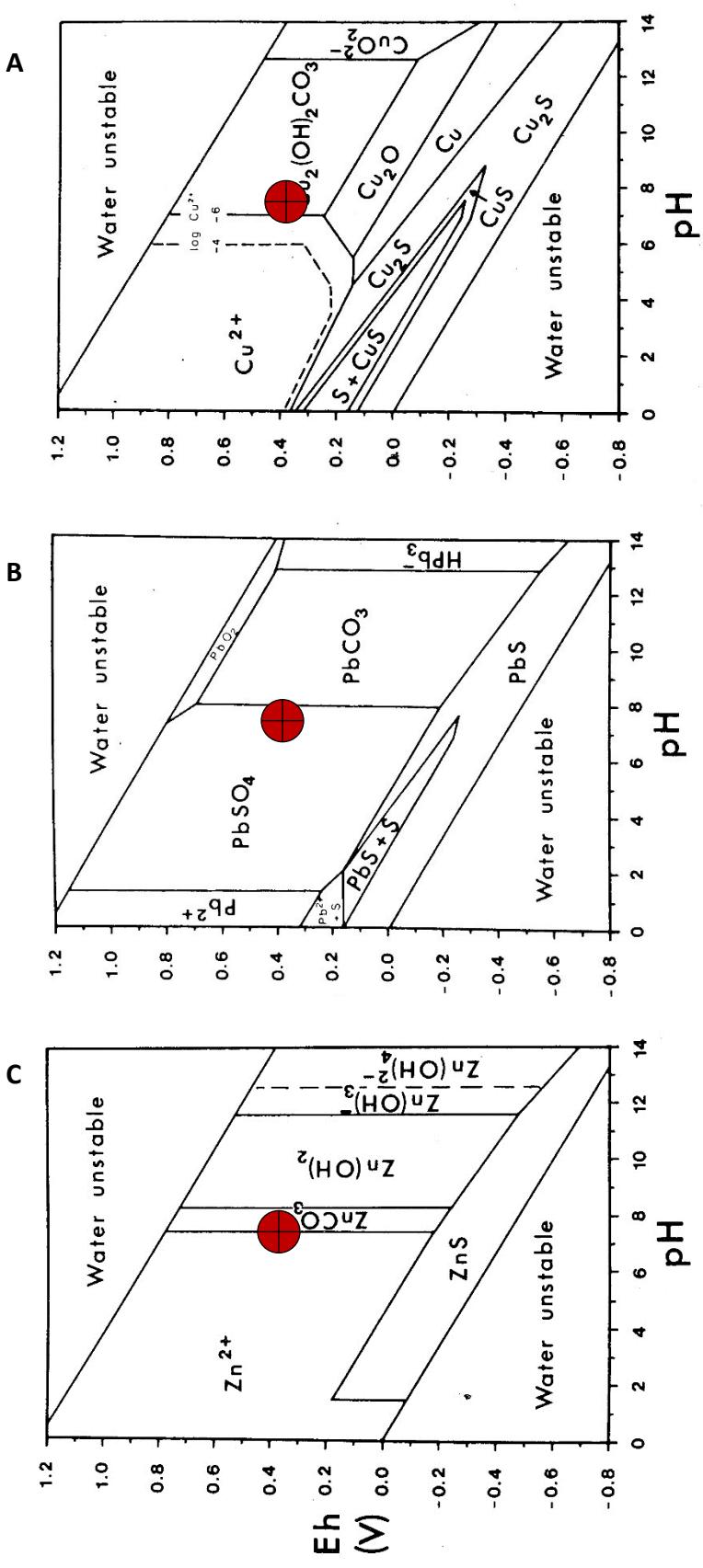

When considering copper (Figure 5.17A), the pH range spans the fields of both Cu^{2+} (dissolved) and $Cu_2(OH)_2CO_3$ (solid), however, the placement suggests a tendency toward the latter. This finding is in agreement with the experimental results presented in section 5.2 and 5.3, which show the majority (> 70 %) of the metals in the filtrate occur in the solid phase. A decrease in the pH of the system (either the basin or within the geotextile containment vessel) may encourage additional solubility of this element. Conversely, if the system were to transition to a reducing environment following filtration, a decrease in the percent dissolved may occur.

The location of the conditional marker on Figure 5.17B suggests any lead occurring in the system should exist in the solid fraction. The conditions in the filtrate mimic (to a degree) conditions the solubility diagram suggests (~99 % in the solid phase). A large increase or reduction in pH (> 11 or < 2) may increase the mobility of lead; however, a simultaneous decrease in the reduction potential would narrow the range at which this may occur.

When considering the placement of the marker on the zinc solubility diagram (Figure 5.17C), it becomes clear why the metal has a higher propensity to occur in the dissolved fraction when compared to the other two elements. The marker straddles the fields of both the charged ion Zn^{2+} as well as the uncharged molecule $ZnCo_3$, with close proximity to the $(Zn(OH)_2$ field. Due to the zinc solubility diagram being heavily partitioned along the pH axis, even a small change in the pH of the system may alter the solubility of the metal. A decrease to a more acidic condition may result in an increase in the amount of soluble zinc present in the system, and may, as a result, increase its mobility.

Conversely, an increase in pH, or if a transition to a reducing environment were to occur, a decrease in the solubility may ensue.

The solubility diagrams presented and discussed in this section provide some explanation as to why the metals appear in their respective fractions in the filtrate. When comparing the measured E_H and pH conditions in the filtrate with these diagrams, copper and zinc should appear more variable with respect to their stability immediately following filtration, while lead should generally remain undissolved. This result is confirmed by the metal concentrations measured in the filtrate throughout the experimentation conducted for this thesis. As mentioned, pH measurements fluctuated between 7.4 and 7.9, which spanned several stability fields for each of the two metals, and as a result, may have had a strong influence on solubility. Although small, the presence of dissolved lead cannot be explained by these diagrams. It is important to remember, however, that the solubility diagrams shown here are representative of ideal laboratory conditions, and do not consider the effect of other metals or constituents which may significantly alter the stability fields. As the sediment exists under field conditions, these diagrams serve to provide some rationale as to the possible range in the geochemical state of the contaminants.

CHAPTER 6: SUMMARY: CONCLUSIONS AND RECOMMENDATIONS

6.1 PREAMBLE

A comprehensive understanding of the fate and migration potential of existing contaminants (metals) is a crucial aspect of ensuring the effectiveness of any remediation technique. This statement is particularly true when assessing the viability of the geotextile filtration dewatering method, as changes in the environment may alter the mobility of certain metals found in the sediment and hence influence the water quality of the filtrate. Laboratory and field-scale experimentation to analyze the fate and transport of three metals (Cu, Pb, Zn) in a contaminated marine sediment extracted from the Boat Harbour wastewater treatment facility was applied to this problem. The primary contributions of this research are:

- The determination of the fate and migratory potential of copper, lead, and zinc, during the geotextile dewatering of the sediment under study.
- Identifying how an established filter cake deposit on the geotextile has influenced the metal transport during these operations.

6.2 SUMMARY

Characterization of the BH sediment confirmed the physical and chemical characteristics, as well as concentrations of metal contaminants, which had previously been reported. An average total copper concentration of 124 mg kg^{-1} was determined for the basin sediment, with 82 mg kg^{-1} and 1255 mg kg^{-1} found for lead and zinc respectively. In addition to the

metal contaminants, the sediment had an in-situ moisture content of greater than > 1000 %, confirming the requirement of an effective decontamination and dewatering method to be implemented during the remediation (i.e., geotubes).

In order to assess the viability of the geotextile dewatering technique and its ability to contain metals of concern, the sediment was diluted to 1 % solid content and conditioned with chemical additives in order to improve the efficiency of the geotextile. The identification of an optimal additive dosage which would encourage the flocculation of material, as well as an effective treatment procedure was determined. This conditioning included 500 ppm of a flocculating agent (7118) and 250 ppm of a cationic polymer (9244).

Two tests were applied in order to determine the efficiency of the treatment. A bench-scale analysis was first conducted to gain an understanding of the retention properties of the geotextile, and identify any influence on transport through the development of a sediment derived filter cake which accumulated on the surface of the geotextile. The filtrate produced upon conditioning and filtration was analyzed to determine the overall effectiveness of the treatment.

A reduction in TSS, from an initial concentration of 13,120 mg L^{-1} to 15.6 mg L^{-1} in the filtrate was determined (reduced by 99.9 %). In addition to TSS, a reduction of over 99.7 % was seen for particle concentration, while particles which were 65 % smaller appeared on average in the filtrate when compared to the untreated material. Total metal concentrations in the filtrate were found to be 99.4 %, 99.6 %, and 99.8 % lower than identified in the 1 % SC slurry for copper, lead, and zinc, respectively. All concentration measurements showed decreasing values as an increased volume of filter cake was deposited on the geotextile. A larger field-scale trial was then implemented to confirm the

results of the bench-scale analysis, as well as to further explore the effect of variable filter cake volume and thickness on metal reduction. All filtrate quality parameters tested during the bench-scale RDT (TSS, particle and metal concentrations) showed improvement when a thicker filter cake was created during the larger test. The effect of the added filtration was a (relatively) cleaner material with respect to particulate and metal contaminants.

Dewatering potential and filter cake analyses were also explored during the field scale trial. A reduction in the flow rate of over 99.8 % was found to occur over the duration of the field-scale experiment, as a thicker filter cake impeded the flow of the filtrate. The filter cake reached a MC which was equal to that of the in situ sediment (~800 % MC) after 24-hours and continued to consolidate over the course of 2-weeks (~500 % MC). The cake was also analyzed for metal concentration and was determined to hold > 99 % of the total mass of the three metals of concern, which was identified in the initial untreated material.

6.3 CONCLUSIONS

The dewatering trials conducted over the course of this thesis have identified the initial fate of the metal contaminants immediately upon collection. The results presented have proven that, with effective conditioning, over 99 % of the three metal contaminants considered during this study are retained by the geotextile. The migratory potential was explored through further chemical and physical analysis of the filtrate and filter cake. Apart from the size of the particles physically inhibiting migration through the geotextile, zeta potential, oxidation-reduction potential, and pH were determined to be significant contributors to the metal mobility. Immediately upon collection, the system was found to

be both a neutral (pH ≈ 7.5) and oxidizing environment ($E_H \approx +375$ mV). These conditions helped to explain the percentage of both total and dissolved metals in the filtrate.

Through the use of bench and field-scale experimentation, this thesis has demonstrated the capability of the geotextile filtration method to effectively contain metal contaminants. As unforeseen changes in the environment may influence future migration, several recommendations have been included.

6.4 RECOMMENDATIONS

- As the sediment which was analyzed during this thesis originates from a real-world contaminated site, the research conducted here may be expanded upon through monitoring of the filtrate and filter cake generated during the upcoming remediation.
- A long-term evaluation of the filter cake (i.e. leaching potential) may also be helpful in confirming the geotextiles ability to retain metals through changing environmental conditions (pH, E_H, etc.) which were discussed in this thesis.
- Additional research into the identity of the organic fraction, through techniques such as fluorescence spectroscopy, may also shed some light on the association of metals with the solid fraction. Determining a propensity to bond to a specific solid fraction present may help aid in containment, and further reduce the concentration of these contaminants in the filtrate.

REFERENCES

Ali, M., & Sreekrishnan, T. R. (2001). Aquatic toxicity from pulp and paper mill effluents: a review. Advances in environmental research, 5(2), 175-196.

Alimohammadi, M., Hoffman, E., Lyons, J. A., Walker, T. R., & Lake, C. B. (2017). Historical Sampling of Dioxin and Furan Contaminated Sediment from Pulp and Paper Effluent. GeoOttawa 2017 Conference Paper (Unpublished).

Alimohammadi, M., Tackley, H. A., Lake, C. B., Holmes, B., Davidson, K., Spooner, I. S., Jamieson, R. C., Walker, T. R. (2019a). Field and Laboratory Physical Property Characterization for a Contami-nated Sediment for Bench Scale Dewatering Purposes. Submitted to Geo-Environmental Engineering.

Alimohammadi, M., Tackley, H., Lake, C. B., Spooner, I., Walker, T. R., Jamieson, R., Gan, C., & Bossy, K. (2019b). Effect of different sediment dewatering techniques on subsequent particle sizes in industrial derived effluent. Submitted to Canadian Journal of Civil Engineering.

Allan, L., Kaufman, E., Underwood, J. (1972) Paper Profits: Pollution in the Pulp and Paper Industry. Council on Economic Priorities. Cambridge: MIT Press.

APHA, AWWA, WEF. (2005). Standard methods for the examination of water and wastewater. 522 21st Edition. Published jointly by the American Public Health Association, American Water 523 Works Association, and Water Environment Federation. New York.

ASTM International. (1998). ASTM E1508-98 Standard Guide for Quantitative Analysis by Energy-Dispersive Spectroscopy. Retrieved from https://doi.org/10.1520/E1508-98

ASTM International. (1999). ASTM D1193-99e1 Standard Specification for Reagent Water. Retrieved from https://doi.org/10.1520/D1193-99E01

ASTM International. (2002). ASTM E1829-02 Standard Guide for Handling Specimens Prior to Surface Analysis. Retrieved from https://doi.org/10.1520/E1829-02

ASTM International. (2014). ASTM D2974-14 Standard Test Methods for Moisture, Ash, and Organic Matter of Peat and Other Organic Soils. Retrieved from https://doi.org/10.1520/D2974-14

ASTM International. (2015). ASTM D2976-15 Standard Test Method for pH of Peat Materials. Retrieved from https://doi.org/10.1520/D2976-15

ASTM International. (2016a). ASTM D5464-16 Standard Test Method for pH Measurement of Water of Low Conductivity. Retrieved from https://doi.org/10.1520/D5464-16

ASTM International. (2016b). ASTM D5673-16 Standard Test Method for Elements in Water by Inductively Coupled Plasma—Mass Spectrometry. Retrieved from https://doi.org/10.1520/D5673-16

ASTM International. (2019a). ASTM D2035-19 Standard Practice for Coagulation-Flocculation Jar Test of Water. Retrieved from https://doi.org/10.1520/D2035-19

ASTM International. (2019b). ASTM D2216-19 Standard Test Methods for Laboratory Determination of Water (Moisture) Content of Soil and Rock by Mass. Retrieved from https://doi.org/10.1520/D2216-19

Bennett, E. (2013). 'We Had Something Good and Sacred Here': ReStorying A'se'k with Pictou Landing First Nation.

Betancur, M., Bonelli, P. R., Velásquez, J. A., & Cukierman, A. L. (2009). Potentiality of lignin from the Kraft pulping process for removal of trace nickel from wastewater: effect of demineralisation. Bioresource Technology, 100(3), 1130-1137.

Boat Harbour Act, SNS 2015, c 4, <http://canlii.ca/t/52rfb> retrieved on 2018-04-02

Brightwell Technologies Inc. (2009). DPA 4100 Flow Microscope. Retrieved from http://www.christison.co.uk/equipment/documents/BrightwellDPA4100Brochure-2.pdf

Cabrera, M. N. (2017). Pulp Mill Wastewater: Characteristics and Treatment. In Biological Wastewater Treatment and Resource Recovery. IntechOpen.

Cameron, J. M. (1972). Pictou County's History. Kentville, NS: Pictou County Historical Society.

Canadian Council of Ministers of the Environment (CCME). (2018). Canadian Sediment Quality Guidelines for the Protection of Aquatic Life. Canadian Environmental Quality Guidelines. Retrieved 2018-11-06 from http://st-ts.ccme.ca/

Catalyst Paper. (n.d.). How We Make Kraft Pulp, Catalyst Paper Corporation. Retrieved from https://www.catalystpaper.com/products/how/pulp. March 2019. (Web)

Chuan, M. C., Shu, G. Y., & Liu, J. C. (1996). Solubility of heavy metals in a contaminated soil: effects of redox potential and pH. Water, Air, and Soil Pollution, 90(3-4), 543-556.

Crist, R., Martin, J., & Crist, D. (2002). Heavy Metal Uptake by Lignin: Comparison of Biotic Ligand Models with an Ion-Exchange Process. Environmental Science Technology, 1485-1490.

Davidson, K. B. (2018). Spatiotemporal assessment of metal concentrations of pre-effluent estuarine sediments in a freshwater kraft pulp mill tailings pond in Pictou County, Nova Scotia, using paleolimnological methods. Unpublished Thesis.

Davidson, K. B. (2020). Assessing Ultraviolet Optical Screening Tool Technology for Delineating an In-Situ Contaminated Sediment Layer. Unpublished Thesis.

Di Luca, G. A., Maine, M. A., Mufarrege, M. M., Hadad, H. R., Sánchez, G. C., & Bonetto, C. A. (2011). Metal retention and distribution in the sediment of a constructed wetland for industrial wastewater treatment. Ecological Engineering, 37(9), 1267-1275.

Dillon Consulting Limited. (2019). Northern Pulp Nova Scotia Effluent Treatment Facility Environmental Assessment Registration Document. Halifax, Nova Scotia. Northern Pulp Nova Scotia. File No. 17-6461-1300

Dore, S. (2018, January 4). Personal communication with Dr. S. Dore [GHD Limited – Buffalo NY].

Fatema, N., & Bhatia, S. K. (2018). Sediment Retention and Clogging of Geotextile with High Water Content Slurries. International Journal of Geosynthetics and Ground Engineering, 4(2), 13.

Fowler, J., Bagby, R. M., & Trainer, E. (2000). Dewatering sewage sludge with geotextile tubes. In Dredged Material Management–Options and Environmental Considerations, Proc. of a conference, MIT Sea Grant College Program (pp. 80-83).

Furley, T. H., & de Oliveira Filho, A. C. (2000). Biomonitoring of heavy metals and organo-chlorinated compounds in a pulp mill effluent using introduced mussels. Aquatic Ecosystem Health & Management, 3(4), 499-507.

Gambrell, R. P., Wiesepape, J. B., Patrick, W. H., & Duff, M. C. (1991). The effects of pH, redox, and salinity on metal release from a contaminated sediment. Water, Air, and Soil Pollution, 57(1), 359-367.

Garrels, R. M., & Christ, C. L. (1965). Minerals, solutions, and equilibria. Minerals, solutions, and equilibria. Harper Row. New York, New York.

Gauthier, G., Burke, A. L., & Leclerc, M. (2012). Assessing XRF for the geochemical characterization of radiolarian chert artifacts from northeastern North America. Journal of Archaeological Science, 39(7), 2436-2451.

GHD Limited. (2018a). Phase 2 Environmental Site Assessment, Boat Harbour Remediation Planning and Design. Pictou County, Nova Scotia. Nova Scotia Lands, Inc. Project No. 11148275, Report No. 6.

GHD Limited. (2018b). Remedial Option Decision Document, Boat Harbour Remediation Planning and Design. Pictou County, Nova Scotia. Nova Scotia Land, Inc. Project No. 11148275, Report No. 5.

Gregory, J., & Barany, S. (2011). Adsorption and flocculation by polymers and polymer mixtures. Advances in colloid and interface science, 169(1), 1-12.

Hach Company (2014). Method 8006: Suspended Solids, Photometric 558 Method (750 mg/L). DOC316.53.01139

Hem, J. D. (1972). Chemistry and occurrence of cadmium and zinc in surface water and groundwater. Water Resources Research, 8(3), 661-679.

Hermann, R., & Neumann-Mahlkau, P. (1985). The mobility of zinc, cadmium, copper, lead, iron and arsenic in ground water as a function of redox potential and pH. Science of the Total Environment, 43(1-2), 1-12.

Hoffman, E., Bernier, M., Blotnicky, B., Golden, P. G., Janes, J., Kader, A., Kovacs-Da Costam R., Pettipas, S., Vermeulen, S., & Walker, T. R. (2015). Assessment of public perception and environmental compliance at a pulp and paper facility: a Canadian case study. Environmental monitoring and assessment, 187(12), 766.

Hoffman, E., Lyons, J., Boxall, J., Robertson, C., Lake, C. B., & Walker, T. R. (2017). Spatiotemporal assessment (quarter century) of pulp mill metal (loid) contaminated sediment to inform remediation decisions. Environmental monitoring and assessment, 189(6), 257.

Holmes, B. E. J. (2018). Application of the paleolimnological method in the environmental assessment of pulp mill effluent-influenced freshwater sediment in Pictou County, Nova Scotia. Unpublished Thesis.

Igathinathane, C., Pordesimo, L. O., Columbus, E. P., Batchelor, W. D., & Methuku, S. R. (2008). Shape identification and particles size distribution from basic shape parameters using ImageJ. Computers and electronics in agriculture, 63(2), 168-182.

JWEL & Beak Consultants Limited. (1992). An Investigation of Sediment Characteristics at Boat Harbour Treatment Facilities. Dartmouth, Nova Scotia. Nova Scotia Department of Supply and Services. Project No. 8109

JWEL & Beak Consultants Limited. (1993). Remediation Alternatives – Phase 2 Boat Harbour Treatment Facility. Dartmouth, Nova Scotia. Nova Scotia Department of Supply and Services. Project No. 8660.

Keppie, J. D. (2000). Geological Map of the Province of Nova Scotia. NS Department of Natural Resources. Minerals and Energy Branch. Map ME2000-1. Scale, 1(500,000).

Lacorte, S., Latorre, A., Barcelo´, D., Rigol, A., Malmqvist, A., & Welander, T. (2003). Organic compounds in paper-mill process waters and effluents. Trends in Analytical Chemistry, 725-737.

Lange, K., Rowe, R. K., & Jamieson, H. (2004). Metal migration in geosynthetic clay liners. In Proceedings of the GeoQuebec2004 (October) Conference Quebec.

Larsson, M., Hill, A., & Duffy, J. (2012). Suspension stability; why particle size, zeta potential and rheology are important. Ann. Trans. Nordic Rheol. Soc, 20, 209-214.

Lassabatere, L., Winiarski, T., & Galvez-Cloutier, R. (2004). Retention of three heavy metals (Zn, Pb, and Cd) in a calcareous soil controlled by the modification of flow with geotextiles. Environmental science & technology, 38(15), 4215-4221.

Lewinsky, A. A. (2007). Hazardous materials and wastewater: treatment, removal and analysis. Nova Publishers.

Lu, G. W., & Gao, P. (2010). Emulsions and microemulsions for topical and transdermal drug delivery. In Handbook of non-invasive drug delivery systems (pp. 59-94). William Andrew Publishing.

Malvern Instruments Ltd. (2019). Zetasizer Nano ZS Specifications. Worcestershire, UK. Retrieved from https://www.malvernpanalytical.com/en/products/product-range/zetasizer-range/zetasizer-nano-range/zetasizer-nano-zs

Martinez, C. E., & Motto, H. L. (2000). Solubility of lead, zinc and copper added to mineral soils. Environmental pollution, 107(1), 153-158.

Mastin, B. J., Lebster, G. E., & Salley, J. R. (2008). Use of Geotube® dewatering containers in environmental dredging. Proceedings of GeoAmericas, 143-151.

Maximova, N., Österberg, M., Koljonen, K., & Stenius, P. (2001). Lignin adsorption on cellulose fibre surfaces: effect on surface chemistry, surface morphology and paper strength. Cellulose, 8(2), 113-125.

McMaster, M. E., Mark Hewitt, L., & Parrott, J. L. (2006). A decade of research on the environmental impacts of pulp and paper mill effluents in Canada: field studies and mechanistic research. Journal of Toxicology and Environmental Health, Part B, 9(4), 319-339.

Moo-Young, H. K., Gaffney, D. A., & Mo, X. (2002). Testing procedures to assess the viability of dewatering with geotextile tubes. Geotextiles and Geomembranes, 20(5), 289-303.

Moo-Young, H., Myers, T. E., Townsend, D., & Ochola, C. (1999). The migration of contaminants through geosynthetic fabric containers utilized in dredging operations. Engineering Geology, 53(2), 167-176.

Mulligan, C. N., Davarpanah, N., Fukue, M., & Inoue, T. (2009). Filtration of contaminated suspended solids for the treatment of surface water. Chemosphere, 74(6), 779-786.

Mulligan, C. N., Yong, R. N., & Gibbs, B. F. (2001). An evaluation of technologies for the heavy metal remediation of dredged sediments. Journal of hazardous materials, 85(1-2), 145-163.

Muthukumaran, A. E., & Ilamparuthi, K. (2006). Laboratory studies on geotextile filters as used in geotextile tube dewatering. Geotextiles and Geomembranes, 24(4), 210-219.

Northern Pulp. (2015). About Bill no. 89: Boat Harbour Act. Retrieved 2019–02-15 from http://nslegislature.ca/.

Northern Pulp. (nd). Kraft Process at Northern Pulp. Northern Pulp Nova Scotia Corporation. Retrieved from http://www.paperexcellence.com/northern-pulp. March 2019. (Web)

Ogden, J. G. (1972). Oxygen demand of effluent from a bleached kraft pulp mill. Water, Air, and Soil Pollution, 1(4), 365-374.

Pettersen, R. C. (1984). The chemical composition of wood. The chemistry of solid wood, 207, 57-126.

Pokhrel, D., & Viraraghavan, T. (2004). Treatment of pulp and paper mill wastewater—a review. Science of the total environment, 333(1-3), 37-58.

Rahman, M. S., Saha, N., Molla, A. H., & Al-Reza, S. M. (2014). Assessment of anthropogenic influence on heavy metals contamination in the aquatic ecosystem components: water, sediment, and fish. Soil and Sediment Contamination: An International Journal, 23(4), 353-373.

Reddy, K. J., Wang, L., & Gloss, S. P. (1995). Solubility and mobility of copper, zinc and lead in acidic environments. Plant and Soil, 171(1), 53-58.

Rima, U. S. (2013). Characterization and centrifuge dewatering of oil sands fine tailings (Doctoral dissertation, Faculty of Graduate Studies and Research, University of Regina).

Rust Associates Ltd. & Nova Scotia Water Resources Commission. (1970). A review of the Boat Harbour waste treatment facilities for Nova Scotia Water Resources Commission; appendix. Montreal.

Sawidis, T., Marnasidis, A., Zachariadis, G., & Stratis, J. (1995). A study of air pollution with heavy metals in Thessaloniki city (Greece) using trees as biological indicators. Archives of Environmental Contamination and Toxicology, 28(1), 118-124.

Siepmann, R., von der Kammer, F., & Förstner, U. (2004) Possible Filtration Techniques to Prevent Particle-Bound Transport of Heavy Metals in Filtration Units for Urban Run-Off.

Skipperud, L., Salbu, B., & Hagebø, E. (1998a). Speciation of trace elements in discharges from the pulp industry. Science of the total environment, 217(3), 251-256.

Skipperud, L., Salbu, B., & Hagebø, E. (1998b). Transfer, pathways, enrichment and discharge of trace elements in the pulp industry measured by means of neutron activation analysis. Science of the total environment, 216(1-2), 133-146.

Smith, M. (2002). Geotextile tubes in environmental applications. Global Synthetics Pty Ltd. Girraween, Australia.

Smook, G. A. (1992). Handbook for Pulp & Paper Technologist: Angus Wilde Publication.

Song, X. (2019). Evaluating 50 Plus Years of Contaminant Migration into a Marine Sediment. Unpublished Thesis.

Spooner, I., & Dunnington, D. (2016): Boat Harbour Gravity Core Sediment Survey. Report to Nova Scotia Lands Inc.

Stantec Consulting Ltd. (2016) Final Report: Geotechnical and Contaminant Assessment. Report to Nova Scotia Lands Inc. File No: 121413919.

Stea, R. R., Conley, H., Brown, Y. (1992). Surficial Geology. NS Department of Natural Resources. Minerals and Energy Branch. Map 92-3. Scale, 1(500,000).

Suhr, M., Klein, G., Kourti, I., Gonzalo, M. R., Santonja, G. G., Roudier, S., & Sancho, L. D. (2015). Best available techniques (BAT) reference document for the production of pulp, paper and board. European Commission.

Tack, F. M., O. W. J. J. Callewaert, and M. G. Verloo. "Metal solubility as a function of pH in a contaminated, dredged sediment affected by oxidation." Environmental pollution 91, no. 2 (1996): 199-208.

TenCate Corporation. (2015). Geotube® Dewatering Container (Standard Dewatering Specification). Version 15.

TenCate Corporation. (n.d.a). Geotube® RDT Test A Fast And Easy Way To Measure Dewatering Efficiency and Polymer Selection. Retrieved from https://bishopwater.ca/wp/wp-content/uploads/2017/01/20160428115925_bro_rdt.pdf

TenCate Corporation. (n.d.b). TenCate Geotube GDT Test A Demonstration of Geotube® Dewatering Technology. Retrieved from https://bishopwater.ca/wp/wp-content/uploads/2017/01/20160428120126_gdt-low-resolution.pdf

TenCate Corporation. (2017). Solutions. Web. Retrieved from https://www.tencategeo.us/en-us/solutions (Web)

Thacker, N. P., Nitnaware, V. C., Das, S. K., & Devotta, S. (2007). Dioxin formation in pulp and paper mills of India. Environmental Science and Pollution Research-International, 14(4), 225-226.

US EPA. (1995). EPA office of compliance sector notebook project: profile of pulp and paper industry. Washington, DC

Watts, M., & Trainer, E. (2010). Disposal of coal mine slurry waste using geotextile containers at the North River Mine, Chevron Mining Inc. Tailings and Mine Waste 2010, 265.

Wong, S. S., Teng, T. T., Ahmad, A. L., Zuhairi, A., & Najafpour, G. (2006). Treatment of pulp and paper mill wastewater by polyacrylamide (PAM) in polymer induced flocculation. Journal of Hazardous Materials, 135(1-3), 378-388.

Yee, T. W., Lawson, C. R., Wang, Z. Y., Ding, L., & Liu, Y. (2012). Geotextile tube dewatering of contaminated sediments, Tianjin Eco-City, China. Geotextiles and Geomembranes, 31, 39-50.

APPENDIX 1: TOTAL METAL CONCENTRATION (ICP – OES)

Table A 1: 1 % Solid content (Slurry).

	mg/kg							
Sample	Ag	Al	As	Ba	Be	Bi	Ca	Cd
Ref. Value	0.7	5719	11	212	<0.5	<5	47709	3
Black Boat Hbr Sludge	6.4	7218	6	390	<0.5	8	31780	14
	Ce	Co	Cr	Cu	Fe	Ga	Ge	In
Ref. Value	<50	10	43	380	43900	<10	<50	<50
Black Boat Hbr Sludge	<50	7	28	124	11585	<10	<50	<50
	K	La	Li	Mg	Mn	Mo	Na	Nb
Ref. Value	988	<5	6	6983	570	4	326	<10
Black Boat Hbr Sludge	1711	<5	13	5530	2000	9	24857	<10
	Ni	P	Pb	S	Sb	Se	Sn	Sr
Ref. Value	43	1355	679	1636	5	<5	231	100
Black Boat Hbr Sludge	30	1570	81	25590	2	<5	<5	97
	Ta	Te	Ti	Tl	V	W	Zn	Zr
Ref. Value	<10	<10	150	<10	12	<5	1160	<5
Black Boat Hbr Sludge	<10	<10	109	<10	85	<5	1253	<5

Table A 2: Undiluted sediment.

	mg/kg							
Sample	Ag	Al	As	Ba	Be	Bi	Ca	Cd
Ref. Value	0.6	5453	11	224	<0.5	<5	47792	3
Black Boat Hbr Sludge #2	5.9	7860	6	368	<0.5	<5	32592	15
	Ce	Co	Cr	Cu	Fe	Ga	Ge	In
Ref. Value	<50	7	56	372	43146	<5	<50	<50
Black Boat Hbr Sludge #2	<50	4	36	125	13428	<5	<50	<50
	K	La	Li	Mg	Mn	Mo	Na	Nb
Ref. Value	910	13	11	7058	573	4	284	<10
Black Boat Hbr Sludge #2	1126	8	26	6021	2152	10	6264	<10
	Ni	P	Pb	S	Sb	Se	Sn	Sr
Ref. Value	43	1277	651	1544	7	<5	239	97
Black Boat Hbr Sludge #2	35	1596	83	18192	2	<5	3	91
	Ta	Te	Ti	Tl	V	W	Zn	Zr
Ref. Value	<10	<10	119	<5	12	<5	1088	2
Black Boat Hbr Sludge #2	<10	<10	94	<5	84	<5	1259	<1

Table A 3: Field scale filter cake

Sample	mg/kg							
	Ag	Al	As	Ba	Be	Bi	Ca	Cd
Ref. Value	<1	11897	17	468	0.5	<5	49338	3
BH Field Scale Filter Cake	5.9	8329	4	342	0.6	<5	31816	15
	Ce	Co	Cr	Cu	Fe	Ga	Ge	In
Ref. Value	<50	12	91	412	72494	<5	<50	<50
BH Field Scale Filter Cake	<50	6	22	131	12915	<5	<50	<50
	K	La	Li	Mg	Mn	Mo	Na	Nb
Ref. Value	2172	730	16	9640	724	5	653	<10
BH Field Scale Filter Cake	585	335	13	4510	2101	2	2778	<10
	Ni	P	Pb	S	Sb	Se	Sn	Sr
Ref. Value	50	1325	681	1768	<10	<10	441	115
BH Field Scale Filter Cake	34	1618	86	21012	<10	<10	<5	90
	Ta	Te	Ti	Tl	V	W	Zn	Zr
Ref. Value	<10	<10	629	<10	27	<5	1152	<5
BH Field Scale Filter Cake	<10	<50	151	<10	102	77	1229	<5

APPENDIX 2: SMALL SCALE DOSAGE VOLUMES

Table A 4: Small scale trial and error dosage volumes.

Sample ID	White Polymer (9244)		Orange Polymer (7118)		Optical Improvement		Selected for Jar Test
	mL	%	mL	%	yes	No	
SS1	1.5	5.00	1	3.333	yes		
SS2	1.5	5.00	3	10.000	yes		
SS3	1.5	5.00	5	16.667		no	
SS4	2	6.67	1	3.333	yes		yes
SS5	2	6.67	3	10.000	yes		
SS6	2	6.67	5	16.667		no	
SS7	2.5	8.33	1	3.333	yes		
SS8	2.5	8.33	3	10.000	yes		
SS9	2.5	8.33	5	16.667		no	
SS10	3	10.00	1	3.333	yes		yes
SS11	3	10.00	3	10.000	yes		
SS12	3	10.00	5	16.667		no	
SS13	1.5	5.00	0.3	1.000		no	
SS14	1.5	5.00	0.9	3.000	yes		
SS15	1.5	5.00	1.5	5.000	yes		yes
SS16	2	6.67	0.3	1.000		no	
SS17	2	6.67	0.9	3.000	yes		
SS18	2	6.67	1.5	5.000	yes		yes
SS19	2.5	8.33	0.3	1.000		no	
SS20	2.5	8.33	0.9	3.000	yes		yes
SS21	2.5	8.33	1.5	5.000	yes		yes
SS22	3	10.00	0.3	1.000	yes		
SS23	3	10.00	0.9	3.000	yes		yes
SS24	3	10.00	1.5	5.000	yes		yes
SS25 PM	1.5	5.00	1.5	5.000	yes		yes

APPENDIX 3: 4000 ML RDT DATA

Table A 5: 4000 mL RDT total suspended solids average and statistical data.

TSS (ug/L)									
Sample ID	mL	Min	Q1	Median	Q3	Max	Average	High Whisker	Low Whisker
1	200	34	43	62	81	86	55.67	30.33	21.67
2	400	32	36	45	54	58	46.33	11.67	14.33
3	600	35	36	43.5	51	53	43.89	9.11	8.89
4	800	34	40	40	41	45	39.89	5.11	5.89
5	1000	31	36	36.5	38	39	36.44	2.56	5.44
6	1200	19	22.00	28.50	36.00	36.00	30.22	5.78	11.22
7	1400	33	36.00	39.50	43.00	43.00	38.22	4.78	5.22
8	1600	32	39.00	44.00	49.00	51.00	43.44	7.56	11.44
9	1800	30	31	33	36	39	34.33	4.67	4.33
10	2000	32	32	37	42	50	37.11	12.89	5.11
11	2200	22	25	26.5	29	30	27.22	2.78	5.22
12	2400	23	24	25	26	27	25.11	1.89	2.11
13	2600	35	35	37	37	38	36.33	1.67	1.33
14	2800	25	29	32.5	36	37	32.44	4.56	7.44
15	3000	19	20	24.5	29	30	25.22	4.78	6.22
16	3200	12	15	20	25	25	20.44	4.56	8.44
17	3400	13	14	18	18	18	16.44	1.56	3.44
18	3600	12	13	15	20	21	16.56	4.44	4.56
19	3800	15	19	21.5	22	23	20.11	2.89	5.11
20	4000	8	10	16	22	23	15.78	7.22	7.78

Table A 6: 4000 mL RDT particle size and concentration average and statistical data.

Particle Concentration (#/mL)				
Trial	Volume	Mean	Min	Max
1	200	304396.6	175580.4	386481.7
2	400	389664	209916.9	513381.1
3	600	382027.9	195700.6	493951.6
4	800	353972.3	201876.8	446161.2
5	1000	312147.6	234924.7	361651.9
6	1200	282584.3	164676.4	351479.1
7	1400	348562.1	308111.7	400988.3
8	1600	382946.5	303770	458215.9
9	1800	278417.7	246562.8	302252.7
10	2000	275580	244023.5	313151.6
11	2200	206894	134484.9	259332.6
12	2400	176238.2	126291.9	215860.3
13	2600	318547.1	292385.1	335484.4
14	2800	236548.6	138228.9	306868.3
15	3000	213960.1	99801.03	284627.9
16	3200	160819.5	66616.16	213365.5
17	3400	148466.5	81359.41	184612.4
18	3600	110483.7	51199.85	146831.8
19	3800	162037.3	136467.3	178821.9
20	4000	101840.5	41234.12	169422

Particle Size (um)				
Trial	Volume	Mean	Min	Max
1	200	3.287	3.000	3.510
2	400	3.050	2.860	3.180
3	600	3.003	2.800	3.110
4	800	2.967	2.690	3.220
5	1000	2.790	2.680	2.920
6	1200	2.743	2.660	2.880
7	1400	2.960	2.810	3.130
8	1600	2.870	2.750	3.040
9	1800	2.827	2.720	2.970
10	2000	2.847	2.780	2.970
11	2200	2.750	2.650	2.840
12	2400	2.803	2.680	2.980
13	2600	2.870	2.780	2.950
14	2800	2.757	2.610	2.920
15	3000	2.773	2.640	2.910
16	3200	2.703	2.490	2.880
17	3400	2.630	2.490	2.720
18	3600	2.663	2.520	2.890
19	3800	2.727	2.660	2.840
20	4000	2.600	2.480	2.670

Metal Data – 4000 mL RDT

Table A 7: 4000 mL RDT copper measurement data for total and dissolved metal.

Copper (ug/L)							
		Mean Total	Min	Q1	Med	Q3	Max
1	200	17.95	12.44	12.78	14.02	26.87	27.62
2	400	11.50333	10.8	11.15	11.52	11.9725	12.03
3	600	7.9145	7.349	7.35875	7.84	8.43675	8.624
4	800	8.585167	6.296	6.50375	8.6225	10.715	10.76
5	1000	7.393889	5.831	5.978	8.057	8.141	8.279
6	1200	5.823833	5.664	5.7525	5.809	5.87675	6.028
7	1400	7.845444	6.062	6.164	7.893	9.367	9.655
8	1600	6.162333	6.035	6.1305	6.1765	6.20975	6.25
9	1800	7.2265	6.182	6.31925	7.219	8.15475	8.253
10	2000	6.513	5.555	5.647	6.585	7.323	7.452
11	2200	5.600333	4.647	4.795	5.582	6.44925	6.52
12	2400	5.834667	4.545	4.691	5.3	7.506	7.686
13	2600	6.252833	5.873	5.99625	6.255	6.54825	6.578
14	2800	4.5995	4.425	4.48	4.5445	4.73725	4.823
15	3000	5.808444	4.829	5	6.108	6.308	6.436
16	3200	5.136833	4.693	4.729	5.109	5.534	5.632
17	3400	4.562667	4.106	4.15425	4.5685	4.97525	5.006
18	3600	4.637667	4.442	4.51175	4.65	4.783	4.791
19	3800	5.839556	5.199	5.503	5.616	6.48	6.566
20	4000	4.429444	3.946	4.083	4.533	4.73	4.757
Mean Dissolved							
2	400	3.707					
6	1200	2.5365					
11	2200	1.831					
15	3000	1.941667					
19	3800	2.352667					
20	4000	2.452667					

Table A 8: 4000 mL RDT lead measurement data for total and dissolved metal.

Lead (ug/L)							
		Mean Total	Min	Q1	Med	Q3	Max
1	200	15.5	10.34	10.51	14.44	21.42	21.92
2	400	7.740833	7.276	7.40275	7.71	8.123	0.008188
3	600	6.778333	6.025	6.109	6.757	7.462	0.007541
4	800	23.359	8.277	8.41075	23.142	38.285	0.03876
5	1000	9.829889	4.442	4.591	8.07	16.77	0.01702
6	1200	5.271833	4.987	5.10375	5.2485	5.47575	0.00554
7	1400	8.561444	4.353	4.45	8.18	12.94	0.00824
8	1600	8.497833	6.342	6.40875	8.4625	10.6025	0.01068
9	1800	17.47167	16.83	17.265	17.45	17.8	0.01798
10	2000	8.012222	3.457	3.591	5.609	14.7	0.01506
11	2200	13.71917	7.342	7.46575	13.584	20.0375	0.02019
12	2400	13.74089	8.008	8.18	15.91	16.9	0.01604
13	2600	14.79667	13.85	14.1225	14.75	15.565	0.01568
14	2800	5.440667	3.775	3.86075	5.416	7.0365	0.007118
15	3000	9.527	5.367	5.432	7.367	15.56	0.01604
16	3200	11.36367	9.19	9.323	11.4035	13.43	0.01345
17	3400	10.54833	4.645	4.77825	10.4455	16.355	0.01654
18	3600	9.117	8.322	8.43775	9.074	9.843	0.009907
19	3800	14.19944	8.273	8.502	15.18	18.86	0.0154
20	4000	6.776556	5.272	5.414	6.735	8.188	0.008353
		15.5	10.34	10.51	14.44	21.42	21.92
Mean Dissolved							
2	400	0.9165					
6	1200	0.07					
11	2200	0.086					
15	3000	0.0615					
19	3800	0.078667					
20	4000	0.942					

Table A 9: 4000 mL RDT zinc measurement data for total and dissolved metal.

Zinc (ug/L)							
		Mean Total	Min	Q1	Med	Q3	Max
1	200	85.88	50.64	51.29	80.9	123.6	126.9
2	400	46.065	37.24	38.19	45.945	54.2925	54.58
3	600	36.03333	32.78	32.96	35.94	39.0325	39.51
4	800	87.30167	33.99	34.805	86.71	140.1	141
5	1000	47.57667	29	29.41	34.21	78.45	79.8
6	1200	27.89667	26.49	26.94	27.69	29.0325	29.34
7	1400	37.43667	21.74	22.37	34.55	55.25	56.23
8	1600	43.02667	27.36	27.455	42.775	58.5825	59.05
9	1800	77.82333	70.4	71.44	77.405	84.6375	85.23
10	2000	58.35	48.07	48.85	61.88	64.04	65.92
11	2200	55.505	32.59	33.215	55.145	77.525	79.26
12	2400	54.75222	38.82	39.51	59.52	64.75	66.04
13	2600	56.515	54.59	55.505	56.055	57.58	58.98
14	2800	27.96167	17.67	17.7525	27.83	38.1325	38.48
15	3000	47.77778	29.04	30.11	52.1	60.06	62.65
16	3200	55.24167	41.88	42.5575	55.105	68.0275	68.65
17	3400	36.405	19.9	20.14	36.135	52.6475	53.3
18	3600	51.98667	41.76	43.0125	52.195	61.2725	61.52
19	3800	55.31222	44.94	45.6	58.54	61.25	62.34
20	4000	32.84333	24.46	24.87	31.55	42.1	42.65
Mean Dissolved							
1	200	35.18					
2	400	24.4					
3	600	18.8					
5	1000	19.16					
8	1600	16.79					
9	1800	20.65					
13	2600	26.02					
16	3200	21.535					
18	3600	18.695					

APPENDIX 4: FIELD TRIAL DATA

Table A 10: Field Trial TSS data.

Sample ID	Time (s)	Total Time (s)	1	2	3	Average
Trial 1	15	15	324	319	355	332.7
	30	30	45	40	45	43.3
	45	45	34	33	32	33.0
	60	60	27	28	26	27.0
	75	75	27	26	25	26.0
	90	90	20	20	20	20.0
	105	105	22	20	20	20.7
	120	120	20	20	20	20.0
	150	150	18	18	17	17.7
	180	180	17	17	16	16.7
	240	240	12	15	16	14.3
	600	600	18	18	18	18.0
Trial 2	15	615	1	2	3	2.0
	30	630	3	2	1	2.0
	45	645	0	1	1	0.7
	60	660	5	4	4	4.3
	75	675	2	1	1	1.3
	90	690	3	2	4	3.0
	105	705	6	4	4	4.7
	120	720	4	3	3	3.3
	150	750	7	6	5	6.0
	180	780	5	5	5	5.0
	300	900	8	6	6	6.7
	600	1200	4	4	4	4.0
	1500	2100	2	1	1	1.3
	3600	4200	4	4	4	4.0
	5400	6000	3	2	2	2.3
	7200	7800	2	2	2	2.0

Table A 11: Field Trial Particle concentration and mean grain size.

Sample ID	Time	Total time	Mean Grain Size (µm)	Particle Concentration (#/ml)
1.15	15	15	2.99	228041.3581
1.30	30	30	2.59	293147.1419
1.45	45	45	2.65	287235.6937
1.60	60	60	3.58	NA
1.75	75	75	2.62	247502.8221
1.90	90	90	2.59	179458.4257
1.105	105	105	2.6	167348.0563
1.120	120	120	2.59	156339.6667
1.150	150	150	2.61	162554.5586
1.180	180	180	2.61	161678.4505
1.240	240	240	2.6	132547.8559
1.600	600	600	2.6	155525.1599
2.15	15	615	3.07	38941.1802
2.30	30	630	3.12	34905.1509
2.45	45	645	3.27	919.4572
2.60	60	660	2.46	4355.4437
2.75	75	675	3.81	6919.8851
2.90	90	690	5.92	8072.0586
2.105	105	705	2.75	16623.2387
2.120	120	720	2.67	16089.3604
2.150	150	750	2.42	10819.0225
2.180	180	780	3.15	49465.8851
2.300	300	900	2.95	13456.473
2.600	600	1200	4.45	4467.2387
2.1500	1500	2100	6.25	6340.3761
2.3600	3600	4200	3.67	28457.5428
2.5400	5400	6000	4.46	9867.6239
2.7200	7200	7800	4.09	14143.214

Table A 12: Field trial copper measurement data for total and dissolved metal.

Copper (mg/L)						
			Mean Total	Min	Med	Max
	15	1.15	0.04063	0.03984	0.04083	0.04122
	30	1.3	0.002237	0.002178	0.002263	0.00227
	45	1.45	0.00258	0.002571	0.002577	0.002593
	60	1.6	0.00268	0.00263	0.002703	0.002706
	75	1.75	0.00274	0.002674	0.002733	0.002813
	90	1.9	0.003222	0.003189	0.003208	0.003269
	105	1.105	0.002093	0.002043	0.002099	0.002136
	120	1.12	0.0018	0.001756	0.001821	0.001823
	150	1.15	0.001915	0.001898	0.001908	0.00194
	180	1.18	0.001298	0.001253	0.001314	0.001327
	240	1.24	0.004507	0.00444	0.004522	0.004559
	600	1.6	0.002723	0.002682	0.002728	0.00276
15	615	2.15	0.002793	0.002774	0.002785	0.002821
30	630	2.3	0.002366	0.002339	0.002341	0.002418
45	645	2.45	0.003237	0.003215	0.003225	0.003271
60	660	2.6	0.003226	0.003218	0.003222	0.003238
105	705	2.105	0.001141	0.00112	0.001147	0.001157
120	720	2.12	0.001881	0.001836	0.001884	0.001923
150	750	2.15	0.00198	0.001945	0.001985	0.002009
180	780	2.18	0.002577	0.002559	0.002565	0.002608
300	900	2.3	0.001349	0.001328	0.001344	0.001374
600	1200	2.6	0.001842	0.001824	0.00184	0.001862
1500	2100	2.15	0.001147	0.00114	0.001141	0.001159
3600	4200	2.36	0.002179	0.002138	0.002182	0.002217
5400	6000	2.54	0.002747	0.002705	0.002744	0.002791
7200	7800	2.72	0.000753	0.000741	0.000755	0.000762
Mean Dissolved						
	30	1.3	0.000851			
	60	1.6	0.000867			
	120	1.12	0.000404			
	600	1.6	0.000403			
15	615	2.15	0.001333			
45	645	2.45	0.001456			
180	780	2.18	0.000295			
3600	4200	2.36	0.000417			
7200	7800	2.72	0.000201			

Table A 13: Field trial lead measurement data for total and dissolved metal.

Lead (mg/L)						
			Mean Total	Min	Med	Max
	15	1.15	0.03624	0.03554	0.03649	0.03669
	30	1.3	0.008231	0.008129	0.008256	0.008308
	45	1.45	0.008226	0.008116	0.008255	0.008306
	60	1.6	0.011663	0.01148	0.01175	0.01176
	75	1.75	0.01435	0.01422	0.01439	0.01444
	90	1.9	0.02346	0.02323	0.02349	0.02366
	105	1.105	0.01418	0.01398	0.01425	0.01431
	120	1.12	0.010703	0.01049	0.01079	0.01083
	150	1.15	0.013803	0.01365	0.01383	0.01393
	180	1.18	0.007306	0.007173	0.007336	0.007409
	240	1.24	0.007178	0.007098	0.007208	0.007227
	600	1.6	0.01478	0.01407	0.01506	0.01521
15	615	2.15	0.007056	0.006991	0.007077	0.007101
30	630	2.3	0.008682	0.008307	0.008806	0.008932
45	645	2.45	0.008301	0.00824	0.008306	0.008356
60	660	2.6	0.007309	0.007255	0.007323	0.007348
105	705	2.105	0.003958	0.003912	0.003967	0.003995
120	720	2.12	0.008211	0.008122	0.008244	0.008267
150	750	2.15	0.012767	0.01263	0.01283	0.01284
180	780	2.18	0.01947	0.01921	0.01958	0.01962
300	900	2.3	0.004937	0.004888	0.004949	0.004975
600	1200	2.6	0.009467	0.009345	0.009522	0.009534
1500	2100	2.15	0.003885	0.003843	0.003898	0.003915
3600	4200	2.36	0.02269	0.02149	0.023	0.02358
5400	6000	2.54	0.022203	0.02116	0.02263	0.02282
7200	7800	2.72	0.0041	0.004059	0.004108	0.004132
Mean Dissolved						
	30	1.3	0.00017			
	60	1.6	0.000192			
	120	1.12	0.000263			
	600	1.6	0.00012			
15	615	2.15	0.000102			
45	645	2.45	0.00008			
180	780	2.18	0.000095			
3600	4200	2.36	0.000117			
7200	7800	2.72	0.000111			

Table A 14: Field trial zinc measurement data for total and dissolved metal.

Zinc (mg/L)						
			Mean Total	Min	Med	Max
	15	1.15	0.4101	0.402	0.4137	0.4146
	30	1.3	0.05493	0.05434	0.05496	0.05549
	45	1.45	0.143967	0.142	0.1448	0.1451
	60	1.6	0.1565	0.1546	0.1572	0.1577
	75	1.75	0.147333	0.1458	0.1474	0.1488
	90	1.9	0.1192	0.1181	0.1196	0.1199
	105	1.105	0.0695	0.06864	0.06964	0.07022
	120	1.12	0.05127	0.05018	0.05172	0.05191
	150	1.15	0.069917	0.06929	0.06997	0.07049
	180	1.18	0.034013	0.03373	0.03406	0.03425
	240	1.24	0.055293	0.05484	0.05525	0.05579
	600	1.6	0.08202	0.0811	0.0823	0.08266
15	615	2.15	0.03115	0.03073	0.03127	0.03145
30	630	2.3	0.039733	0.03904	0.04002	0.04014
45	645	2.45	0.05064	0.0502	0.05073	0.05099
60	660	2.6	0.037033	0.03668	0.03705	0.03737
105	705	2.105	0.030577	0.03027	0.03058	0.03088
120	720	2.12	0.05399	0.05315	0.05421	0.05461
150	750	2.15	0.07957	0.07851	0.08006	0.08014
180	780	2.18	0.088043	0.08724	0.08823	0.08866
300	900	2.3	0.034447	0.03403	0.03465	0.03466
600	1200	2.6	0.047967	0.04755	0.04806	0.04829
1500	2100	2.15	0.01905	0.01875	0.0192	0.0192
3600	4200	2.36	0.065287	0.06416	0.06576	0.06594
5400	6000	2.54	0.092317	0.09157	0.09245	0.09293
7200	7800	2.72	0.023967	0.02374	0.02392	0.02424
Mean Dissolved						
	30	1.3	0.013357			
	60	1.6	0.09242			
	120	1.12	0.009454			
	600	1.6	0.016573			
15	615	2.15	0.006619			
45	645	2.45	0.006164			
180	780	2.18	0.01383			
3600	4200	2.36	0.010517			
7200	7800	2.72	0.008045			

Table A 15: Field test flow rate data.

Trial 1							
Sampling Time (s)	Time Difference	Marked Height	Head	Vol. (cm^3)	Vol. L	Vol. Dif.	Flow Rate (L/s)
0	0	0	68.2	103700.2	103.7002	0	0
15	15	23	45.2	68727.99	68.72799	34.97221	2.331481
30	15	27.2	41	62341.76	62.34176	6.38623	0.425749
45	15	29.5	38.7	58844.54	58.84454	3.497221	0.233148
60	15	31.1	37.1	56411.69	56.41169	2.432849	0.16219
75	15	32.5	35.7	54282.95	54.28295	2.128743	0.141916
90	15	33.8	34.4	52306.26	52.30626	1.97669	0.131779
105	15	35	33.2	50481.62	50.48162	1.824637	0.121642
120	15	36.4	31.8	48352.88	48.35288	2.128743	0.141916
150	30	38.6	29.6	45007.71	45.00771	3.345168	0.111506
180	30	40.6	27.6	41966.65	41.96665	3.041062	0.101369
600	420	48.7	19.5	29650.35	29.65035	12.3163	0.029325
900	300	54.4	13.8	20983.33	20.98333	8.667026	0.02889
1560	660	64.6	3.6	5473.911	5.473911	15.50941	0.023499
Trail 2							
Sampling Time (s)	Time Difference	Marked Height	Head	Vol. (cm^3)	Vol. L	Vol. Dif.	Flow Rate (L/s)
0	0	68	68	103396.1	103.3961	0	0
15	15	3.4	64.6	98226.29	98.22629	5.169805	0.344654
30	15	4.2	63.8	97009.87	97.00987	1.216425	0.081095
45	15	4.7	63.3	96249.6	96.2496	0.760265	0.050684
60	15	5.2	62.8	95489.34	95.48934	0.760265	0.050684
75	15	5.6	62.4	94881.12	94.88112	0.608212	0.040547
90	15	6	62	94272.91	94.27291	0.608212	0.040547
105	15	6.3	61.7	93816.75	93.81675	0.456159	0.030411
120	15	6.5	61.5	93512.65	93.51265	0.304106	0.020274
150	30	6.8	61.2	93056.49	93.05649	0.456159	0.015205
180	30	7.3	60.7	92296.22	92.29622	0.760265	0.025342
300	120	8.9	59.1	89863.37	89.86337	2.432849	0.020274
600	300	14.1	53.9	81956.61	81.95661	7.90676	0.026356
1500	900	22.7	45.3	68880.05	68.88005	13.07657	0.01453
2100	600	27.6	40.4	61429.45	61.42945	7.450601	0.012418
2520	420	30.3	37.7	57324.01	57.32401	4.105433	0.009775
3000	480	33.6	34.4	52306.26	52.30626	5.017752	0.010454
3600	600	37.1	30.9	46984.4	46.9844	5.321858	0.00887
5400	1800	47.3	20.7	31474.99	31.47499	15.50941	0.008616
6360	960	52	16	24328.49	24.32849	7.146495	0.007444
7200	840	55.3	12.7	19310.74	19.31074	5.017752	0.005974
7860	660	58	10	15205.31	15.20531	4.105433	0.00622
9600	1740	64	4	6082.123	6.082123	9.123185	0.005243

Table A 16: Field test filter cake moisture and solid content.

MC and SC								
ID		Tin Weight	Tin + Sample (W)	Sample Wet	Tin + Sample (D)	sample (dry)	MC (%)	SC (%)
24.1	Middle 1	1.04	20.53	19.49	3.12	2.08	835.53	10.69
24.2	Middle 2	1.02	22.63	21.62	3.23	2.22	874.62	10.26
24.3	Middle 3	1.07	22.57	21.51	3.31	2.24	858.85	10.43
24.4	Edge 1	1.04	24.02	22.98	4.02	2.98	670.47	12.98
24.5	Edge 2	1.02	24.26	23.25	3.80	2.79	734.49	11.98
24.6	Edge 3	1.04	26.74	25.69	4.01	2.97	766.28	11.54
48.1	Middle 1	1.04	26.03	25.00	3.80	2.76	805.36	11.05
48.2	Middle 2	1.03	30.07	29.04	4.23	3.19	810.00	10.99
48.3	Middle 3	1.08	28.54	27.46	4.13	3.05	800.69	11.10
48.4	Edge 1	1.04	30.37	29.33	4.61	3.57	721.69	12.17
48.5	Edge 2	1.02	24.92	23.90	3.86	2.84	741.11	11.89
48.6	Edge 3	1.04	25.60	24.56	4.04	3.01	716.22	12.25
168.1	Middle 1	1.03	28.73	27.70	4.61	3.59	672.53	12.94
168.2	Middle 2	1.03	18.46	17.43	3.23	2.20	692.86	12.61
168.3	Middle 3	1.01	23.81	22.80	4.10	3.09	637.28	13.56
168.4	Edge 1	1.06	26.97	25.91	4.51	3.45	651.23	13.31
168.5	Edge 2	1.03	23.34	22.32	3.87	2.85	684.36	12.75
168.6	Edge 3	1.06	25.76	24.70	4.43	3.37	633.03	13.64
336.1	Middle 1	1.05	18.09	17.04	3.69	2.64	544.52	15.52
336.2	Middle 2	1.04	24.90	23.86	4.76	3.72	541.85	15.58
336.3	Middle 3	1.02	25.65	24.64	4.77	3.76	556.17	15.24
336.4	Edge 1	1.05	24.34	23.29	4.75	3.69	530.43	15.86
336.5	Edge 2	1.01	15.39	14.38	3.36	2.34	513.48	16.30
336.6	Edge 3	1.05	17.70	16.65	3.81	2.76	504.03	16.56

APPENDIX 5: SEM DATA

Table A 17: SEM weight percentage data corresponding to figure 5.15.

Figure 5.15A						
Site		1	2			
C		99.42	54.29			
O			35.75			
Mg			0.2			
Al		0.17	0.4			
Si		0.15	8.73			
Cl			0.18			
K			0.07			
Ca		0.08	0.21			
Mn		0.18				
Fe			0.16			
Figure 5.15B						
Site		1	2	3	4	5
C		58.76	49.12	65.2	68.84	61.54
O		15.5	18.16	27.13	25.9	29.54
Na		0.11	0.06	0.19	0.16	0.34
Mg		0.78	0.86	0.52	0.56	0.84
Al		2.63	4.27	1.47	0.73	1.42
Si		7.13	11.2	2.25	1.31	3.36
S		2.51	2.86	0.94	0.72	0.63
Cl		1.6	1.9	0.62	0.5	0.35
K		2.63	1.06	0.28	0.17	0.43
Ca		4.39	6.8	0.82	0.61	0.43
Mn		0.93	0.96		0.13	0.34
Fe		3.01	2.75	0.57	0.38	0.77

Table A 18: SEM weight percentage data corresponding to figure 5.16.

Untreated (A)						
Site	1	2	3	4	5	
Na	7.96	12.21	4.44		13.14	
Mg	5.09	6.79	15.97		8.14	
Al	5.28	10.2	10.2		9.2	
Si	14.75	28.03	40.16		19.78	
S	19.76	13.19	7.4		15.62	
Cl	21.2	14.35	8.69		20.14	
K	2.34	2.28	2.74		2.3	
Ca	14.12	7.97	4.86		7.33	
Mn	1.51					
Fe	5.7	3.76	4.55		4.35	
Cu	2.29	1.22	0.99			
Conditioned (Flocs) (B)						
Site		2	3	4	5	6
Na		4.87	4.55	1.02	2.44	9.65
Mg		13.75	4.9	1.14	7.72	6.76
Al		10.11	10.96	15.27	4.2	11.96
Si		36.1	25.25	68.57	25.42	20.47
S		10.85	12.98		14.33	14.78
Cl		10.85	14.57	1.77	16.39	17.15
K		2.23	3.65	7.32	3.48	2.99
Ca		4.72	13.88	1.06	16.87	8.68
Mn		0.69	1.5			
Fe		4.3	7.76	2.97	9.14	6.12
Cu		1.54				1.44
Filter Cake (C)						
Site	1	2	3	4		
Na	1.33	1.52		1.53		
Mg	7.17	6.6	5.05	9.59		
Al	12.39	15.36	9.54	11.21		
Si	29.23	32.79	21.97	31.72		
S	13.4	15.84	19.01	17.12		
Cl	5.87	10.73	8.26	10.5		
K	2.78	3.4	2.39	3.06		
Ca	22.1	8.58	18.51	8.04		
Mn			1.61	0.89		
Fe	5.71	5.18	13.66	5.02		
Cu				1.33		
Particles in Filtrate (D)						
Site	1	2	3	4	5	
Na			1.91		2.97	
Mg	5.32	7.12	5.58	11.1	6.3	
Al	16.65	11.82	13.93	11.73	12.08	
Si	14.72	33.27	33.26	31.25	19.05	
S	16.16	12.41	12.05	14.69	17.57	
Cl	8.59	13.08	8.61	6.93	11.7	
K		2.73	2.27	2.49	1.82	
Ca	29.96	9.16	9.71	12.91	16.78	
Mn	3.23	3.29	2.02	1.75	2.57	
Fe	5.38	7.11	9.55	5.08	5.9	
Cu				2.08	3.27	